Regulation of Integrin Activation and Migration in Fibroblasts

Kemp-O'Brien, Karl William

Awarding institution:
King's College London

Regulation of Integrin Activation and Migration in Fibroblasts

A thesis submitted to King's College London for the degree of Doctor of Philosophy

by

Karl Kemp-O'Brien

Randall Division of Cell and Molecular Biophysics, King's College London, 2014

Acknowledgements

I would like to thank my supervisors, Dr Maddy Parsons and Dr Simon Ameer-Beg for all of their efforts in supporting me through my thesis work. I would also like to thank everyone in the Randall Cell Motility groups, past and present, for their support, help, advice and friendship over the last few years. Special thanks must go to Penny and Asier without whom I may have lost my sanity. I would also like to thank my mother for not sugar coating her advice and for always being there for me, and my Nan for always supporting me in every way imaginable. I could not have completed this work without Mali, Giulia, Rumena, Valen and Matt who all, in different ways and at different times, gave me so much support and motivation. I would also like to thank Sweta, John, Ah-Lai, Lizzy, Jo, Anneri, Tim, Ester, Mags, Anne, Claudia, Mark, Matthias, Gareth, Helen and everyone else in the lab who has enriched my work life with moments of fierce humour, kindness and support from day one.

Abstract

Cell adhesion and migration is essential for normal tissue organisation and function and dysregulation of these processes is involved in a number of different diseases. Focal adhesions are the major sites of adhesion to the extracellular matrix in migrating cells and integrins are a major component of these structures. Integrins are heterodimeric transmembrane receptors that undergo cycles of activation and inactivation at the plasma membrane to control assembly of focal adhesions. Integrins can be activated in two different ways; outside-in activation by binding to an extracellular ligand, or inside-out activation though the binding of cytoplasmic proteins to the integrin cytoplasmic tail. Talin and kindlin proteins are the two known families of activators of integrins, and act through binding to the cytoplasmic tail on the integrin beta subunit. Both kindlins and talin contain phospholipid-binding domains and have been shown biochemically to be able to bind to PIP2 or PIP3. The aim of this study is to characterize the recruitment of talin and kindlins to integrins and their individual roles in the sequence of receptor activation. The role of PIP2 and PIP3 in regulating the recruitment of integrin activators to adhesion sites and the role of each of these protein families in controlling integrin dynamics at focal adhesions was also addressed in fibroblast cells on both 2D and 3D matrices. Data demonstrates that kindlin2 plays the key role in fibroblast migration on 2D and 3D matrices and that this correlates with a reduction in active integrin levels. Moreover, live cell imaging revealed that kindlins appear at focal adhesions prior to talin suggesting a role for these proteins in 'priming' the receptor for activation by talin. Finally, these recruitment and adhesion maturation events all depend on the balance of PIP2 local to focal adhesions. These findings shed novel light on the mechanism of integrin activation in migrating cells.

Table of Contents

List of Figures

List of Tables

Abbreviations

ADP	Adenosine diphosphate
APS	Ammonium persulphate
Arp2	Actin related protein 2
Arp3	Actin related protein 3
ATP	Adenosine triphosphate
BSA	Bovine Serum Albumin
CCD	Charged coupled device
CDM	Cell derived matrix
CHO	Chinese hamster ovary cells
DMEM	Dulbecco's modified Eagle's media
DMSO	Dimethyl sulfoxide
DNA	Deoxyribonucleic acid
ECM	Extracellular matrix
EDTA	Ethylenediaminetetra-acetic acid
EGF	Epidermal growth factor
EGFR	Epidermal growth factor receptor
EM	Electron microscope
F-actin	Filamentous actin
FAK	Focal adhesion kinase
FAT	Focal adhesion-targeting domain
FBS	Fetal bovine serum
FERM	Four point one protein, ezrin, radixin and moesin
FRAP	Fluorescence Recovery After Photobleaching
FRET	Fluorescence Resonance Energy Transfer
GAPDH	Glyceraldehyde 3-phosphate dehydrogenase
GDP	Guanosine diphosphate
GFP	Green fluorescent protein
GTP	Guanosine triphosphate
HDF	Human dermal fibroblasts
HRP	Horseradish peroxidase
IF	Immunofluorescence
ILK	Integrin-linked kinase
IP	Immunoprecipitation
kDa	Kilodaltons
LDV	Leucine-aspartic acid-valine
LIM	Lin11, ISL-1, Mec-3
MEFs	Mouse embryo fibroblasts
MMP	Matrix metalloproteinase

PBS	Phosphate buffered saline
PFA	Paraformaldehyde
PH-domain	Pleckstrin-homology domain
PI3K	Phosphoinositide-3-kinase
PI(3,4)P2	Phosphatidylinositol (3,4)-bisphosphate
PI(4,5)P2	Phosphatidylinositol (4,5)-bisphosphate
PIP3	Phosphatidylinositol (3,4,5)-trisphosphate
PKC	Protein kinase C
PTEN	Phosphatase and tensin homolog
PY	Phosphotyrosine
RGD	Arginine-glycine-aspartic acid
RIPA	RadioImmuno precipitation assay
SDS	Sodium dodecyl sulphate
SEM	Standard error of the mean
SH2	Src homology 2 domain
SH3	Src homology 3 domain
SOC	Super optimal broth with catabolite repression
TEMED	Tetramethylethylenediamine

1. Introduction

1.1 Cell Migration

Cell migration is a fundamental process in large complex multicellular organisms such as mammals, down to small single-celled organisms (Vicente-Manzanares et al., 2005; Ridley et al., 2003). In multicellular organisms, cell migration is crucial to development and the functioning of our immune system, but when incorrectly regulated it can lead to a wide range of diseases. Cell migration is required for gastrulation of the early embryo, and for the movement of neural crest cells in order to form our nervous system. Failure to correct errors in these processes results in perturbed development and embryonic lethality (Locascio and Nieto, 2001; Klämbt, 2009). Indeed, even after embryonic development, cell migration is required for maintaining skin tissue and for closing open wounds (Wen et al., 2010).

It is often remarked that the cost of being multicellular animals, which often leads us to our death, is uncontrolled cell division. Uncontrolled tumour growth can often be operable, however it is when secondary tumours are formed throughout the body that the prognosis for patients decreases. A key stage in lethal cancer development is therefore the development of metastasis throughout the body (van Zijl et al., 2011). Cell migration and adhesion signalling must be damaged or dysregulated in order for cancer cells to migrate out of their primary site, enter the circulatory system, and

then adhere to and invade a secondary site to form a new metastatic tumour (van Zijl et al., 2011).

Abercrombie *et al*, were the first to study migration in detail in cell cultured fibroblasts (Abercrombie, Heaysman, and Pegrum, 1970a; 1970b; 1970c). Fibroblasts were seen to push out ruffling lamellipodia, which were largely flat and thin. In the years since a great deal of work has gone into understanding the molecular details of migration. Single cells have been shown to be able to move in two different migration modes, amoeboid and mesenchymal. Amoeboid migration occurs without mature focal adhesions or stress fibres, making the cells appear rounded (Friedl et al., 2001; Lämmermann and Sixt, 2009). Within the amoeboid migration type cells can migrate either through use of a blebbing forward pushing migration type, instead of a pulling propulsive force, or through forming small filopodia at the front of the cell, providing some degree of contact with the substrate. This latter type of migration is is sometimes called pseudopodal movement (Friedl and Wolf, 2010; Sanz-Moreno and Marshall, 2009). The other main type of migration mode is termed mesenchymal migration, and relies upon adhesive contacts to the substrate and actin stress fibres in order to generate force and allow the cells to migrate (Friedl and Wolf, 2010). This mesenchymal migration will now be the focus of this literature review.

In order for cells to successfully migrate using mesenchymal migration, four distinct steps are involved (Figure 1.1); first cells extend membrane protrusions at the front of the cell, second, nascent adhesions are formed between the cell and the extracellular matrix (ECM), third, the cell body undergoes cell contraction inducing movement which is anchored by more mature adhesions and finally, adhesions at the rear of the cell disassemble and the cell rear retracts (Vicente-Manzanares et al., 2005; Moissoglu and Schwartz, 2012; Gardel et al., 2010). This basic model of migration is observed in most motile cells on 2D substrates and leads to cell polarity with a broad lamella at the leading edge of the cell, and trailing edge at the rear of the cell. Traditionally, cell migration has been studied on 2D surfaces, such as plastic or glass, to allow for a greater understanding of the fundamental mechanics of cell migration. However more recently, use of *in vivo* imaging and more physiologically relevant models has enabled the study of cell migration within 3D substrates and revealed differences with data arising from 2D studies.

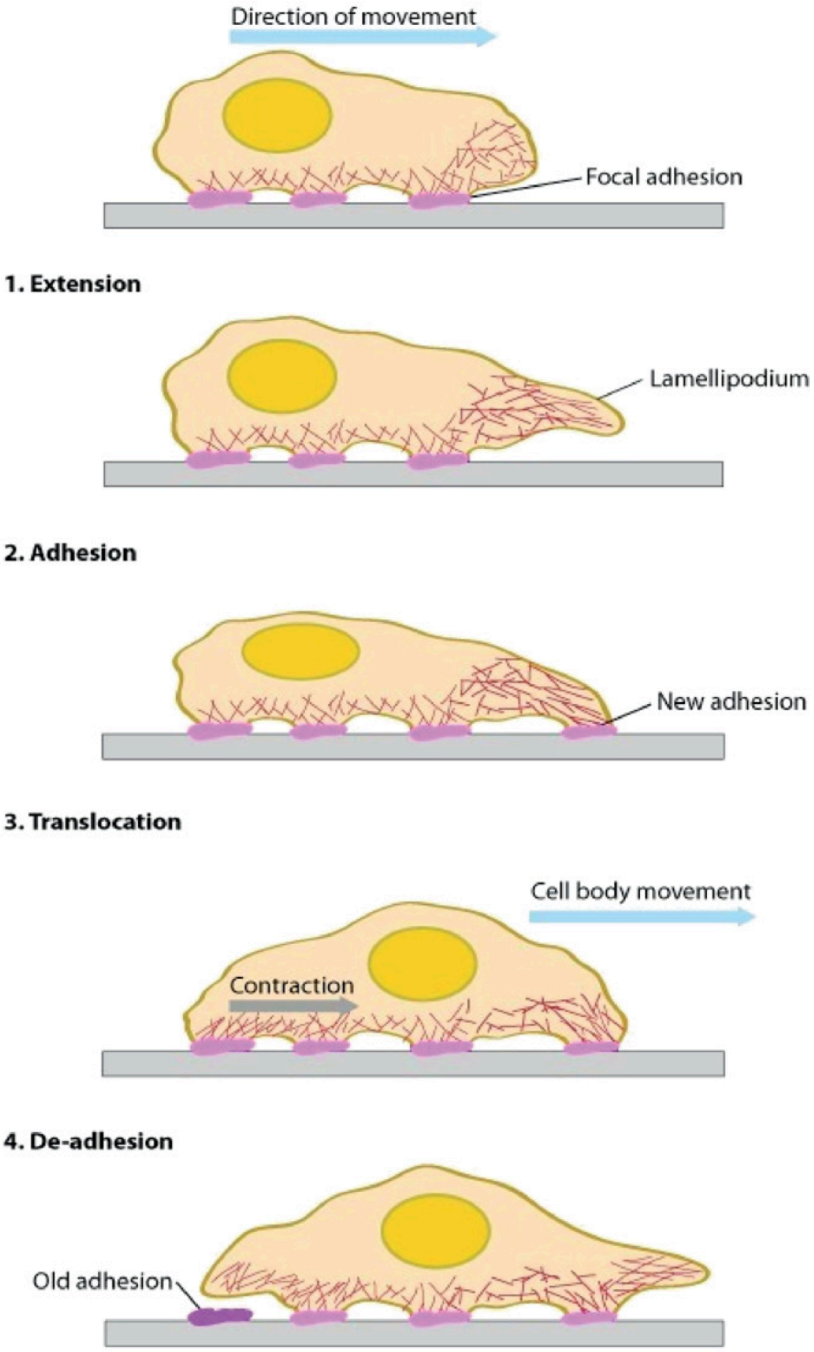

Figure 1.1. Schematic model of migration of a cell across a 2D substrate.
1. Actin-based protrusions are formed at the leading edge of cells, typically lamellipodia or filopodia. **2.** Membrane protrusions come in contact with the substrate and facilitates the binding of transmembrane adhesion receptors called integrins. **3.** Acto-myosin contractility and actin retrograde flow contribute to a contraction of the cytoskeleton at the read of the cell, anchored by adhesions. **4.** Increased force and other proteins contribute to the disassembly of older adhesions at the rear of the cell and the subsequent retraction of the cell. Adapted from (Ladoux and Nicolas, 2012).

Fibroblasts within 3D matrix models and within stromal collagen I environments *in vivo* have been shown to adopt a more extended, elongated shape than fibroblasts on traditional 2D substrates (Cukierman et al., 2002; 2001; Jayo and M. Parsons, 2012; Hakkinen et al., 2011; Harunaga and Yamada, 2011; Tamariz and Grinnell, 2002). Cells migrating through 3D matrix produce protrusions, mostly at the leading edge of the cell, and use actomyosin tension to generate force in order to propel through the matrix. Fibroblasts normal function within skin is to produce the fibrous matrix in which other cells exist. Consistent with this, fibroblasts have been shown to be able to degrade and remodel surrounding matrix potentially through extension of membrane protrusions (Tamariz and Grinnell, 2002; Kobayashi et al., 2014). Indeed, this remodeling and degrading of ECM has led to a renewed focus on fibroblasts within the context of cancer cell extravasation and invasion (Kharaishvili et al., 2014).

1.2 Focal adhesions

In order for a cell, such as a fibroblast, to be able to migrate, contacts between the cell and the substrate must be made in order to generate force. These adhesions are structures that offer a platform for protein recruitment, signal transduction and a physical connection between the cell's cytoskeleton and the cells external substrate and were first described

in the 1970s (Heath and Dunn, 1978; Abercrombie and Dunn, 1975; Abercrombie et al., 1971). Adhesions contain many proteins and the dynamic regulation and turn over of these proteins are crucial to understanding the role of adhesion, and integrin activation, in migration. These adhesions can be broadly separated into different groups based upon their size (Shown in Figure 1.2), localisation and composition, these are nascent adhesions, focal complexes, focal adhesions and fibrillar adhesions in addition to a fifth group for specialised adhesions in 3D (Scales and M. Parsons, 2011). Nascent adhesions are small, very short lived adhesions, typical lasting < 1 min, formed at the leading edge of cells in 2D culture which are migrating or spreading, and these adhesions quickly disassemble or mature to become focal complexes (Izzard, 1988; Riveline et al., 2001; Zamir et al., 2000). Focal complexes are slightly longer lived than nascent adhesions lasting for < 1 min (Izzard, 1988). Focal adhesions are larger, 1-5 μm compared with 0.5 μm for focal complexes and have slower turnover of proteins than nascent adhesions or focal complexes and are much longer lived lasting upwards of 10-60 min (Zamir et al., 2000). Fibrillar adhesions are larger still and are more elongated than focal adhesions and are found aligned with extracellular fibers and induce fibronectin fibrillogenesis (Pankov et al., 2000). Adhesions of one type can mature into larger adhesions of another type and in doing so lose or gain additional proteins. A key step in this maturation process is the generation of actomyosin tension and is illustrated in Figure 1.2.

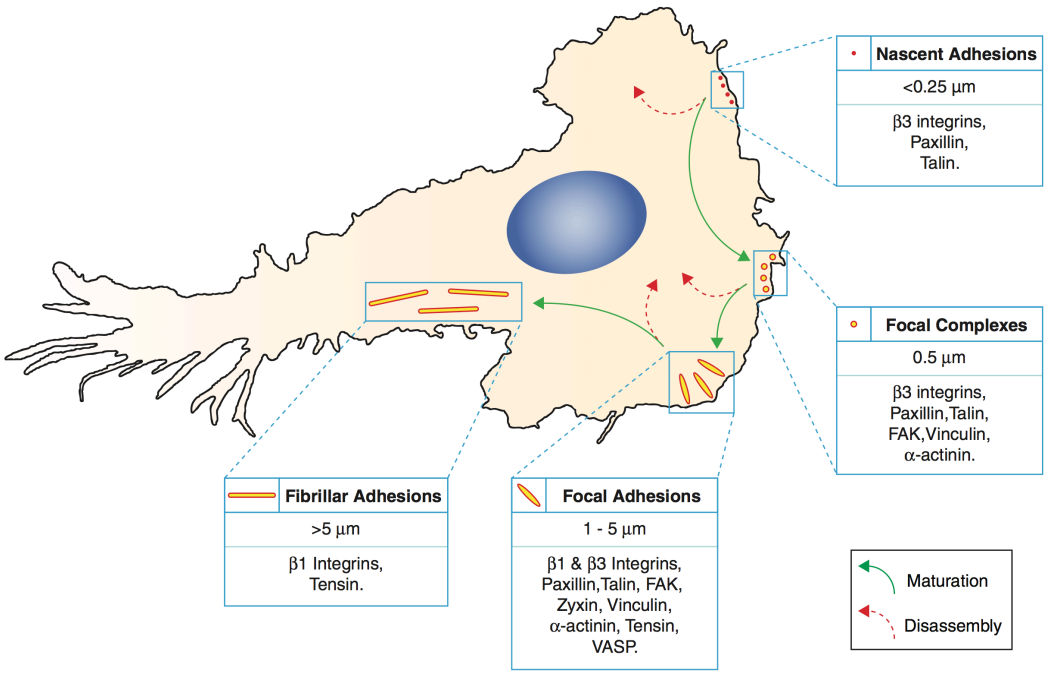

Figure 1.2. Schematic of the classification of different integrin-based adhesions and their known protein components.

Initial adhesions are called nascent adhesions. They form at the cell periphery and are small <0.25µm total area and are rapidly disassembled or mature to for form focal complexes. Focal complexes are larger, ~0.5µm, and have more proteins associated with them. Focal complexes can mature further to focal adhesions, which can vary in size from 1-5µm. Focal adhesions may disassemble or further mature to form fibrillar adhesions, which are long adhesions typically over 5µm in total area size. Adapted from (Scales and M. Parsons, 2011).

1.3 Actin

Actin is a highly conserved globular protein with three isoforms. α-actin is mostly found in muscle but β- and γ-actin are ubiquitously expressed and make up the fibroblasts actin cytoskeleton (Khaitlina, 2001). Monomeric actin when ATP bound, can polymerise to form polymeric filamentous actin or F-actin. F-actin is polarised with a plus end, where additional actin monomers can be added to the filament, and a minus end, where the actin filament is depolymerised and the monomeric actin is once again released (Le Clainche and Carlier, 2008). This continuous polymerisation and depolymerisation of actin filaments results in F-actin being able to maintain its length while being continuously polymerized which is known to be crucial to different cellular functions including the extension of neuronal growth cones (Gomez and Letourneau, 2014). This retrograde flow of actin monomers within filaments was termed 'treadmilling' when originally discovered, but can also be called retrograde flow (Y. L. Wang, 1985). Motor proteins such as myosin move along actin filaments and are key to generating actomyosin force in addition to various other roles in transporting cargo such as vesicles (Doherty and McMahon, 2008). Actin polymerization, elongation, depolymerisation, branching, bundling and cross-linking is regulated by a large host of proteins such as Arp2/3, mDia and fascin (Le Clainche and Carlier, 2008). In addition to actomyosin tension, bundles of actin generate protrusions by pushing on the plasma membrane. These protrusions include filopodia, containing long parallel

bundles of F-actin, and lamellipodia, broad flat branched networks of actin with leading edge membrane ruffles, as first characterised by Abercrombie, *et al.* 1970 (Le Clainche and Carlier, 2008; Abercrombie, Heaysman, and Pegrum, 1970b).

Adhesion proteins link the actin cytoskeleton directly to the extracellular matrix via integrins. It has been shown that there are distinct layers within adhesions, with each layer named after its primary function (Kanchanawong et al., 2010). Broadly, integrins bind directly to the extracellular matrix and allow for signal transduction across the plasma membrane and for the recruitment of adhesion proteins. The proteins in this layer make up the integrin signaling layer and include proteins such as focal adhesion kinase (FAK), paxillin and the talin head domain, as shown in Figure 1.3 (Kanchanawong et al., 2010). Some adhesion proteins physically link integrins to the actin cytoskeleton and make up what was called the force transduction layer as some protein components within this layer are mechanosensitive shown in Figure 1.3 (Kanchanawong et al., 2010). The mechanosensitive properties of some of these proteins, such as talin or vinculin, allow for force dependant signal transduction through force dependent recruitment of proteins (Kanchanawong et al., 2010). Above this layer is the actin regulatory layer and the actin cytoskeleton itself shown in Figure 1.3 (Kanchanawong et al., 2010). This architecture of integrin-based adhesions is useful when thinking about the complexity of adhesions and the signal transduction that then occurs.

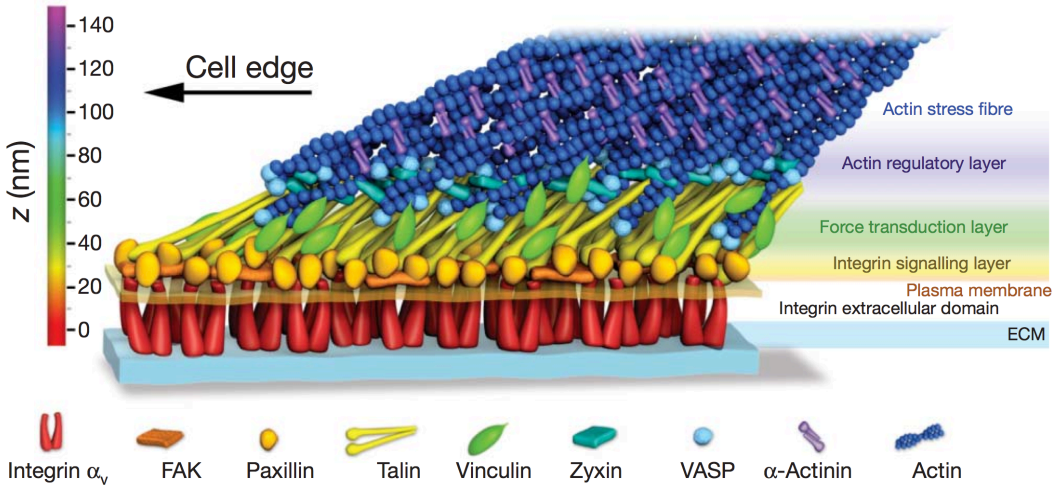

Figure 1.3. The architecture of focal adhesions.

Schematic model based upon iPALM microsocopy data of the nano-scale architecture of focal adhesions depicting where in relation to the substrate adhesion proteins and actin are found. The adhesion has been subdivided into distinct layers, notably the integrin signaling, force transduction and actin regulatory layers. The schematic shows the localisation of several key adhesion proteins including talin, paxillin and vinculin. Adapated from (Kanchanawong et al., 2010)

1.4 Integrins

Integrins are a major component of adhesions and their main role is in controlling cell adhesion to the ECM that ultimately acts to regulate cell fate, growth, differentiation, migration and apoptosis (Hynes, 2002a). Integrins are a family of heterodimeric type I transmembrane receptors consisting of an α and β subunit which are non-covalently linked (Harburger and Calderwood, 2009). The large extracellular domain of each subunit interact to form the 'ligand-binding domain of the integrin. The α subunit β propeller and thigh domains, and the β subunit β-I , hybrid, PSI and I-EGF-1 domains for the top part of the extracellular integrin which is important for binding to ligand. This ligand binding head domain is connected to the transmembrane region through calf 1 and calf 2 domain in α subunits, and I-EGF-2, -3, -4 and β tail domains in β subunits (Xiong et al., 2001; Jianghai Zhu et al., 2008). This lower extracellular portion is connected to the upper ligand binding head domain via a region flexible enough to allow for a conformational change commonly called the 'knee' region (Jieqing Zhu et al., 2013). These regions are then connected to the transmembrane regions which are then connected to the α and β subunit tails in the cytosol (Gahmberg et al., 2009).

In mammals there are currently 18 known α-subunits, 8 β-subunits which give rise to 24 possible integrin receptor heterodimers with different binding properties and different tissue distributions (Hynes, 2002a;

Campbell and M. J. Humphries, 2011). These 24 different possible combinations of α and β subunits allow for integrin ligand specificity. Some β integrin subunits are only known to exist as in combination with one other α subunit, whereas others can be part of many heterodimers such as β1 which can exist in combination with 12 different α-subunits (J. D. Humphries et al., 2006). Ligand recognition is a key part of integrin signaling and it is a key way for cells to recognize local composition of tissues. Integrins can be placed into four different groups based upon the ligands they can recognise, as illustrated in Figure 1.4 (J. D. Humphries et al., 2006; Hynes, 2002a). These groups are the RGD-binding integrins, LDV-binding integrins, I-domain β1 integrins and non-α-I-domain-containing laminin-binding integrins (J. D. Humphries et al., 2006).

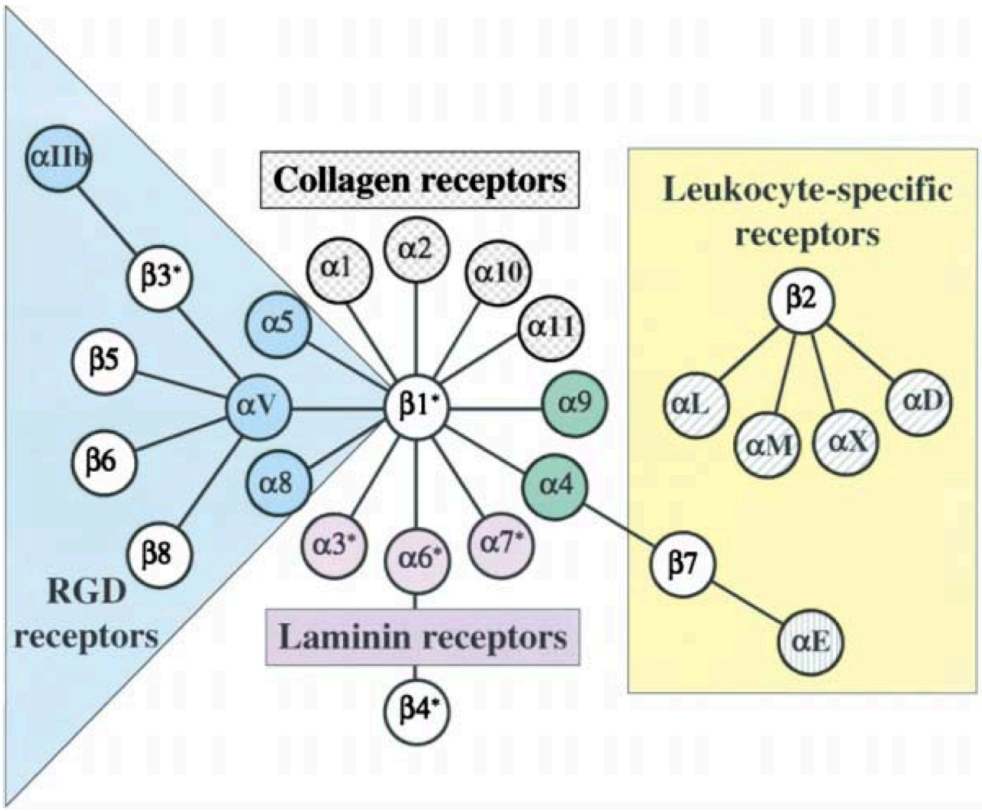

Figure 1.4. Diagram of the integrin heterodimer family.

Integrins are composed of a combination of α and β subunit. There are 18 α subunits and 8 β subunits giving rise to the 24 heterodimer αβ pairs indicated in this figure. Adapted from (Hynes, 2002a).

Within the first group of integrins that are able to recognise ligands containing the RGD peptide, there are all five αV integrin containing heterodimers, αIIbβ3 and two β1 containing integrins (α5β1 and α8β1) (Hynes, 2002b; J. D. Humphries et al., 2006). This group of integrins are able to bind to and recognise a large range of extracellular matrix components and soluble ligands, however the affinity for specific ligands by each integrin varies even within this group (J. D. Humphries et al., 2006). The interaction site between the integrin and RGD-peptide is in the integrin head domain where binding occurs between the integrin subunits. The exact site as revealed by crystal structures of αIIbβ3 and αVβ3 is the cleft between the β-propeller domain of the α-subunit and the β-I-domain in the β subunit with the arginine of the RGD peptide fitting next to the β propeller domain and the aspartic acid residue of the RGD peptide to the β-I-domain (Xiong et al., 2001; Xiao et al., 2004). It is thought that the different affinities of RGD-binding integrins for specific RGD-containing ligands may be due to differences in how exact a fit there is between the peptide and the specific binding site between the two integrin subunit head domains (Campbell and M. J. Humphries, 2011).

The second group of integrins recognise the acidic LDV motif that is functionally similar to the RGD peptide and it is thought that binding of integrins to LDV is similar to that with RGD peptide between the α subunit and the β subunit head domains, but structural data is still lacking

(Campbell and M. J. Humphries, 2011). The LDV-binding integrins are the α4 containing integrins (α4β1, α4β7), α9β1, αEβ7 and the four β2 containing integrins (α1β2, αMβ2, αXβ2 and αDβ2) (Campbell and M. J. Humphries, 2011; J. D. Humphries et al., 2006). Of the LDV binding integrins five are leukocyte specific, αEβ7 and the four β2 containing integrins (Hynes, 2002a). The four β2 containing integrins bind to ligands in a way similar to the others but the major interaction with the ligand takes place via an inserted I-domain in the α subunit. A major difference between these β2 integrin ligand is that instead of using an aspartate residue for cation coordination, like β1 and β7 ligands, β2 integrin ligands instead employ a glutamate residue (J. D. Humphries et al., 2006; Campbell and M. J. Humphries, 2011).

The third group of integrins are the I-domain β1 integrins which can bind to laminin or collagen. Integrins in this grouping all are composed of β1 subunits combined with α-subunits containing an α-I-domain (α1, α2, α10 and α11) (J. D. Humphries et al., 2006). The crystal structure for the binding of the α2-I-domain and collagen was solved and showed that the structural basis of the interaction was dependent upon a critical glutamate residue within a GFOGER motif thought to be the key cation-coordinating residues in this interaction (Emsley et al., 2000). The precise details of how these integrins bind to laminin is still unclear (J. D. Humphries et al., 2006; Campbell and M. J. Humphries, 2011).

The final group of integrins is the non-α-I-domain-containing integrins which are highly selective laminin binding integrins, namely α3β1, α6β1, α7β1 and α6β4 (J. D. Humphries et al., 2006). The active site involved with the binding of these integrins to laminin, like that of the I-domain containing integrins, is not known.

1.5 Integrin conformation upon activation

Integrins are bidirectional adhesion receptors capable of being activated via outside-in or inside-out signaling. Outside-in signaling is when a ligand binds to the extracellular head domain of integrins triggering a large conformational change leading to transduction of the signal to the inside of the cell (Gahmberg et al., 2009). On the other hand, inside-out signaling is when cytosolic proteins bind to the intracellular tails of the integrins leading to a conformational change and the activation of the integrin (Ye et al., 2011; Anthis and Campbell, 2011). Additionally, clustering of integrins may also contribute to inside-out activation (Gahmberg et al., 2009).

Activation of an integrin is intrinsically linked to its conformation. Structural work on integrin αVβ3 has been critical to the current models of integrin activation. αVβ3 was found to be compact and to adopt a 'bent' conformation with a large flexible bend in the integrin between the head and the 'legs' of the integrin (Xiong et al., 2001; Mould and M. J.

Humphries, 2004). This conformation positions the ligand-binding domain closer to the plasma membrane (Figure 1.5). Various studies have shown that integrins are inactive when bent and that when they become active, they straighten and adopt an extended conformation which allows the head domain to move closer to ligand in the substrate for easier binding (Chigaev et al., 2003; Nishida et al., 2006; Campbell and M. J. Humphries, 2011; Takagi et al., 2002). Even when in the inactive bent conformation integrins were shown to still be able to bind ligand albeit with very low affinity (Adair et al., 2005).

The change from a bent inactive state, to an extended active state is not completely understood due to technical limitations, however a movement of the hybrid domain is thought to be central to the change in conformation of the integrin. This was shown by angles between the hybrid and β-I-domain changing from an acute to an obtuse angle once the integrin is ligand bound (Takagi et al., 2002). Further evidence came from the use of activating antibodies that bind to regions of the integrin close to the hybrid domain (Mould et al., 2003). The movement of the hybrid domain away from the α subunit would pull the β-I-domains α7 helix region down which would then move the α1 helix upwards (Xiao et al., 2004). Further proof of the importance of this action is in data showing that mutation of the integrin to favour a downward movement of the α7 helix of the β-I-domain (Hato et al., 2006; Mould et al., 2003). Changes in the conformation of the extracellular portion of integrins change the conformation along its whole

length and results in the separation of the integrin transmembrane and cytoplasmic tail domains (Figure 1.5). Although there is structural evidence to suggest that some integrins can be ligand bound when bent, more recent evidence using FRET-FLIM analysis of adherent cells showed that integrins in focal adhesions are in the extended high ligand affinity conformation (Chigaev et al., 2003; Xiong et al., 2001; Askari et al., 2010).

Additionally, integrins can be activated through changes in their conformation on the inside of the cell. The α and β subunit cytoplasmic tail membrane proximal regions are stabilised by a salt bridge and disruption of this interaction due to protein binding leads to activation of the integrin and the first protein to be discovered to be able to contribute directly to this mode of activation was the talin family of proteins (Anthis, Wegener, et al., 2009; Campbell and M. J. Humphries, 2011).

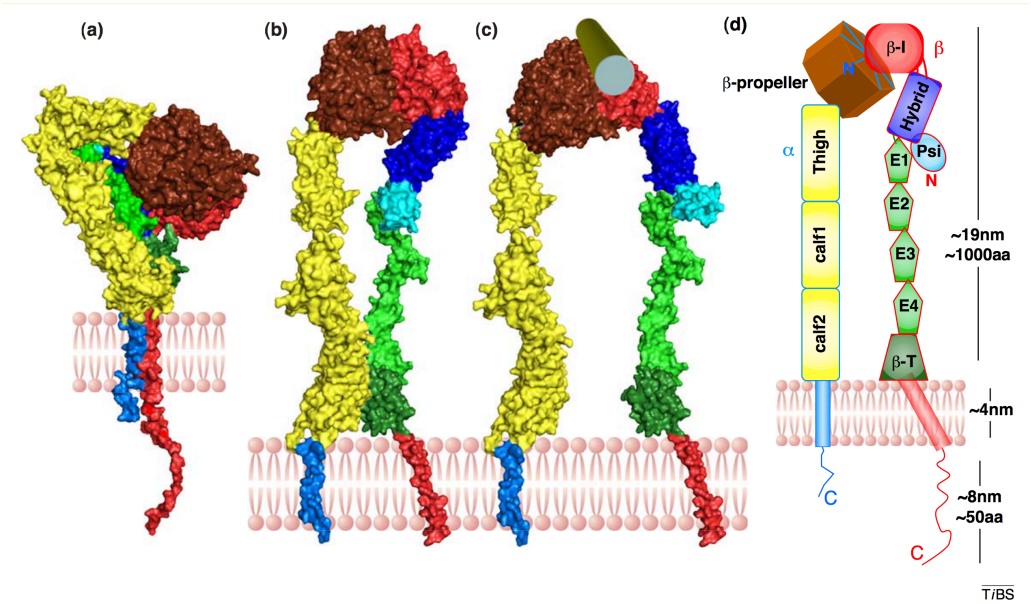

Figure 1.5. Schematic view of integrin conformation at different activation states.

A) Integrin structure when in an inactive or low-affinity state, the integrin extracellular domain is bent with the head domain pointed towards the cell membrane. B) Integrins are thought to be able to adopt an intermediate or primed extended conformation due to a rotation in the integrin separating the cytoplasmic tails somewhat (full -engtth cytoplasmic tail not shown). C) Structure of an integrin in a high affinity or fully activated ligand bound state, with the hybrid domain of the β subunit having swung out, resulting in a large separation of the cytoplasmic tails (full length cytoplasmic tail not shown). D) schematic view of the integrin subdomains with approximate sizes at the fully extended conformation. Adapted from (Anthis and Campbell, 2011).

1.6 Talin

Talin was the first protein to be found to directly activate integrins through the inside-out mechanism (Calderwood et al., 1999). There are two isoforms of talin, talin-1 and talin-2, with talin-1 being ubiquitously expressed and the expression of talin-2 being found mainly in muscle cells and brain tissue (Senetar et al., 2007). Talin-1is a ~270 kDa protein that consists of a N-terminal head domain, and a C-terminal rod domain, ~50 kDa and ~200 kDa respectively (Critchley, 2009). The head contains a FERM (protein 4.1, ezrin, radixin, moesin) domain which itself is composed of F1, F2 and F3 domains along with an atypical F0 domain in an extended conformation, rather than a cloverleaf formation typical for a FERM domain (Elliott et al., 2010; Critchley, 2009). The F3 subdomain is notable as it resembles a phosphotyrosine-binding (PTB) domain. It is this domain that binds to the flexible integrin β subunit tail at the membrane proximal NPXY motif, in addition to potentially binding to FAK, TIAM1, and phosphatidylinositol 4-phosphate 5-kinase type Iγ (PIPKIγ) (de Pereda et al., 2005; Lawson et al., 2012; S. Wang et al., 2012; Calderwood et al., 2013).

The head domain is linked to the rod domain through a large unstructured linker region that can extend and gives the molecule some flexibility between its two main domains (Calderwood et al., 2013). The rod domain of talin is formed of 62 α-helicies grouped into 13 bundles (R1-13) with a

lone α-helix at the C-terminal end (Figure 1.6). This single α-helix is also called the DD or dimerisation domain as it is where talin can bind to another talin molecule (Molony et al., 1987). Talin links integrins to the actin cytoskeleton and to this end the rod domain contains two binding sites for actin, in addition to several sites for binding for other proteins such as RIAM, and vinculin, which itself can bind to actin and strengthen the link to the cytoskeleton, shown in Figure 1.6 (Critchley, 2009; Calderwood et al., 2013). Additionally, the rod domain also contains a second integrin binding site, at positions R11-12, which has been shown to be able to bind to β3 integrins at the same place where αIIb integrins are bound and therefore this integrin binding site for talin can only be employed once the integrin is activated and the integrin tails have separated (Rodius et al., 2008).

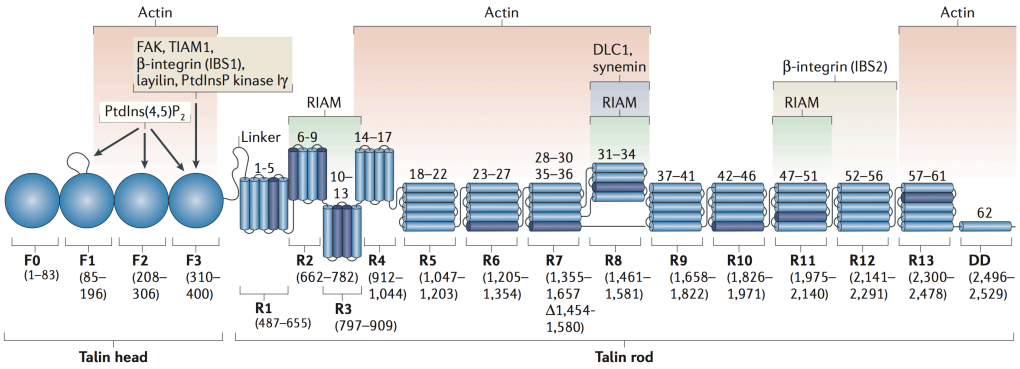

Figure 1.6. Diagram of the structure of talin.

Talin is composed of a head domain connected by a flexible linker to a large rod domain. The head domain consists of an atypical FERM domain, which is itself composed of an F0 domain and F1-3 domains. The talin rod domain is formed of 13 α helix bundles and a final α helix called the DD domain where talin is able to form a dimer with another talin. The various known interaction and binding sites on talin have been shown. Adapted from (Calderwood et al., 2013).

The protease calpain-2 can cleave talin, releasing the head domain from the rod domain that has been shown to result in increased binding to the β3 integrin tail (Yan et al., 2001). Talin dimers are autoinhibited through the binding of the talin rod R9 domain to the F3 region of the head domain. This results in a donut structure with the head domains occupying the space in the middle of the ring of rod domains and calpain cleavage relieves this autoinhibition (Goult et al., 2013). Calpain-2 can also cleave talin between the R13 domain and dimerization domain in the talin rod domain which may relieve autoinhibition. The current model suggests that talin cleavage by calpain results in adhesion disassembly, and the resultant talin head domain may facilitate integrin activation and potentially adhesion remodeling before it is targeted for degradation (Franco et al., 2004; Calderwood et al., 2013). Additionally, talin-PI(4,5)P2 phospholipid interactions have been shown to increase binding of talin to integrins (Moore et al., 2012).

The binding of the talin F3 domain to the membrane proximal NPXY motif on β integrin subunits has been shown to be required for integrin activation *in vitro* and *in vivo* (Tadokoro et al., 2003; Petrich, 2009). The mechanism for talin-induced integrin activation is triggered by talin through increasing the tilting angle of the rigid β integrin transmembrane domain which destabilises integrin α and β subunit transmembrane domain interactions, moving them apart (Ye et al., 2011) The integrity of the rigid β integrin

transmembrane domain has been demonstrated to be critical to talin-induced integrin activation through breaking the transmembrane domain into two halves which can then adopt different tilting angles which blocks integrin activation (Kim et al., 2011). Additionally, a salt-bridge forms between the talin F3 domain and β integrin membrane proximal region that may disrupt the interaction with the integrin α subunit tail which has been shown to be inhibitory, thus contributing to integrin activation (Anthis, Wegener, et al., 2009). Acidic phospholipids such as PI(4,5)P2 have been shown to increase the affinity of integrin β3 tails for talin as the talin head domain contains regions known to bind to acidic phospholipid and that this may play a role in orientating talin head domains to increase affinity of the talin-β integrin interaction (Moore et al., 2012; Elliott et al., 2010).

1.7 Kindlins

The kindlins are a family of proteins that have been shown to be able to regulate integrin activation through binding to the integrin β subunit cytoplasmic tail. There are three known members of the kindlin family of proteins, kindlin 1, kindlin 2, and kindlin 3. Kindlin expression varies by tissue, kindlin 1 is predominantly expressed in epithelial cells, kindlin 2 is ubiquitously expressed and kindlin 3 is expressed in hematopoietic and endothelial cells (Meves et al., 2009; Montanez et al., 2008; Siegel et al., 2003). Kindlin 1 and kindlin 2 have the greatest sequence similarity with

kindlin 3 showing lowest sequence similarity to the other two (Siegel et al., 2003). Loss of function mutations in kindlin 1 has been shown to lead to Kindler syndrome. Patients with this disease suffer from skin blistering, increases photosensitivity, early onset periodontal disease, gingivitis, progressive poikiloderma, gastrointenstinal problems, skin atrophy and squamous cell carcinoma (Ashton, 2004; Lai-Cheong et al., 2010). In *C. elegans* the homologue is known as UNC-112 and when a loss of function mutation was introduced resulting worms were paralysed and died (Siegel et al., 2003). In mice, Kindlin 1 knock-out animals developed skin atrophy and intestinal epithelial dysfuntion that resulted in their death (Ussar et al., 2008). In both cases an adhesion defect was shown to be one of the molecular causes of these phenotypes. Recently, a loss a kindlin 1 in the epidermis and at hair follicles of mice resulted in Kindler's syndrome like symptoms including, skin pigment changes similar to poikiloderma and skin blistering at the dermal-epidermal junction which was found to be a result of a lack of kindlin 1-β1 integrin binding (Rognoni et al., 2014). Kindlin 1 was also shown to control cutaneous epithelial stem cell homeostasis through controlling TGF-β and Wnt-β-catenin signaling pathways (Rognoni et al., 2014). The release of TGF-β, which suppresses stem cell proliferation, was shown to be triggered through activation of αVβ6 integrin by kindlin 1. Kindlin 1 knockout specifically in keratinocytes or treatment with αVβ6 blocking antibody resulted in cells being unable to release TGF-β. Importantly, kindlin 2 could not compensate for a loss of kindlin 1 in this pathway. This is because kindlin 2 is unable to bind to β6

integrin (Rognoni et al., 2014). Additionally, due to the reported roles of TGF-β and Wnt signaling in cancer, the kindlin 1 keratinocyte knockout mice were treated with carcinogenic drugs and it was found that a loss of kindlin 1 resulted in an increased susceptibility of skin tumour development further exemplifying the importance of kindlin 1 in disease (Rognoni et al., 2014).

Kindlin 2 is ubiquitously expressed and knock-out of kindlin-2 results in inhibited β1 integrin activation and is lethal in mice where it causes a detachment of cells form the basement membrane (Montanez et al., 2008). Kindlin 2 was found to be the only kindlin expressed in cardiac tissue and kindlin 2 knockdown in both zebrafish and mice were found to lead to failures in heart development due to a failure of intercalated disc formation and failure of attachment of myofibrils (Dowling et al., 2008). Kindlin 2 defects are not currently known to be involved directly with any congenital diseases. Kindlin 3 expression is limited to hematopoeitc cells and has more recently been shown to be expressed in endothelial cells where it is important for adhesion and tube formation (Ussar et al., 2006; Calderwood et al., 2013; Bialkowska et al., 2010). Kindlin 3 knockout mice survive gestation but die within a week after birth after suffering with osteopetrosis and hemorrhages in their skin, bladder, brain and gastrointestinal tract due to severe platelet dysfunction (Moser et al., 2008). Additionally, loss of kindlin 3 resulted in platelet spreading defects and a lack of β1 or β3 integrin activation (Moser et al., 2008). Leukocyte

adhesion deficiency type III (LAD-III) syndrome is a hereditary disease that results in severe bleeding and frequent infections, the cause of this disease was found to be due to mutations in the gene encoding kindlin 3 (Mory et al., 2008; Svensson et al., 2009). The result of these mutations is a failure to activate β1, β2, or β3 integrins in blood cells thereby impairing platelet activation and leukocyte adhesion resulting in bleeding (Malinin et al., 2009). Recently it was discovered that, like talin, calpain can cleave kindlin 3 in platelets and leukocytes (but not Kindlin 1 or kindlin 2) and this cleavage favours cell migration but reduces cell adhesion (Zhao et al., 2012).

Structurally the kindlin proteins are similar to each other and to the talin head domain, each consisting of a FERM domain interrupted by a pleckstrin homology (PH) domain. Kindlins have an F0 domain followed by an F1 and F2 domain, the FERM domain is interrupted within the F2 domain by the PH domain before the remaining FERM subdomain (Meves et al., 2009). The F1 domain is interrupted by an unstructured F1 loop which was shown to be important for membrane targeting and integrin activation (Bouaouina et al., 2012). Complete solved structures for kindlin 1 and kindlin 2 are not currently available however the structure of kindlin 3 was found to adopt a linear rather than globular structure similar to the talin head domain (Yates et al., 2012).

1.8 Integrin binding proteins and control of receptor activation

Kindlins have been shown to bind to integrin β subunit cytoplasmic tails at the membrane distal NPXY motif via their F3 domain and point mutations in this domain, or near the NPXY motif, inhibit the interaction of kindlins with integrins (Harburger et al., 2009; Bledzka et al., 2012). The sequence in between the first and second NPXY motif in the integrin β subunit tail was found to dispensable for talin binding, but indispensible for kindlin binding (Moser, Legate, et al., 2009). Within kindlin there are three regions shown to be important for lipid binding and activation of integrins. The F0 domain in kindlin 2 has been shown to contain an ubiquitin fold with a positively charged surface which would allow for binding to negatively charged phospholipids in the membrane, such as PI(4,5)P2, and disruption of this binding resulted in reduced integrin activation (Perera et al., 2011). Secondly, the PH domain of kindlin 2 was found to contain a distinct binding pocket that was shown to be able to bind to PIP3, and defects in this region prevented kindlin 2 induced activation of integrins (J. Liu et al., 2011). Kindlin 2 binding to PIP3 was also found to induce a conformational change in the PH domain of kindlin which was thought to anchor kindlin 2 to the plasma membrane in order to facilitate integrin binding and activation (Y. Liu et al., 2012). The PH domain in kindlin 1 was found to have an isoform specific salt bridge across the pocket where phospholipids were thought to bind (Yates et al., 2012). Modeling data suggested that the kindlin 1 PH domain was able to switch between open

and closed pocket formation transiently (Yates et al., 2012). Additionally, the kindlin 1 PH domain was found to have high affinity for the phospholipid PI(3,4)P2 (Yates et al., 2012). Finally, the kindlin 1 F1 domain contains a conserved unstructured F1 loop that was shown to be important for the activation of kindlin 1 and kindlin 2 of αIIbβ3 but not for binding to the integrin tails, and this loop was shown to bind to acidic membrane phospholipids (Goult et al., 2010; Bouaouina et al., 2012).

Talin has been shown to be sufficient to activate integrins directly through binding to the integrin β subunit cytoplasmic tail of αIIbβ3 in an in vitro system and that this leads to integrin extension (Ye et al., 2010). Kindlins too have been shown to be important to bind to integrins and in some cases are essential for integrin activation. However, over-expression of kindlin alone has been shown to inhibit integrin activation but co-expression of both talin head domain and kindlin was shown to increase integrin activation suggesting that kindlin may mediate talin binding to and activation of integrins rather than activating integrins directly (Montanez et al., 2008; Ma et al., 2008; Harburger et al., 2009; Moser, Bauer, et al., 2009). It has been shown that integrin β tails, talin head domain and kindlin can form a complex and that the formation of this complex may be required for integrin activation in cells (Bledzka et al., 2012). Kindlin may also act to recruit other proteins or to displace inhibitors of integrin activation from the integrin β subunit cytoplasmic tail. Kindlin has been shown to be able to bind to migfilin and recruit it to integrins, and migfilin in

turn has been shown to be able to act as a molecular switch in integrin activation by displacing filamin from integrins (Tu et al., 2003; Ithychanda et al., 2009).

Filamin has been shown to bind to integrin β subunit cytoplasmic tails in a region overlapping with the membrane proximal NPXY motif that is required for talin binding and activating of integrins (Kiema et al., 2006). Therefore, kindlin may bind to or near to integrins and recruit migfilin, which displaces filamin and allows for the recruitment of talin to integrins. ICAP1 is another known inhibitor of integrin activation that can bind to integrins overlapping with the kindlin binding site such that kindlin binding or KRIT1 binding to ICAP1 may displace ICAP1 from integrin tails, removing its inhibition of activation (W. Liu et al., 2013). Additionally, phosphorylation sites have been found at the tyrosines of both membrane proximal and membrane distal NPXY motifs in integrin β subunit cytoplasmic tails and when phosphorylated by Src family kinases (SFKs) they prevent talin and kindlin binding, but enhance binding of integrin inhibitor DOK1 (Bledzka et al., 2010; Oxley et al., 2008; Anthis, Haling, et al., 2009).

SHARPIN is another known inhibitor of integrin activation that binds to the integrin α subunit and inhibits recruitment of talin and kindlin to integrins, and was shown to be able to inhibit β1 integrin function and upon re-expression cells were seen to have increased β1 integrin activity (Rantala

et al., 2011). Interestingly, data has shown that kindlin increases integrin activation and binding through clustering of integrins, rather than directly through activation, opening up another facet to the increasingly complex dynamics of integrin activation by talin and kindlin (Ye et al., 2013).

1.9 Other focal adhesion proteins

Adhesions are large macromolecular complexes that are formed of many proteins that each play different parts in order to facilitate extracellular linkage via integrins, connection to the actin cytoskeleton, signal transduction, mechanosensing and adhesion turnover. Two of the most well studied adhesion proteins are paxillin and focal adhesion kinase (FAK). FAK is a non-receptor tyrosine kinase that is recruited to clustered integrins and forms a complex with Paxillin (Schaller and J. T. Parsons, 1995; Choi et al., 2011). A 3D nanoscale fluorescent microscopy study has grouped FAK, paxillin, talin head domain and integrin cytoplasmic tails to the same membrane proximal region forming a signaling layer at adhesions (Kanchanawong et al., 2010). Recently however, data has emerged that has suggested that FAK may recruit talin to early adhesions as in FAK-null cells on fibronectin, talin was not seen at nascent adhesions but was seen at mature focal adhesion after 60 mins with paxillin recruitment being unaffected (Lawson et al., 2012). FAK has been hypothesised to be able to be recruited to nascent adhesions via its FERM

domain, although expression of the FERM domain alone was not seen to be able to be recruited to adhesions; It is instead now thought that the FERM domain of FAK functions to recruit the actin nucleating complex Arp2/3 (Serrels et al., 2007; Lawson and Schlaepfer, 2012). Additionally, FAK has been implicated in contributing to PI(4,5)P2 production at adhesions via phosphorylation of PIPKIγ, and since talin has been shown to bind to PI(4,5)P2 and to PIPKIγ (Ling et al., 2002) which may contribute to the FAK-dependent recruitment of talin to nascent adhesions . The conventional model is that FAK binds to paxillin and talin at adhesions via the FAT domain and upon binding it can recruit Arp2/3 or become activated by integrin clustering or by binding of other proteins leading to recruitment of Src and phosphorylation of regulators of small GTPases Rap1, Rac and RhoA which are important in cell migration control and cytoskeleton organization (Cai et al., 2008) . The FAK-Src complex is also known to be able to phosphorylate paxillin thereby recruiting Cdc42 and β-PIX (Klooster et al., 2006).

Paxillin is a 68 kDa LIM-domain containing protein which is what anchors paxillin to the adhesions where it exists as a molecular scaffold protein that is recruited early in adhesion formation (Deakin and Turner, 2008). Paxillin has been shown to associate with both β1 and β3 integrins and to play a role in stimulating microtubule catastrophes at focal adhesions (Cantor et al., 2008; Efimov et al., 2008; Deakin and Turner, 2008). Paxillin has also been indicated to be involved with adhesion turnover and cell migration

(Sero et al., 2012; Quizi et al., 2012). Paxillin and FAK have both been shown to form tetramers in nascent adhesions, and when paxillin is phosphorylated, the complexes of paxillin and FAK get larger with increased turnover indicating a role for paxillin and FAK in nascent adhesion formation and maturation (Choi et al., 2011).

Vinculin is another well studied protein that is recruited early to forming adhesions and can bind directly to F-actin and other focal adhesion proteins (Geiger et al., 2001). Talin contains several vinculin binding sites (VBS) within its rod domain and when talin is stretched by actomyosin tension on one side, and integrin-ECM interactions on the other, these cryptic VBS are revealed and able to recruit vinculin (Yao et al., 2014). The binding of vinculin to talin is shown to stabilise talin in an elongated conformation (Yao et al., 2014). Talin is able to activate vinculin through this stretching and paxillin could contribute to this activation (del Rio et al., 2009; Pasapera et al., 2010). Vinculin also binds to actin and is part of a force transduction layer of the focal adhesion along with talin that links the signaling layer at the membrane to the actin cytoskeleton directly (Kanchanawong et al., 2010). Additionally, vinculin has been shown to be important for the recruitment and stabilization of many other core focal adhesion components including FAK, p130Cas, Arp2/3, paxillin, zyxin, ILK and parvin and is critical to prevent disassembly of the focal adhesion (Carisey et al., 2013).

The composition of proteins at focal adhesions in cells within 3D matrix cultures and also *in vivo* have been seen to be different than when cells are studied in conventional 2D cultures. 3D adhesions were characterized following the discovery that fibroblasts in 3D matrix had unsual adhesions with high amounts of α5 integrin and paxillin parallel to fibronectin fibers (Cukierman, 2001). Adhesions in cells within 3D CDM were found to be longer, but not wider, than adhesions on a flattened 2D CDM substrate, indicating that the dimensionality of the matrix is important in determining the size and shape of 3D adhesions (Hakkinen et al., 2011). In early studies paxillin, phospho-paxillin, vinculin and FAK could be seen colocalised with 3D adhesions (Cukierman et al., 2001; 2002). However, phospho-FAK was found to be absent from these 3D adhesions and were not seen to colocalise with α5 integrin, and in later work it was found that phospho-FAK is present at 3D adhesions, but phosphorylation levels are low indicating differences in signaling events between adhesions in 2D and 3D (Yamada et al., 2003; Cukierman et al., 2001). In MDA-MB 231 breast cancer cells, paxillin was found to be important in regulating adhesion assembly and disassembly times but only of 3D adhesions and not of adhesions on 2D substrates; additionally paxillin was found to be required for persistent migration in 3D CDM (Deakin and Turner, 2011). The exact composition and dynamics of proteins at adhesions in 3D matrices is still not fully detailed. This may be due to the technicalities of studying 3D adhesions as indicated in recent correspondences wherein it was made clear some of the technical requirements to visualize 3D

adhesions, such as expression levels of fluorescently labeled proteins (Fraley et al., 2010; Kubow and Horwitz, 2012). Additional complexity also comes from differences in the type of 3D model used to study adhesions as it has been shown that factors such as matrix stiffness and the structure of the substrate can alter the nature of adhesions in 3D (Harunaga and Yamada, 2011; Hakkinen et al., 2011; Jayo and M. Parsons, 2012).

1.10 Lipid Rafts and Phospholipids

The structure of the lipid bilayer has been known for decades but the complexities and fundamental roles they play in controlling cell signalling is only now being fully understood (Gorter and Grendel, 1925). The formation of the lipid bilayer is due to lipids containing a hydrophilic head domain and hydrophobic tails which interact and form a bilayer with the hydrophobic tails on the inside, allowing the head groups to interact with each other (Shevchenko and Simons, 2010). Lipid bilayers in eukaryotes contain a variety of lipids that are grouped into 3 categories; glycerol-phospholipids, sphingolipids and sterols, such as cholesterol (which occupies space between sphingolipids) (Simons and Sampaio, 2011). These lipids contain a high degree of heterogeneity, varying by head group, or length and saturation of fatty acid chains (Simons and Sampaio, 2011). Cholesterol is the predominant sterol in eukaryotic plasma

membranes and has been shown to increase the stiffness and thickness of the plasma membrane and allow for transmembrane protein sorting (Lundbæk et al., 2003; Roduit et al., 2008).

The ‘fluid mosaic’ model was used to describe how the plasma membrane functions by Singer and Nicolson, whereby the lipids and proteins in the plasma membrane randomly shuffle so as to adopt the lowest free energy state that their interactions would allow (Singer and Nicolson, 1972). This model was shown to be incorrect in that the organisation of some plasma membrane components was not random. The concept of lipid rafts were then described to initially explain regions of the apical membrane of epithelial cells that were rich in glycophospholipids (Simons and van Meer, 1988). This later became a general principle of how membranes sub-compartmentalise. In 1997, Simons and Ikonen suggested the existence of lipid rafts, which were then described as the partitioning of an area of the membrane by a presence of a high amount of sphingolipids, phospholipids and cholesterol (also called liquid ordered phase) with tight packing of lipids that can move within the membrane and serve as a platform for protein recruitment (Simons and Ikonen, 1997)). They postulated that proteins exhibited a preference for partitioning within either an ordered or disordered phase, and hence they would then be included or excluded from lipid rafts. These lipid rafts, it was suggested, would then serve as sites of signal transduction with increased rates of protein-protein interactions given to the increase in spatial constriction.

It was shown that adhesions are regions of high membrane order; that is they have high concentrations of sphingolipids, proteins and cholesterol (Gaus et al., 2006). More recently it has been shown that lipid rafts can cluster. This clustering is dependent upon cholesterol, upon actin tethering to lipid rafts and acto-myosin activity (Goswami et al., 2008). Actin filaments are also required for the lateral movement of GPI-anchored proteins which was shown to be dependent upon myosin activity (Gowrishankar et al., 2012). These data show that the regulation of lipid rafts is an active process that is dependent upon actin, myosin, cholesterol and membrane anchored proteins.

Adhesions are known sites of actin nucleation and polymerisation, as discussed earlier, additionally several key adhesion molecules have been shown to be able to bind to, and be activated by specific phospholipids which themselves are known to partition into lipid rafts, therefore the role of specific phospholipids in modifying which proteins are recruited to lipid rafts is crucial to the understanding of adhesion biology (Simons and Sampaio, 2011).

Phosphotidylinositol composes ~10% of the total lipid amount in most cells, and constitute a diverse group of lipids that are formed of a D-myo-inositol-1-phosphate linked to diacylglycerol (Saarikangas et al., 2010). Phosphotidylinositol can be phosphorylated reversibly at three different

positions in the inositol ring, giving rise to seven different species of phosphoinositide that can interchange between species through phosphotidyinositol phosphatases and kinases (Saarikangas et al., 2010; Erneux et al., 2011). PI(4,5)P2 is the most abundant phospholipid in blood cells, hepatocytes and lymphocytes with a high concentration to be found in most mammalian cells (McLaughlin et al., 2002; Hagelberg and Allan, 1990; J E Ferrell and Huestis, 1984). Several adhesion proteins have been shown to be able to bind PI(4,5)P2 or require its production including talin, vinculin, FAK, the kindlin F0 domain and potentially the F1 loop region of kindlin (Legate et al., 2011; Cai et al., 2008; Bouaouina et al., 2012; Perera et al., 2011). Indeed, focal adhesions have been found to have a high level of PI(4,5)P2 which is thought to play a key role in facilitating protein recruitment and lipid raft formation (Ling et al., 2002) . PI(4,5)P2 can be phosphorylated at the 5 position of the inositol ring by Class I PI3-kinase to become PI(3,4,5)P3 or PIP3. PIP3 is a critical recruiter of key enzymes which are involved with controlling cell growth, survival and division (Wong et al., 2010). PIP3 has also been implicated in playing a key role in adhesion biology after PIP3 was shown to be able to bind to ILK and to the PH domain in kindlins (Pasquali et al., 2007; J. Liu et al., 2011). PIP3 can be dephosphorylated into PI(4,5)P2 by PTEN or into PI(3,4)P2 by SHIP2 (Leslie et al., 2008; Mondal et al., 2012). PI(3,4)P2 was found to directly regulate Akt and has been shown to be important for recruitment of the Ena/VASP protein lamellipodin (Bae et al., 2010; Franke et al., 1997). Additionally, the actin-associated protein profilin has been

shown to regulate levels of PI(3,4)P2 and thereby lamellipodin and migration (Bae et al., 2010).

In summary, data has shown that many adhesion proteins have interactions with phospholipids that are crucial to their function in adhesions and migration, however, the interplay of phospholipids, adhesion proteins and integrins has not been well studied in the context of a dynamic pool of interchanging phospholipid species.

1.11 Hypothesis and aims

Hypothesis:

The hypothesis of this thesis is that talin and kindlins act in concert to differentially activate β1 and β3 integrins in migrating fibroblasts on 2D and within 3D matrices and that phospholipids directly regulate these adhesion dynamics.

Aims:

- To define the spatial segregation of integrin activators within fibroblasts on 2D and in 3D matrices with relation to specific integrins.
- To analyse the relative contribution of talin, kindlin 1 and kindlin 2 to integrin activation and fibroblast migration on 2D and in 3D matrices.
- To determine which integrin activator arrives first to sites of forming adhesions in fibroblasts.
- To determine if kindlins contribute to the recruitment of talin to focal adhesions in fibroblasts.
- To analyse the effects of inhibiting phospholipid synthesis on talin, kindlin 1 and kindlin 2 recruitment, and integrin activation.
- To determine if there is a local change in levels of specific phospholipids before or after initiation of adhesion formation.

- To determine whether specific integrins influence the phospholipid composition of adhesion sites on 2D and in 3D matrices.
- To investigate the effects of integrin activation upon the levels of specific phospholipids at adhesion sites.
- To determine if inhibition or activation of integrins, or inhibition of phospholipid synthesis affects the binding between integrin activators and specific integrin β subunits.

2. Materials and Methods

2.1 Reagents

Table 2.1 Cell Culture Reagents

Reagent	Source
Dimethyl sulphoxide (DMSO)	Sigma Aldrich
Fetal Bovine Serum (FBS)	Sera Laboratories International Ltd.
L-Gltuamine	PAA
Penicillin/Streptomycin	Gibco
High Glucose Dulbecco's Modified Eagle's Media	Sigma Aldrich
Trypsin/EDTA	PAA
Optimem	Gibco
Lipofectamine 2000	Invitrogen
Fugene HD	Promega
Interferon-γ	Invitrogen
Polybrene (hexadimethrine bromide)	Sigma Aldrich
Phosphate Buffered Saline (PBS)	Lonza
G418	PAA
Newborn Calf Serum (NBCS)	PAA
Puromycin	Sigma Aldrich
Di-4-ANEPPDHQ	Molecular Probes/Invitrogen
Gluteraldehyde	Alfa Aesar
Ascorbic acid	Sigma Aldrich
Gelatin	Sigma Aldrich
Fibronectin	Milipore
Ammonium hydroxide	Sigma Aldrich

Table 2.2 Molecular Biology Reagents

Reagent	Source
Agarose	Sigma Aldrich
Ampicillin	Sigma Aldrich
Bovine Serum Albumin (BSA)	New England Biolabs
Kanamycin	Sigma Aldrich
Midiprep Kit	Qiagen
Miniprep Kit	Qiagen
Safeview	NBS Biologicals
OneShot TOP10 Chemically Competent *E.coli*	Invitrogen
Luria Bertani Agar and Broth	Sigma Aldrich
Hyperladder I	Biolabs
Restriction Enzymes	New England Biolabs

Table 2.3 Biochemical Assay Reagents

Reagent	Source
1.5mm Cassettes	Invitrogen
2-mecaptoethanol	Sigma Aldrich
30% Acrylamide/Bis solution	Biorad
Ammonium persulphate (APS)	Sigma Aldrich
Bromophenol Blue	Sigma Aldrich
Calyculin A	Sigma Aldrich
ECL Plus western blotting detection system	GE Healthcare
Floursave Mounting Media	Calbiochem
Glycine	Sigma Aldrich

Reagent	Source
Glycerol	VWR International
Hybond ECL Nitrocellulose Membrane	Amersham Biosciences
Medical X-Ray Film	Fuji
Milk Powder	MERCK
Paraformaldehyde (PFA)	Sigma Aldrich
PeqGOLD Protein Marker V	PeqLab
Pierce BCA Protein Assay Kit	Thermo Scientific
PBS Tablets	Oxoid
Pierce ECL Western Blotting Substrate	Thermo Scientific
Ponceau S Solution	Sigma Aldrich
Protein A/G Beads 25% Slurry	Alpha Diagnostic International Ltd.
Sodium Chloride	Sigma Aldrich
Sodium Dodecyl Sulphate	Sigma Aldrich
Sodium Flouride	Sigma Aldrich
Tetramethylethylenediamine (TEMED)	Sigma Aldrich
Tris-Base	Sigma Aldrich
Tris-HCl	Sigma Aldrich
Triton X-100	Sigma Aldrich
Tween-20	Sigma Aldrich
Saponin	Scientific Laboratory Supplies (SLS)
Protease Inhibitor Cocktail set I (Stock 100x) containing: AEBSF, Hydrochloride - 500 µM Aprotinin, Bovine lung, crystalline – 150 nM E-64 Protease Inhibitor - 1 µM EDTA Disodium – 0.5 mM Leupeptin, Hemisulphate – 1 µM	Calbiochem

Table 2.4 Materials and solutions for biochemical assays

Buffer/Soltuion	Composition
5% Stacking Acrylamide Gel	30%-acrylamide mix, 125mM Tris-HCl (pH6.8), 0.1% Sodium dodecyl sulphate (SDS), 0.1% ammonium persulphate (APS), 1% TEMED
8% Stacking Acrylamide Gel	30%-acrylamide mix, 400 mM Tris (pH 8.8), 0.1% SDS, 0.1% APS, 0.05% TEMED
10% Stacking Acrylamide Gel	30%-acrylamide mix, 400 mM Tris (pH! 8.8), 0.1% SDS, 0.1% APS, 0.05% TEMED
RIPA Lysis Buffer	10 mM Tris, 150 mM NaCl, 1 mM EDTA, 1% Triton X-100, Protease inhibitor cocktail set 1
IP Lysis Buffer	50mM Tris Base, 150mM NaCl, 1mM EDTA, 50mM Sodium fluoride, 1% NP-40, 0.2%Triton X-100, Protease inhibitor cocktail set 1, 1µm Calyculin A, pH to 7.4
IP Wash Buffer	50mM Tris Base, 50mM NaCl, 1mM EDTA, 50mM Sodium fluoride, 0.2%Triton X-100, Protease inhibitor cocktail set 1, 1µm Calyculin A, pH to 7.4
Running Buffer (10x)	0.25 M Tris base, 1.92 M glycine, 1% SDS
Transfer Buffer (10x)	0.25 M Tris base, 1.86 M glycine, 10% methanol
PBS-Tween	10 tablets of Phosphate buffered saline dissolved in 1L water, 0.1% Tween-20
SDS Sample Buffer 2x	60mM Tris-HCl (pH 6.8), 25% Glycerol, 2.5% SDS, 0.02% Bromophenol blue, 2% β-mercaptoethanol
SDS Sample Buffer 5x	250 mM Tris-HCl (pH6.8), 10% SDS, 30% Glycerol, 0.02% Bromophenol blue, 5% β-mercaptoethanol

2.2 Antibodies

Table 2.5 Antibodies

Reagent	Species	Dilution	Source
Anti-Kindlin 1	Mouse	1:1000 (WB) 1:300 (IF)	Millipore
Anti-Kindlin 2	Mouse	1:1000 (WB) 1:300 (IF)	OriGene
Anti-Talin	Mouse	1:1000 (WB) 1:500 (IF)	Invitrogen
Anti-Paxillin	Mouse	1:400 (IF)	BD Biosystems
Anti-Phosphotyrosine	Mouse	1:600 (IF)	Sigma Aldrich
Anti-Paxillin	Rabbit	1:400 (IF)	Novus Biologicals
Anti-PI-3,4-P2	Mouse	1:100 (IF)	Medical and Biological Laboratories Co., LTD.
Anti-PI-4,5-P2	Mouse	1:100 (IF)	Echelon Biosciences Inc
Anti-PI-3,4,5-P2	Mouse	1:100 (IF)	Medical and Biological Laboratories Co., LTD.
Anti-Fibronectin	Mouse	1:400 (IF)	Abcam
Anti-Collagen	Mouse	1:400 (IF)	Invitrogen
Anti-GAPDH	Mouse	1:5000 (WB)	Chemicom
Anti-B1 integrin	Rabbit	10ug (IP)	Milipore
Anti-B3 integrin	Mouse	10ug (IP)	Emfret
9EG7	Rat	1:300 (IF)	BD Pharmagen
Phalloidin 633		1:200 (IF)	Invitrogen
Phalloidin 568		1:200 (IF)	Invitrogen
Anti-Mouse HRP	Goat	1:1000-10,000 (WB)	Dako
Anti-Rabbit HRP	Goat	1:1000-2000 (WB)	Dako
IgG Negative Control	Rabbit	10ug (IP)	Dako
Anti-mouse Alexaflour 488	Goat	1:200-1:400	Molecular Probes

Reagent	Species	Dilution	Source
Anti-mouse Alexaflour 568	Goat	1:200-1:400	Molecular Probes
Anti-rabbit Alexaflour 488	Goat	1:200-1:400	Molecular Probes
Anti-rabbit Alexaflour 568	Goat	1:200-1:400	Molecular Probes
Anti-Rat FITC	Goat	1:200-1:400	Sigma Aldrich

2.3 Methods

2.3.1 Molecular Biology and Cloning

2.3.1.1 Generation of shRNA lentiviral knockdown plasmids

Unvalidated shRNA plasmids in a pLK.0 backbone were purchased from OpenBiosystems and their targeting sequences are detailed in table 2.6.

Table 2.6 shRNA lentiviral constructs.

Clone/Clone ID	Target	Sequence (sense, loop, antisense)
K1-1/TRCN0000173934	Kindlin 1	CCGGGATGAGGACCTCTTCCACAAACTCGAGTTTGTGGAAGAGGTCCTCATCTTTTTTG
K1-2/ TRCN0000173772	Kindlin 1	CCGGCAGAGGTCATCAGCATCCTTTCTCGAGAAAGGATGCTGATGACCTCTGTTTTTTG

Clone/Clone ID	Target	Sequence (sense, loop, antisense)
K1-3/ TRCN0000173840	Kindlin 1	CCGGCCATGAGTACATTGGTGGCTACTCG AGTAGCCACCAATGTACTCATGGTTTTTTG
K1-4/ TRCN0000176070	Kindlin 1	CCGGGTGGAGATTCGCCAATATGAACTCG AGTTCATATTGGCGAATCTCCACTTTTTTG
K1-5/ TRCN0000175332	Kindlin 1	CCGGCACCTACTACCTTGTCAGATTCTCG AGAATCTGACAAGGTAGTAGGTGTTTTTT G
K2-1/ TRCN0000191858	Kindlin 2	CCGGGCCTTTGTGTTACAATATGAACTCG AGTTCATATTGTAACACAAAGGCTTTTTTG
K2-2/ TRCN0000191859	Kindlin 2	CCGGGATGAGGAGATGTTCTACAAACTCG AGTTTGTAGAACATCTCCTCATCTTTTTTG
K2-3/ TRCN0000190504	Kindlin 2	CCGGGCCTACCTTGATATGCCGTATCTCG AG ATACGGCATATCAAGGTAGGCTTTTTTG
K2-4/ TRCN0000200833	Kindlin 2	CCGGGAAGTATAAGAGCAAACAGATCTCG AGATCTGTTTGCTCTTATACTTCTTTTTTG
T1/ TRCN0000108756	Talin1	CCGGGCCCATTGTAATCTCTGCTAACTCG AGTTAGCAGAGATTACAATGGGCTTTTTG
T2/ TRCN0000108757	Talin1	CCGGGCCACCAACAATCTGTGTGAACTCG AGTTCACACAGATTGTTGGTGGCTTTTTG
T3/ TRCN0000108755	Talin1	CCGGCGCTCCAAGAGTATTATTAATCTCG AGATTAATAATACTCTTGGAGCGTTTTTG

2.3.1.2 Bacterial Transformation

Transformations were performed as per Invitrogen's One Shot Top 10 protocol. Briefly, a vial containing One Shot Top10 *E.coli* was allowed to thaw on ice before 25µl of bacteria were pipetted into a sterilised eppendorf tube on ice. 1-2.5µl of plasmid DNA was added to the bacteria and was incubated on ice for 30mins to ensure equal distribution of plasmid in the bacterial suspension. The bacteria were then heat-shocked

at 42°c for 45 seconds before being placed immediately back on ice for 2 mins. 200µl of S.O.C. media was added to the bacteria and incubated in a shaking incubator for 45 mins at 37°c. The bacterial suspension was then pipetted onto LB agar plates containing the appropriate antibiotic and spread evenly before being incubated inverted overnight at 37°c.

2.3.1.3 Midiprep

A single colony of *E.coli* was selected from bacterial growth observed on LB agar plates and incubated in 50-100ml of LB media containing the appropriate antibiotic overnight at 37°c in a shaking incubator. 50ml of this bacteria containing media was centrifuged at 13,000 RPM for 30 mins at 4°c and the supernatant discarded. The pellet was then resuspended in 4ml of Buffer P1 from the QIAGEN Plasmid Plus Midi Kit. 4ml of Buffer P2 was then added to the bacterial suspension and inverted 4-6 times before being incubated at room temperature for 3 mins, as the LyseBlue reagent was added to Buffer P1 the bacterial suspension turned blue to indicate cell lysis. 4ml of Buffer S3 was added to the bacterial lysate and inverted 4-6 times gently until the lysates went colourless. Buffer S3 rapidly neutralises the pH of the solution, ending lysis, and forms a white precipitate made up of genomic DNA, SDS and cell debris. The bacterial lysate was then transferred to a QIAfilter cartridge and incubated at room temperature for 10mins. After this time a plunger was inserted into the cartridge and the filtered solution was collected, to which 2ml of Buffer BB

was added. This solution was then inverted 4-6 times before being transferred to a QIAGEN Plasmid Plus Midi spin column which had already been inserted into a QIAvac 24 Plus. A vacuum pressure was then exerted to draw the solution through the column. The DNA in the column filter was then washed with 0.7ml of Buffer ETR and buffer PE. The column was then transferred to a tabletop micro centrifuge and centrifuged for 1min at 9,700 RPM to removal any residual wash buffer. The column was then placed into a clean 1.5ml eppendorf tube and 200µl of Buffer EB, pre warmed to 37^{o}c, was added directly to the column filter and incubated for 5 mins. The column was then centrifuged for 1 min and the resulting DNA collected in the tube was assessed for its concentration and quality using a Nanodrop Spectrophotometer.

2.3.2 Cell Culture

2.3.2.1 Cell Lines

β1-GFP or β3-GFP mouse embryo fibroblasts (MEFs) (Parsons et al., 2008; Worth et al., 2010) were grown in Dulbecco's modified Eagle's media (DMEM) containing 10% heat-inactivated fetal bovine serum (FBS), 1% Penicillin/streptomycin, 1% Glutamine, 2 µg/ml G418 and 2.36 µg/ml interferon-γ. Both β1-GFP and β3-GFP MEF cells were maintained at

33°C in a water saturated incubator with an atmosphere containing 5% CO_2.

NIH3T3 fibroblasts (ATCC) were maintained in DMEM containing 10% heat- inactivated New Born Calf Serum (NBCS), 1% penicillin/streptomycin and 1% glutamine. Primary cultured human dermal fibroblasts (HDFs) (TCS Cellworks) were grown in DMEM plus 10% heat-denatured NBCS. 293T cells (ATCC) were grown in DMEM containing 10% FBS, 1% Penicillin/streptomycin and 1% Glutamine. Both HDFs, 293T and NIH3T3 cells were maintained at 37°C in a water saturated incubator with an atmosphere containing 5% CO_2.

To passage all cell lines, cells were washed twice with PBS (without calcium or magnesium) once 80% confluent and trypsinised (trypsin in EDTA, 0.05% concentration). Once detached, cells were centrifuged at 1200RPM for 3 minutes and resuspended in an appropriate amount of media and plated into T-75cm^2 sterilised tissue culture flasks. To thaw frozen cell stocks, a cryovial of frozen cells was removed from liquid nitrogen storage and allowed to thaw briefly before addition to a 25 cm^2 tissue culture flask containing 5 ml media and incubated overnight at 33°c (MEF) or 37 °c (HDF, 293T, NIH3T3). 24 hours later the media was changed to remove any residual dimethyl sulfoxide (DMSO). To freeze cells, trypsinised cells (from a 75 cm^2 tissue culture flask) were added to 2 ml normal growth media and centrifuged at 1200RPM for 3 minutes.

Growth media was removed from the pellet and cells were re-suspended in 2 ml of freezing media (normal media plus an extra 10% serum and 10% DMSO) and split into 2 1ml cryovials. Cryovials were frozen at -80^{0}c overnight and then transferred to liquid nitrogen.

2.3.2.2 Generation of lentivirus from 293T cells

In order to produce lentiviral particles, two helper plasmids must be used in combination with a lentiviral vector encoding the desired shRNA. One of these lentiviral constructs is the packaging plasmid pΔ8.91 (Addgene) and the other is the envelope/coat plasmid pMD2.G (Addgene). 8µg of DNA in total, 4µg total of pMD2.G and pΔ8.91 lentiviral plasmids, 4µg of desired plasmid (see Table 2.6), were added to 240µl of Optimem. Lipofectamine was diluted in a separate eppendorf tube 20µl of Lipofectamine in 240µl of Optimem. The lipofectamine mix was then added to the DNA mix and this was left for 20 minutes. 293T cells were grown to 50% confluence in a T-75cm^2 flask and were washed with PBS before 5ml of pre-warmed Optimem was added and then the transfection mix was added. 293T cells were incubated for 5 hours in the transfection mix before the Optimem was removed and replaced with complete media. 24 hours later the media was replaced with fresh complete media and left for 2 days to produce virus. The virus containing media was then collected and any detached cells/debris was removed by centrifugation and filtration through a 0.45µm filter.

2.3.2.3 Lentivirus infection of fibroblasts

Fibroblasts were grown to 50% confluence in a T-25cm^2 flask before the media was replaced with 2ml of complete media and 2-3ml of virus containing media warmed to 33^{o}c. Cells were left for 2 days for infection and expression of the plasmids to occur. Selection by puromycin resistance at 2 µg/ml was then conducted for 2 days before lysing the cells and performing a western blot to assess knockdown efficiency.

2.3.2.4 Transient transfection of fibroblasts

Fibroblasts were grown to 50% confluence in a 6-well tissue culture plate. 1-2 µg of the desired DNA was diluted in 120µl of Optimem. Lipofectamine 2000 was diluted in Optimem at a ratio of 1:2.5 of DNA to Lipofectamine. The diluted Lipofectamine was then added to the diluted DNA and mixed by flicking and incubated at room temperature for 20-30mins. The cells to be transfected were washed twice with Optimem. The DNA/Lipofectamine solution was then added drop wise to the well containing fibroblasts and 1ml of Optimem. This was then swirled before being incubated at 37^{o}c for 4 hours. After this time the Optimem was aspirated, and the cells were washed twice in complete media before being incubated for 48 hours to allow for expression of the construct.

2.3.2.5 Treatment of fibroblasts with Di-4-ANEPPDHQ

Di-4-ANEPPDHQ was diluted to a final concentration of 5µM in Optimem which was then added directly to fibroblasts in Optimem that were to be imaged. The cells were incubated with the dye for 30 mins at 37^{o}c before the dye was aspirated and the cells washed once in Optimem. Imaging media was then added to the cells which contained 10% serum and HEPES buffer in Optimem.

2.3.2.6 Cell derived matrix generation

Primary cultured human dermal fibroblasts (HDFs) were plated at 80-90% confluence onto gelatin coated, glutaraldehyde cross-linked coverslips. These were grown for 10-14 days in complete media with 35 µg/ml Ascorbic acid and 5 µg/ml fibronectin with the media being replaced every 24 hours. Cells were denudated by incubation with 20 mM NH4OH and 0.5% Triton X- 100 PBS, and then incubation with DNaseI to remove any DNA. Matrices were blocked with 0.1% heat-denatured BSA before seeding of cells. CDM thickness was sufficient for plated cells to be fully embedded within it as confirmed by confocal microscopy and this was checked multiple times for each preparation.

2.3.3 Biochemical analysis

2.3.3.1 SDS-PAGE analysis

Sodium dodecyl sulphate-polyacrylamide gel electrophoresis (SDS-PAGE) was used to separate proteins based on their molecular weights. SDS loading buffer (2x or 5x) was added to the samples which broke down the proteins tertiary structure to a primary structure through denaturing. The SDS also induced a negative charge to proteins so that when an electrical charge was applied the protein would migrate towards the positive cathode pole. SDS-PAGE gels of 8%, 10% or 12 % were made in 1.5 mm cassettes with stacking gel on top and resolving gel beneath. Along with the samples, 10 µl of PeqGold Protein Marker V was run which includes molecular weight standards of known sizes. A constant voltage of 80 V was ran through the gel for 15 minutes, or until the samples entered into the gel. The voltage was then increased to 150 V for an hour or until the gel band-front had moved sufficient distance to allow for resolution of the proteins of interest.

2.3.3.2 Western Blotting

Cells were cultured and lysed in Radio Immuno Precipitation Assay (RIPA) buffer before being incubated on ice for 20 mins and centrifuged at 13,000

RPM for 10 mins to remove insoluble protein. The lysates were either used immediately or stored at - 20^{o}c. A Pierce BCA Protein Assay Kit was used to determine the concentration of the lysate samples, and this was then equalised through addition of additional RIPA buffer. Either 2x or 5x SDS sample buffer was then addd to the equalised lysates. Lysates were then boiled at 95^{o}c and centrifuged to clear insoluble protein before use. Total cell lysate samples were loaded onto SDS-PAGE gels in 1.5 mm cassettes and subjected to electrophoresis as described above.

Proteins were transferred onto nitrocellulose membranes using either Invitrogen XCell IITM transfer apparatus (35V for an hour) or Biorad Transfer Kit (100V for 1.5 hours) with fresh transfer buffer. Blots were then blocked immediately in 5% Milk/PBS for 60 minutes at room temperature. Membranes were then incubated with primary antibodies overnight at 4^{o}c or for 3 hours at room temperature at the specified concentrations. The blots were washed three times for 10 minutes each with PBS-Tween (0.1%) prior to incubation with horseradish peroxidase(HFP)-conjugated secondary antibodies for an hour at room temperature. Membranes were then washed a further three times and proteins were detected by ECL chemiluminescence kit, and exposed on Medical X-ray film and developed using a Xograph compact X4 developer or by using a Biorad developer. For reprobing, blots were stripped with Re-blot strong diluted in dH_2O for 10 minutes at room temperature and blocked in 5% milk/PBS again before incubation with antibodies. Western films were scanned into Photoshop CS2 or generated using the Biorad Image Lab software.

2.3.3.3 Immunoprecipitation

Cells were cultured until 50% confluent in 145 cm^2 tissue culture dishes. Any treatments were carried out in Optimem at 37^{o}c before cells were placed on ice and washed in cold PBS twice. Proteins were cross-linked on ice with cold dithiobis(succinimidylpropionate) (DSP) diluted to 0.5mM in PBS for 2 hours. Cells were then washed twice in cold PBS before the excess DSP was quenched by incubation with 50mM Tris HCl (and protease inhibitor) on ice for 30mins. Cells were washed once again twice in cold PBS before lysis in 2 ml IP lysis buffer. Cells were then scraped and the cell suspension was kept on ice for a further 20 mins to ensure efficient lysis, after which lysates were passed through a 26 gauge needle and centrifuged to pellet insoluble protein. The A/G agarose affinity matrix suspension was washed 3 times with IP lysis buffer prior to use. Lysates were pre-cleared with 50 µl washed A/G agarose affinity matrix bead suspension rotating at 4 ^{0}C for 45 mins, and 50 µl lysate was kept (1:1 IP buffer: sample buffer) prior to pre-clearing at -20 ^{0}c for use as an input sample. Pre-cleared lysates + A/G beads were centrifuged and the supernatants were collected. Each IP experiment had a duplicate of primary antibody and control IgG. 50ul washed protein A/G beads was incubated with 10µg of antibody for 2 hour at 4^{o}c tumbling end over end. The beads were pelleted and washed twice in IP lysis buffer before 600µl pre-cleared cell lysate was added to the beads+antibody and was

incubated tumbling at 4°c for two hours. After antibody, lysate and A/G agarose affinity matrix suspension incubation, the mixtures were centrifuged and the supernatant was removed and the A/G agarose affinity matrix suspension was washed three times for 10 mins in IP wash buffer. 45 µl of freshly prepared 2x sample buffer was added to each samples beads. Samples were either used immediately or stored at -20°c. Samples were boiled at 95 °c and centrifuged to pellet A/G beads. 40 µl of each sample was loaded in each well of 8% SDS-PAGE gels in 1.5 mm cassettes and subjected to SDS-PAGE, and then the Western blotting protocol was followed. Each IP was performed at least 3 times.

2.3.4 Microscopy

2.3.4.1 Immunofluorescence

13mm coverslips were acid washed and sterilised by autoclaving. Coverslips were then placed into appropriately sized wells in a tissue culture plate and coated with 10 µg/ml of fibronectin for an hour at 37°c or overnight at 4°c. Coverslips were then washed once in sterile PBS. Cells were then plated onto fibronectin or CDM coated coverslips and incubated overnight in normal growth media. Cells were washed in PBS and fixed in 4% PFA/PBS for 20 minutes at room temperature and then washed three times in PBS.

Cells were permeabilised with 0.2% Triton X- 100/PBS for 10 minutes and washed a further two times in PBS. For phospholipid staining, cells were instead permeabilised using 0.5% saponin in PBS. Cells were blocked in 3% BSA/PBS for 30 minutes and then incubated with primary antibody for at least 2 hours at room temperature in the dark. They were then washed three times with PBS and incubated with secondary fluorescent-conjugated antibody for at least 1 hour at room temperature in the dark. Cells were washed a further three times in PBS and if further staining was required, the protocol was repeated from the primary antibody step. If no more staining was required cells were washed once in distilled water and were mounted onto slides with Fluorsave^{TM}. Images of fixed cells were acquired on a confocal microscope with a 60x oil immersion objective.

2.3.4.2 Random migration assay

For the random migration assay, control or talin, kindlin 1 or kindlin 2 knockdown cells were seeded into 12 well plates coated with fibronectin or 8 well Ibidi chambers containing CDM. The cells were plated in complete media and left overnight to spread. The media was changed immediately prior to imaging to Optimem containing 10% serum and 25mM HEPES buffer pH 7.2-7.5 to help control for any pH changes. The cells were imaged with time-lapse microscopy performed on Zeiss Axiovert 100 microscope using an automated scanning stage. Images were acquired by

phase contrast imaging using a 10x N-Achroplan Phase contrast objective (numerical aperture 0.25). Images were acquired every 10 minutes for 10 hours using Andor iQ 1.5 software. Subsequently, all the acquired time-lapse sequences were tracked using the ImageJ Manual Tracking plugin and the nuclear position was used as the point of reference for tracking the cells. At least 60 cells were tracked for each sample as a sufficiently large enough pool from which to draw comparison. Tracking resulted in the generation of a sequence of position coordinates relating to each cell in each frame. Motion analysis was then performed on these sequences using Wolfram Mathematica 6 to quantify the speed and persistence of the cell tracks.

2.3.4.3 Confocal microscopy

Images of fixed cells were acquired on a Nikon A1R inverted confocal microscope (Nikon Instruments UK) with an environmental chamber maintained at 37^{o}c. Images were taken using a 60x Plan Fluor oil immersion objective with a numerical aperture of 1.4. Excitation wavelengths of 488nm (argon laser), 568nm (diode laser) or 633nm (diode laser) were used. Images were acquired using NIS Elements imaging software version 4.0 and were saved in the .nd2 or .tiff file formats for analysis purposes and for processing in ImageJ. For interference reflection microscopy (IRM), cells were imaged with the 488nm argon laser and the

reflection signal was recovered at 457-514nm, with the 488 fluorescent-conjugated secondary antibody or GFP emitting fluorescence at 520-560nm. Only single cells were imaged on both 2D fibronectin as well as CDM-based experiments, furthermore only cells fully embedded within CDM were imaged and used for analysis. Cells that were not embedded were visible by moving the area of focus in the Z-axis, additionally cells not embedded in CDM would adopt a flatter more spread out morphology than those embedded within CDM. For live imaging of cells incubated with the membrane order dye di-4-ANEPPDHQ, the dye was excited at 488nm (argon laser) shown as a blue line in Figure 2.3. Two separate emission spectra could then be detected. The first peak was at ~560nm which was for dye in the ordered phase (green line), with a second peak that could be detected at ~620nm which was for the dye in the disordered phase (red line) as shown in the emission spectra in Figure 2.3.

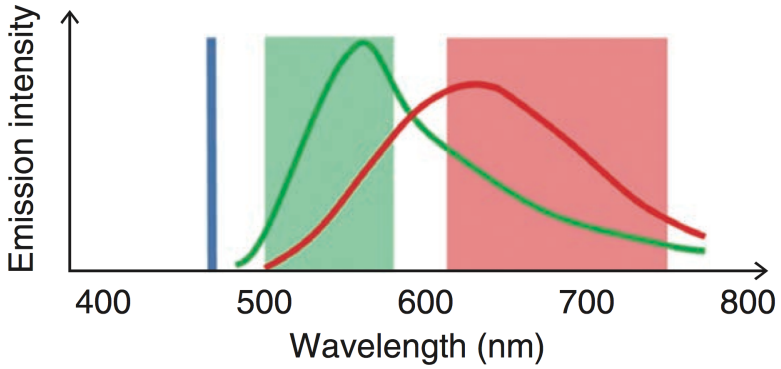

Figure 2.3. Emission and excitation spectra of Di-4-ANEPPDHQ.

Adapted from (Rentero et al., 2011)

2.3.4.4 Image analysis

Colocalisation analysis: Images were all taken at the same laser settings and objectives using Nikon Imaging Software Elements and the same Nikon A1R confocal microscope. The scale of the images was set in ImageJ (URL: http://rsbweb.nih.gov/ij/) using the scale bars saved into the image file. Images were split into three channels and the phalloidin stain was thresholded to generate the outline of the cell. The outline was selected and transferred onto the RGB version of the image and this was cropped to remove unwanted cells resulting in a single cell with all channels being present and saved as a new file. The image was then split into three separate channels again and the Pearson's coefficient between the green and red channels were generated using the ImageJ JACOP plugin (URL: http://imagej.nih.gov/ij/plugins/track/jacop.html). Images used for analysis were checked by eye to ensure that they did not contain artifacts that may skew the results, furthermore just the areas within the cells were used to minimize any distortion of the data. Images were acquired carefully so that only cells that were similar in shape and size were quantified. Similarly, efforts were taken to ensure the images used showed clear focal adhesion staining so as to ensure a fair comparison across all data sets and conditions.

2.3.4.5 Focal Adhesion Analysis

Quantification of focal adhesion size and number was performed in ImageJ by manual thresholding of the desired channel to the same value for each repeat or condition. The 'Analyze Particle' function was used and was limited by size to identify only particles between 0.5 and 3µm in area to capture the full focal adhesion population. This range was chosen as it is the sizes at which focal adhesions have been characterised to exist (Scales and Parsons, 2011). Furthermore, to ensure no false adhesions were detected each image was checked by eye to ensure each identified focal adhesion matched with a visible adhesion and was not an artifact. Focal adhesion number and size per cell were then pooled for each experiment and plotted in excel. Similarly, colocalisation

2.3.4.6 Analysis of Di-4-ANEPPDHQ membrane dye

Membrane order dye analysis: Analysis was performed as previously described in Owen *et al*, 2011. During image acquisition a calibration image was acquired by imaging the undiluted dye alone at laser powers 50% higher and 50% lower than the experimental acquisitions. The calibration image was used to determine the G-factor as per Owen *et al*, 2011; for studies presented in this thesis, the G-factor was 0.75. From the acquired images, separate channels were split into separate files, one for the ordered channel, one for the disordered channel. Images were then opened within the 'GP image analysis' ImageJ plugin and a threshold

value was used that was then consistent for all analysed images. A false-coloured HSB image was generated allowing for visualisation of differences in the membrane order, in addition to a separate greyscale image, which gave each pixel a value between 0-255. These values were then counted using the 'Analyze > Histogram' function in ImageJ. This was then copied into a Microsoft Excel spreadsheet. Alongside the raw data GP values of between -1 and +1 were calculated using the formula GP= DN/127.5-1 where DN was the 'digital number' ie. the grey value of the pixel. The data was normalised by dividing the pixel count for each value by the corresponding GP value, which then allowed for the GP histograms to be plotted with an x-axis from -1 to +1. The mean of these histograms was also used to allow for direct statistics and comparisons to be made between histograms.

2.3.4.7 Live cell focal adhesion analysis

Movies were separated into separate channels and a maximum intensity projection of the individual frames over time was produced in ImageJ for the GFP channel as the signal was strongest. The resulting image was thresholded and the resultant individual focal adhesions were allocated a number. Focal adhesions were excluded if they were below 0.5µm or above 3µm in size. The thresholded image acted as a mask allowing for the selection of the regions of interest. Adhesions that were observed

forming over the length of the recorded movie were selected for analysis. The individual focal adhesions were isolated and the integrated density for each frame was measured using the 'Measure' function within ImageJ. The integrated density at each point was normalised to the highest point of the trace and these normalized values were plotted on a line graph in excel to demonstrate the relative arrival of each protein over time.. The time to the peak of the intensity of each channel was measured from when the adhesion first started to form as seen from the IRM channel.

2.3.4.8 Statistical analysis

All statistical tests were performed using Students T-tests (Excel). Data are expressed as means ± s.e.m. Significance was taken as $p<0.001$, 0.005 and 0.05 and significance values were assigned in specific figures/experiments as shown.

3. Defining the spatial segregation of integrin activators in fibroblasts

Introduction

In order to understand the regulation of specific integrin β-subunits it was important to first characterise the colocalisation of these receptors with the integrin activators talin and kindlin. Talin is a well studied protein which is known to be able to activate integrin β-subunits via the inside-out mechanism of integrin activation (Calderwood et al., 1999).

Alongside talins, a more recently discovered family of proteins have also been shown to be able to activate integrin β-subunits via the inside-out mechanism, the kindlins. It is thought that talins and kindlins work together in concert to activate integrins through binding to the β-subunit cytosolic tails (Calderwood et al., 2013). However, it is not clear whether these proteins play specific or redundant roles in fibroblast migration and more specifically, integrin activation. Moreover, talin and kindlins are both able to bind to the cytoplasmic domains of β1 and β3 integrins but the potential preference for each receptor within the context of an intact fibroblast remains unclear (Harburger et al., 2009).

Traditionally, adhesion and migration has been studied in cells on a 2D substrate, typically coated glass or plastic. In order to provide a more physiologically relevant model for firbroblast migration and adhesion

formation, some of the experiments in this thesis have been performed using cell-derived matrix (CDM). CDM is a fibrillar extracellular matrix meshwork deposited by primary fibroblasts over a period of 10-14 days to provide a 3D ECM environment similar to that seen in the human dermis (Cukierman et al., 2001). Studies have shown that the composition, size and number of focal adhesions in cells in 3D substrates are different to those on 2D substrates. Mouse fibroblast cell lines were used that were knockout for endogenous integrins and engineered to re-express near-endogenous levels of GFP-tagged integrin β1 or β3. These cells show a similar phenotype to wild-type fibroblasts in terms of adhesion and migration and the integrins localise normally to adhesions (Worth and Parsons, 2010).

These cells were used in this thesis for two reasons: firstly the commercial reagents available for immunostaining mouse integrins are extremely poor, and secondly; the use of GFP-integrin cells offers the opportunity to perform live imaging analysis on receptor kinetics. High tyrosine phosphorylation is a known marker of focal adhesions due to the clustering of many tyrosine phosphorylated proteins during the formation and maintenance of adhesions and alongside paxillin are well studied adhesion markers.

The aim of the experiments in this chapter was to analyse the co-localisation of integrin activators and see how this may differ in cells in a

more physiologically relevant 3D CDM substrate. The relative contribution to integrin activation of either talin or kindlin proteins has not been well studied, particularly not in cells within a 3D matrix. This chapter aimed to address this as well as analysing the role of these proteins in 2D and CDM based fibroblast migration.

Results

3.1 Endogenous talin, kindlin 1 and kindlin 2 colocalise with integrin β1-GFP in fibroblasts on 2D fibronectin

Talin and kindlins have both been shown to be able to activate integrins via the 'inside-out' mechanism (Calderwood et al., 1999; Ma et al., 2008; Montanez et al., 2008). β1 and β3 integrin-positive adhesions have also been shown to occupy slightly different areas of the cell, with β3 integrin-positive adhesions localised more towards the leading edge of migratory cells and in smaller adhesions and β1-positive adhesion being found towards the middle and rear of the cell in larger types of adhesions. It was therefore important to first characterise the co-localisation between β1 or β3 integrin with talin and kindlin-1 or -2 to identify if there were biases towards preferential co-localisation between a particular integrin/integrin activator pair.

Mouse embryonic fibroblasts (MEFs) were isolated and cultured from integrin β1 or β3 KO mice, and the corresponding integrin tagged with GFP on the C-terminus was re-expressed stably, as previously published from our group (Parsons et al., 2008; Worth et al., 2010). For both cell lines, re-expression of the integrin has previously been shown to rescue functional defects in these cells and function as endogenous integrin (Worth et al., 2010). β1-GFP MEFs were plated onto glass coverslips

coated with fibronectin before being fixed, and stained for endogenous talin, kindlin 1 or kindlin 2. Staining for endogenous phosphotyrosine or paxillin acted as general markers to determine co-localisation of integrins with all focal adhesions. Images were acquired by confocal microscopy. In the first two panels of images at the top of Figure 3.1, phosphotyrosine and paxillin can be clearly seen co-localising with the same areas as integrin β1-GFP, shown in the zoomed-in insets in the top right of each image. Phalloidin staining clearly shows actin stress fibres terminating at integrin β1-GFP rich adhesions. The integrin β1-GFP localised to adhesions at the cell edges (Figure 3.1), with some smaller adhesions visible under the cell body (data not shown) (Figure 3.1).

Endogenous talin signal (shown in third panels in Fig 3.1) was seen to overlap with integrin β1-GFP signal similar to phosphotyrosine and paxillin. Kindlin 1 staining (shown in the foruth panel in Fig 3.1) was largely perinuclear, however in regions around the cell periphery, kindlin 1 co-localised with integrin β1-GFP. Kindlin 2 staining (shown in the last panels in Fig 3.1) was much stronger than kindlin 1 staining, with lower signal around the nucleus/cytoplasm and stronger signal at the periphery of the cell, co-localising with integrin β1-GFP signal within focal adhesions.

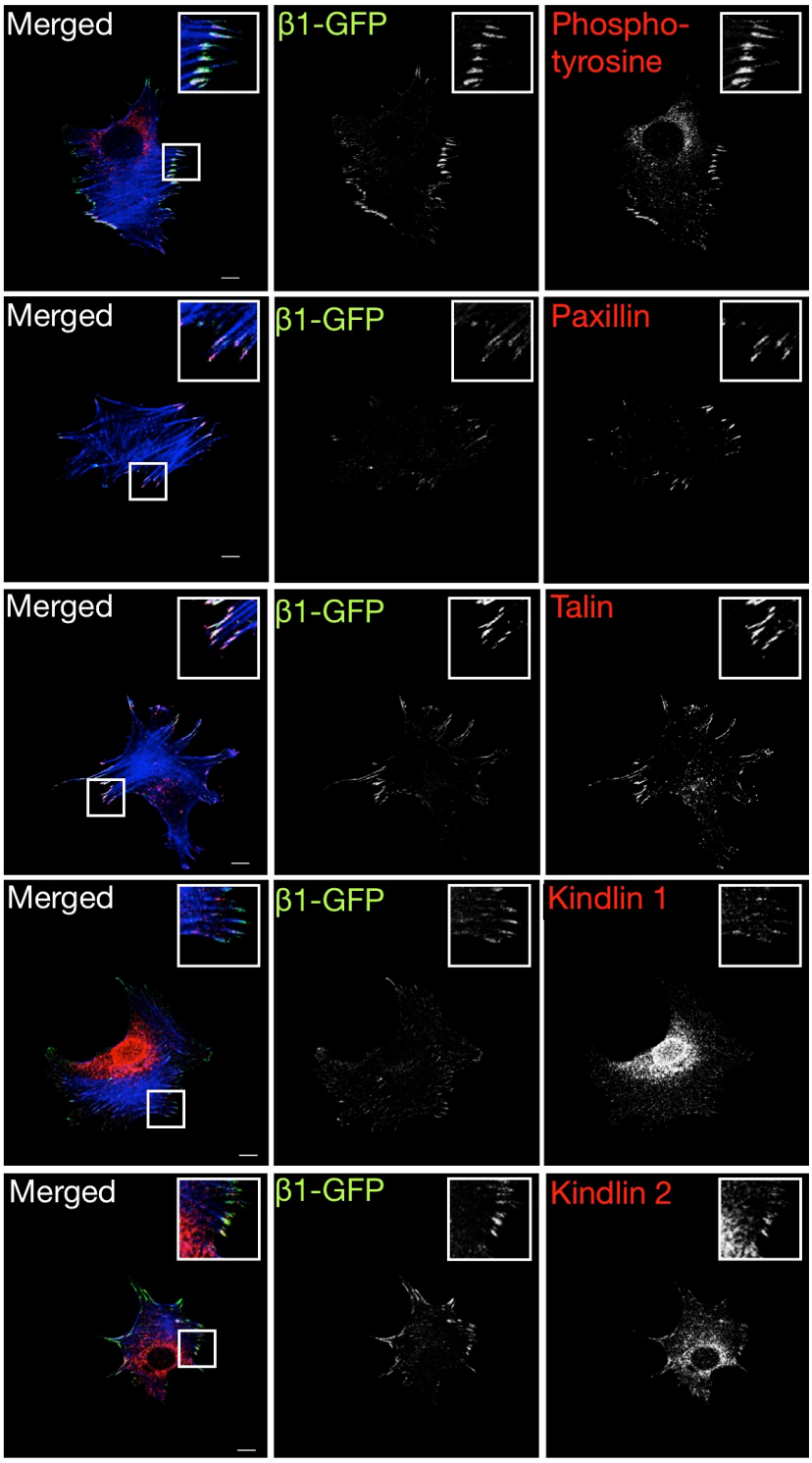

Figure 3.1 Endogenous talin, kindlin 1 and kindlin 2 colocalise with integrin β1-GFP in fibroblasts on 2D fibronectin.
Single slice confocal images of fixed β1-GFP expressing MEF's plated on fibronectin coated glass coverslips. Endogenous phosphotyrosine proteins, paxillin, talin, kindlin 1 or kindlin 2 were stained for followed by Alexa 568 secondary antibodies (red). Actin was stained for using phalloidin-Alexa633 (blue) shown in the merged images only. Zoomed in images of the highlighted areas are shown inset in the merged, and individual channels. Scale bar = 10μm.

3.2 Endogenous talin, kindlin 1 and kindlin 2 colocalise with β3-GFP integrin in fibroblasts on 2D fibronectin

β3-GFP MEF were plated onto glass coverslips coated with fibronectin before being fixed, and stained for endogenous phosphotyrosine, paxillin, talin, kindlin 1 or kindlin 2 and imaged by confocal microscopy as in Figure 3.1. As with β1 adhesions, phosphotyrosine and paxillin co-localised with β3-GFP integrin, shown in the zoomed-in insets in the top right of each image. Phalloidin staining shows actin stress fibres terminating at integrin β3-GFP rich adhesions. The β3-GFP adhesions were localised at the cell edges in Figure 3.2, and unlike β1-GFP, β3-GFP signal was not as clear under the cell body (data not shown). This suggest that β3-GFP containing adhesions are more common at the cell periphery and less common in larger adhesions which typically reside towards the centre and rear of adherent cells.

Endogenous talin signal was seen to overlap with β3-GFP signal similar to that seen with phosphotyrosine and paxillin and with β1-GFP. Kindlin 1 staining was again seen to be largely perinuclear, however some peripheral staining showed partial overlap with β3-GFP integrin. Kindlin 2 again had stronger signal at the periphery of the cell, and co-localised with β3-GFP.

The data presented in Figures 3.1 and 3.2 confirms that integrin β1-GFP and β3-GFP integrins co-localise to focal adhesions as shown by their co-

localisation with phosphotyrosine and paxillin. Furthermore, these images suggest that integrin activators also co-localise, to different degrees, with β1-GFP and β3-GFP.

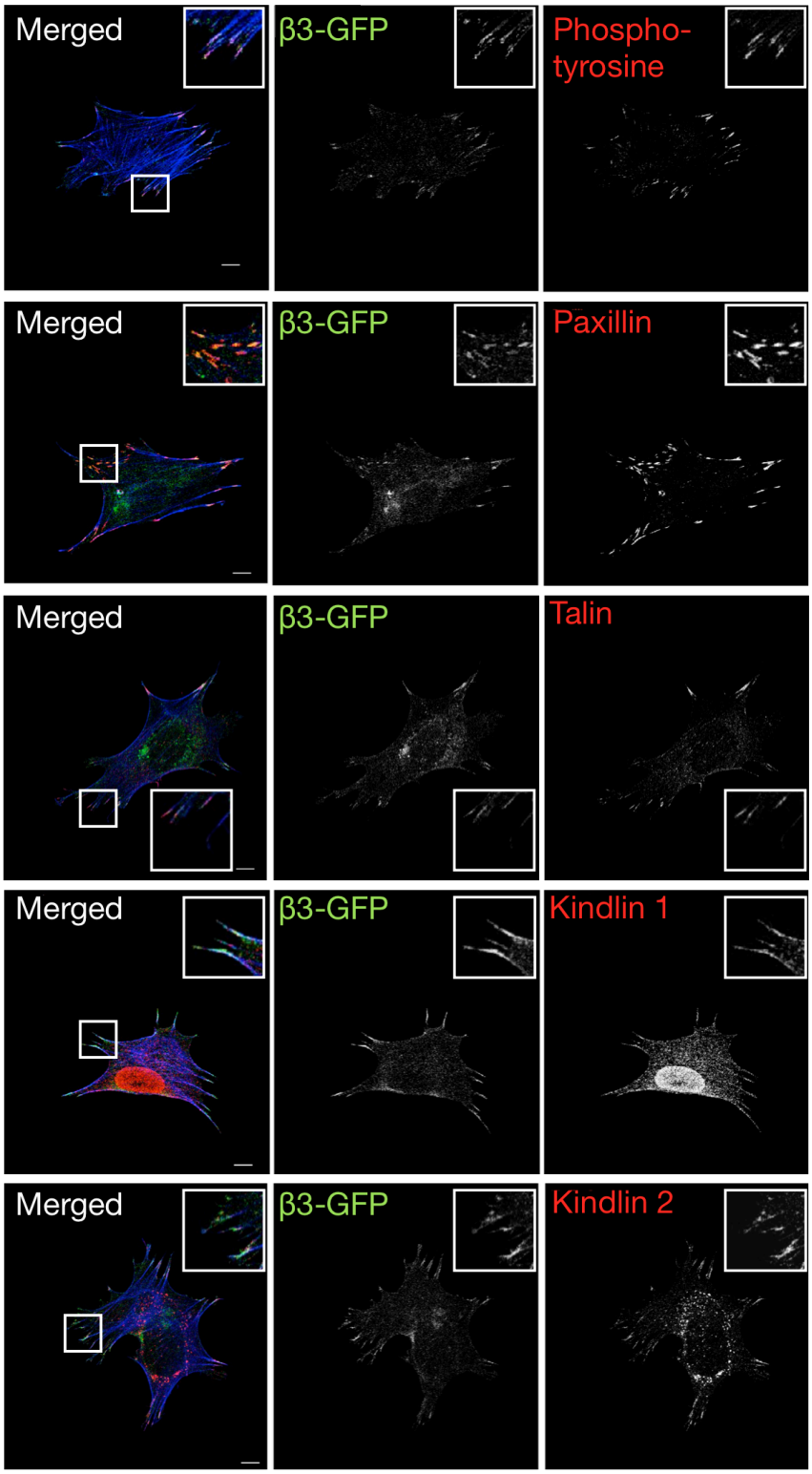

Figure 3.2. Endogenous talin, kindlin 1 and kindlin 2 colocalise with β3-GFP integrins in fibroblasts on 2D fibronectin.
Confocal images of fixed β3-GFP expressing MEF cells on fibronectin coated glass coverslips. Endogenous paxillin, talin, kindlin 1 or kindlin 2 was stained for in the 568 channel and is shown in red. Actin was stained for using phalloidin 633 and is shown in blue. Zoomed in images of the highlighted areas are shown inset in the merged, and individual channels. Scale bar = 10μm.

3.3 β1-GFP integrins show higher co-localisation with talin and lower co-localisation with kindlin 1 than β3-GFP on 2D fibronectin

In order to determine the degree to which integrin activators co-localised with specific β-integrin subunits, further analysis of multiple images from experiments shown in Figures 3.1 and 3.2 was performed. Images were analysed and the degree of co-localisation was quantified by determining the Pearson's correlation coefficient between the stained for endogenous proteins and either integrin β1-GFP or β3-GFP, where 1 is perfect co-localisation, and 0 is no co-localisation at all.

The data in Figure 3.3 shows that phosphotyrosine showed significantly higher co-localisation with β3-GFP integrin than with β1-GFP integrin. Paxillin and kindlin 2 did not show a significant difference in their co-localisation with either integrin β-subunit. The integrin activator talin showed significantly greater co-localisation with β1-GFP, whereas kindlin 1 showed higher co-localisation with β3-GFP than β1-GFP. The data suggests that β1 and β3-GFP positive adhesions are different in their composition or relative abundance or integrin activators.

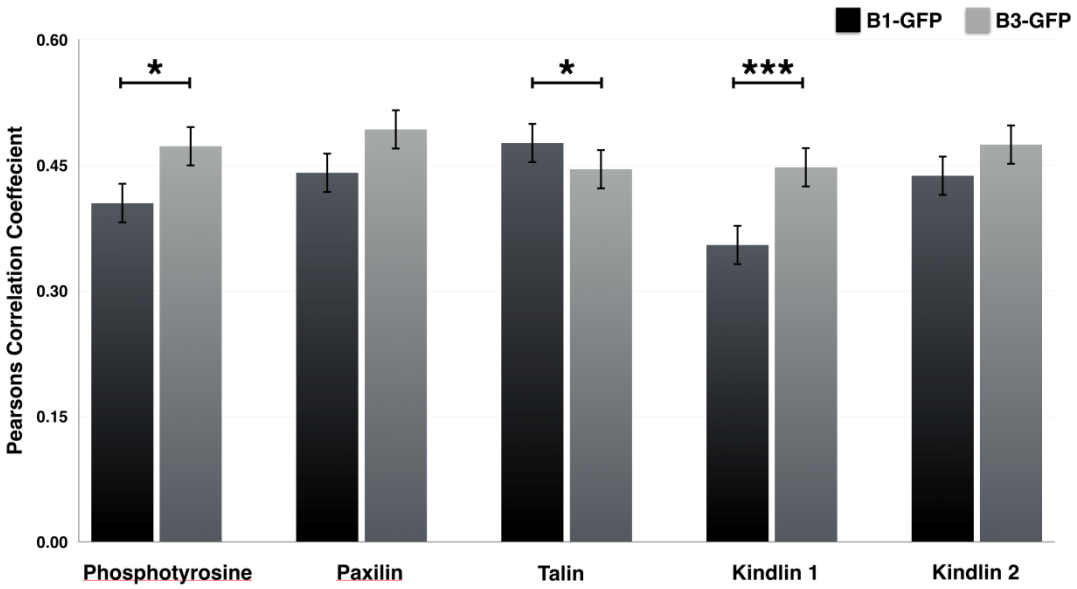

Figure 3.3: β1 Integrin has higher co-localisation with talin and lower co-localisation with kindlin 1 than β3 integrin in cells on 2D fibronectin.

Quantification was performed on confocal images as shown in figure 3.1 and 3.2 using Pearsons correlation coefficient analysis to determine the degree of correlation where 1 is perfectly correlation and 0 is no correlation. Analysis was performed on MEF plated on fibronectin coated glass coverslips, expressing integrin β1-GFP or β3-GFP stained with antibodies against endogenous phosphotyrosine, paxilin, talin, kindlin 1 or kindlin 2. Error bars are S.E.M., n= >30 cells per condition, graph is representative of three independent experiments, * = P<0.05, * * = P<0.001, * * * = P<0.0001

3.4 Composition and structure of CDM and the morphology of fibroblasts on CDM

Having characterised different types of adhesions on 2D substrates, it was important to determine whether these differences in segregation of integrin activation proteins between integrin subtypes also occurred in cells within more physiologically relevant 3D matrices. Cell derived matrix (CDM) is a fibrillar matrix that is deposited by primary human dermal fibroblasts upon culturing over 10-14 days. The CDM contains intact and bundled fibronectin and collagen fibres as shown in confocal images in Figure 3.4a. The matrix produced allows the cells plated within it to adopt a morphology that is more similar to what is seen *in-vivo*. As images in Figure 3.4b demonstrate, fibroblasts when plated on CDM adopt a elongated morphology, spreading along the fibres, is in contrast to the very flat and spread out morphology seen on 2D FN. Adhesions in fibroblasts on CDM were spread along the whole cell length, unlike 2D adhesions which generally were more numerous at the cell edges and less numerous under the cell body. There were also fewer F-actin protrusions in fibroblasts in CDM compared to FN.

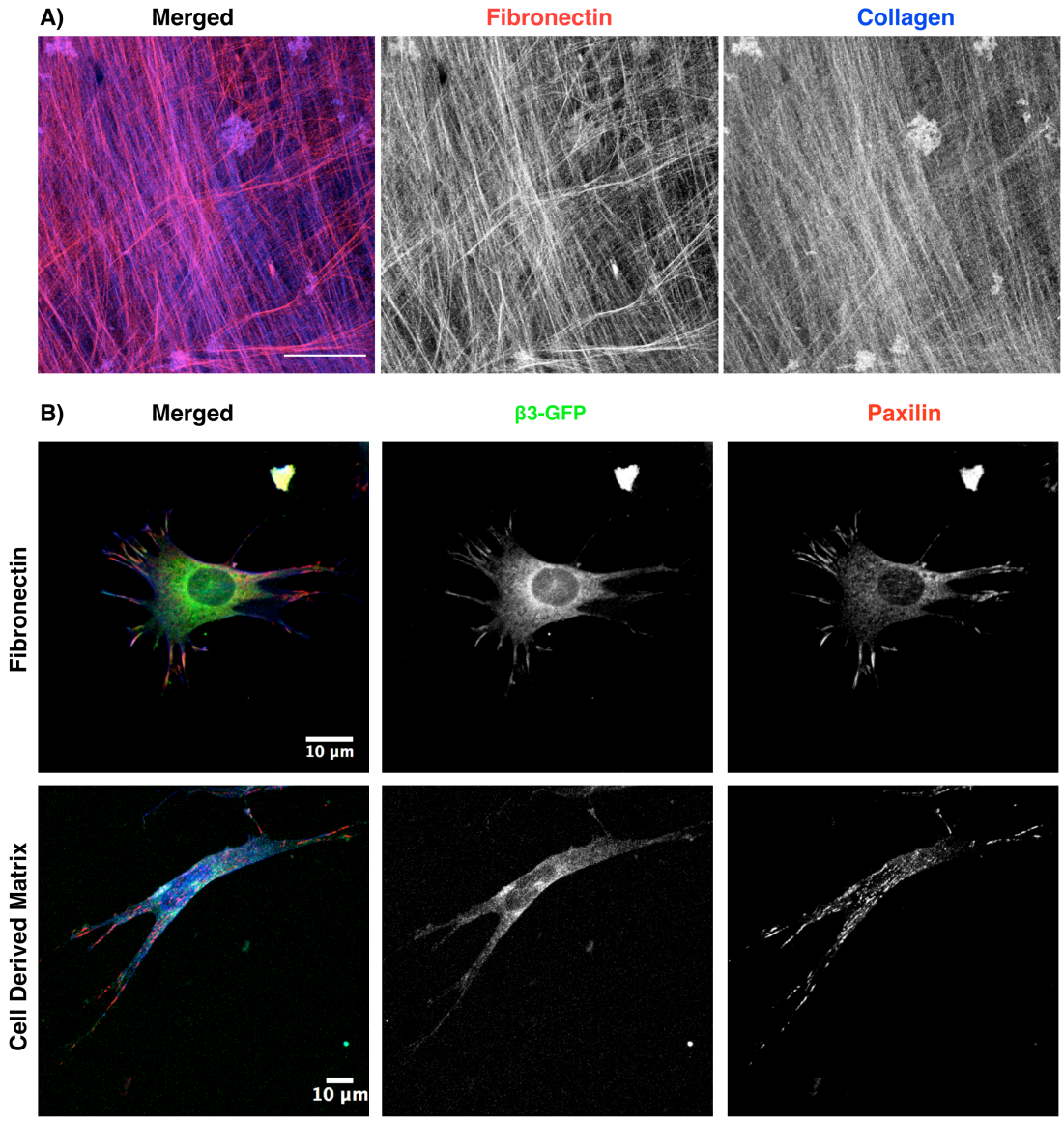

Figure 3.4. Composition and structure of CDM and the morphology of fibroblasts on CDM.

A) Human dermal fibroblasts were grown for 14 days before removal, and subsequent deposited CDM was stained with antibodies against fibronectin (Alexa- 568 secondary, red) or collagen (Alexa-633 secondary, blue) and imaged by confocal microscopy. B) Integrin β3-GFP expressing MEF cells were seeded onto either a 2D fibronectin substrate, or 3D CDM substrate, and were then fixed and stained for endogenous paxillin in the 568 channel, shown in red, and endogenous actin with phalloidin 633, shown in blue. Scale bar = 10µm.

3.5 Endogenous talin, kindlin 1 and kindlin 2 colocalise with β1 integrin in cells within CDM

Having characterised the co-localisation between integrin β1-GFP or integrin β3-GFP and integrin activators in 2D, we next wanted to examine if the co-localisation pattern would change when cells were plated within a more physiologically relevant 3D ECM environment, in this case CDM. Specifically, the question being addressed was whether this change in ECM environment would alter the co-localisation between integrins and the activation molecules.

β1-GFP integrin expressing MEF were plated in CDM and allowed to elongate and integrate with the matrix before fixation and stained for endogenous focal adhesion markers phosphotyrosine and paxillin or integrin activators, talin, kindlin 1 and kindlin 2 as was described for Figure 3.1. Cells were then imaged by confocal microscopy and z-stacks were acquired to enable the full depth of the cells and associated adhesions within different focal planes to be assessed. Figure 3.5 shows the maximum intensity projections from example representative images and demonstrates that MEF show a highly elongated morphology within CDM as compared to morphology on 2D fibronectin.

β1-GFP integrin co-localised with phosphotyrosine generally at the tips of filopodial-like protrusions as shown in figure 3.5. Paxillin and phosphotyrosine (PY) also showed colocalisation with β1-GFP and

colocalisation could be seen near the tips of protrusions. Endogenous talin staining was more cytosolic than seen in cells in 2D, however talin could still be seen co-localising with β1-GFP at adhesions. Endogenous kindlin 1 staining was predominantly localised to the nucleus, but some signal was seen at specific sites, which co-localised with β1-GFP. Endogenous kindlin 2 staining showed clear adhesion staining and co-localised with β1-GFP at these sites.

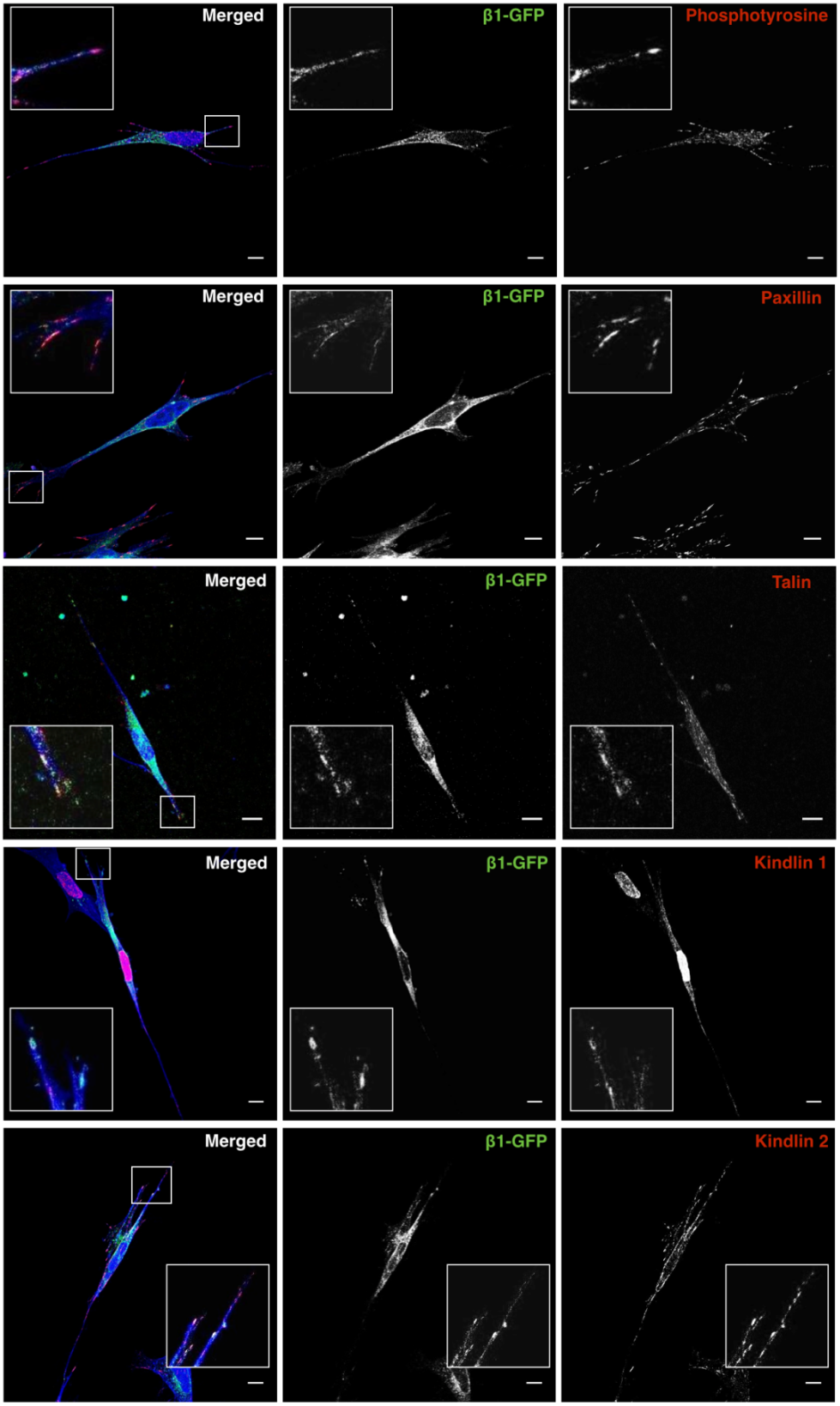

Figure 3.5: Endogenous talin, kindlin 1 and kindlin 2 colocalise with β1 integrin in cells within CDM

Confocal maximum intensity projections of images of fixed β1-GFP (green) expressing MEFs plated on cell derived matrix (CDM). Endogenous paxillin, talin, kindlin 1 or kindlin 2 was stained using Alexa568 secondary antibody (red). Zoomed in images of the highlighted areas are shown inset in the merged, and individual channels. Scale bars = 10μm.

3.6 Endogenous talin, kindlin 1 and kindlin 2 colocalise with β3 integrin in cells within CDM

To determine whether β3 integrin also associated with adhesions in 3D ECM, MEF expressing β3-GFP integrin were seeded onto CDM and left to spread and integrate before being fixed and stained with antibodies against endogenous focal adhesion markers and integrin activators. Cells were then imaged by confocal microscopy to produce z-stacks of the stained cells in CDM, and examples of maximum intensity projections are shown in Figure 3.6.

Phosphotyrosine and paxillin localised to adhesion-like structures in cells in CDM that overlapped with regions of intense β3-GFP signal. The GFP signal in these images appeared more cytosolic and less localised than those shown in 2D as generation of maximum intensity projections leads to flattening of the overall signal. Endogenous talin showed a similar level of overlap with β3-GFP to that was seen with phosphotyrosine and paxillin. Kindlin 1 staining was again seen to be largely perinuclear, however partial colocalisation with β3-GFP was evident at protrusions. Kindlin 2 again had stronger signal at the periphery of the cell, where it overlapped with β3-GFP.

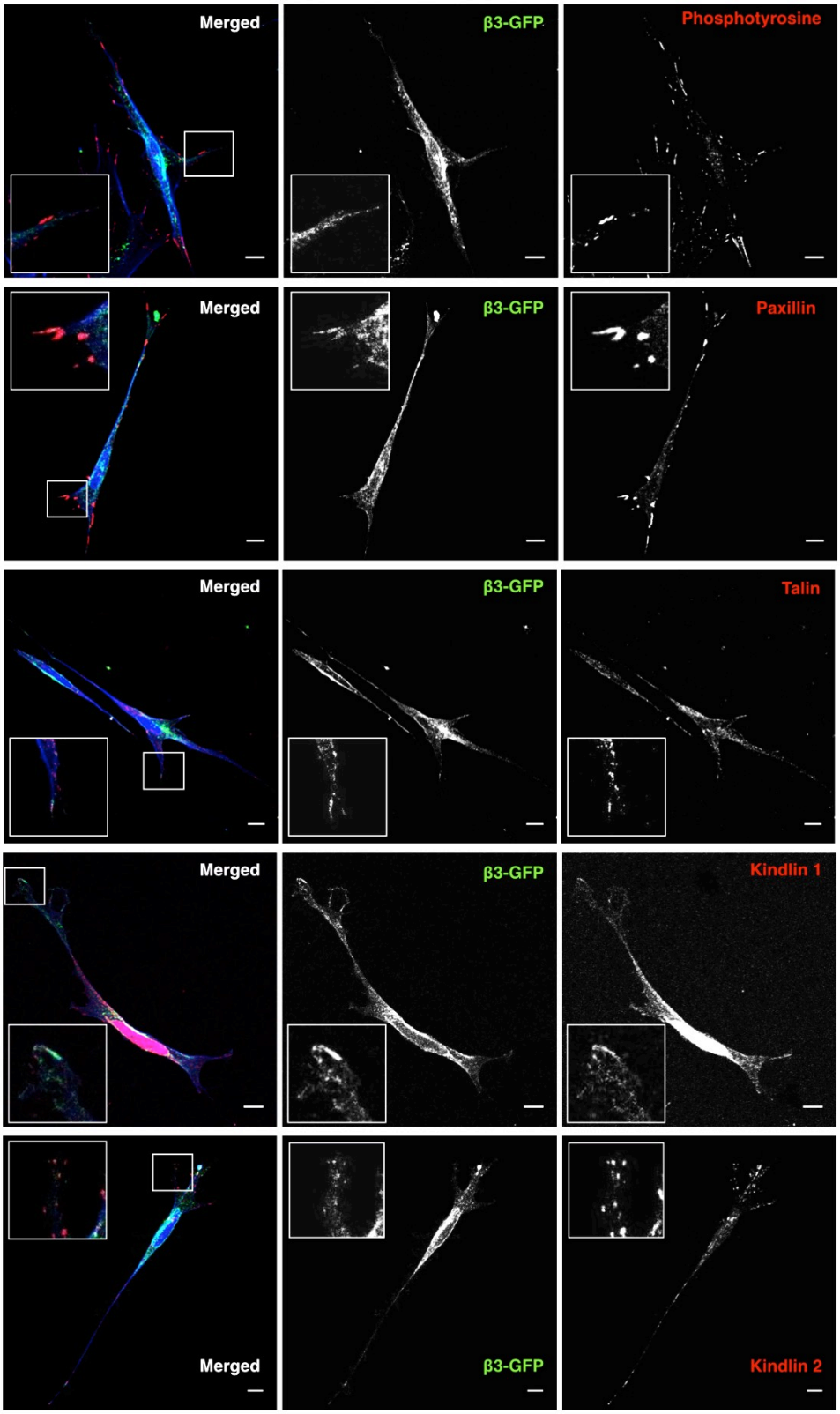

Figure 3.6: Endogenous talin, kindlin 1 and kindlin 2 colocalise with β3 integrin in cells within CDM.
Confocal maximum intensity projections of images of fixed β3-GFP (green) expressing MEFs plated on cell derived matrix (CDM). Endogenous paxillin, talin, kindlin 1 or kindlin 2 was stained using Alexa568 secondary antibody (red). Zoomed in images of the highlighted areas are shown inset in the merged, and individual channels. Scale bars = 10μm.

3.7 Kindlin 1 shows higher co-localisation with β3 integrins than β1 integrins in cells in CDM

In order to quantify these observed differences in subcellular distribution, colocalisation between GFP-tagged integrin β-subunit and focal adhesion markers was determined from multiple cells using Pearsons correlation coefficient analysis. Rather than a maximum intensity projection which can artificially mask intensity signals, individual slices of the acquired z-stacks of confocal images from cells were analysed to increase accuracy.

As shown in Figure 3.7, phosphotyrosine and paxillin both co-localised with β1 integrin significantly more than β3 in cells in CDM. Interestingly, talin and kindlin 2 did not show preferential co-localisation with either β-integrin subunit. However, kindlin 1 showed significantly higher colocalisation with β3 integrin than with β1.

This data, combined with data shown in Figure 3.4, shows that integrin β-subunits co-localise differently with major focal adhesion markers and with integrin activators, and that being in a more physiologically relevant 3D CDM can alter this co-localisation.

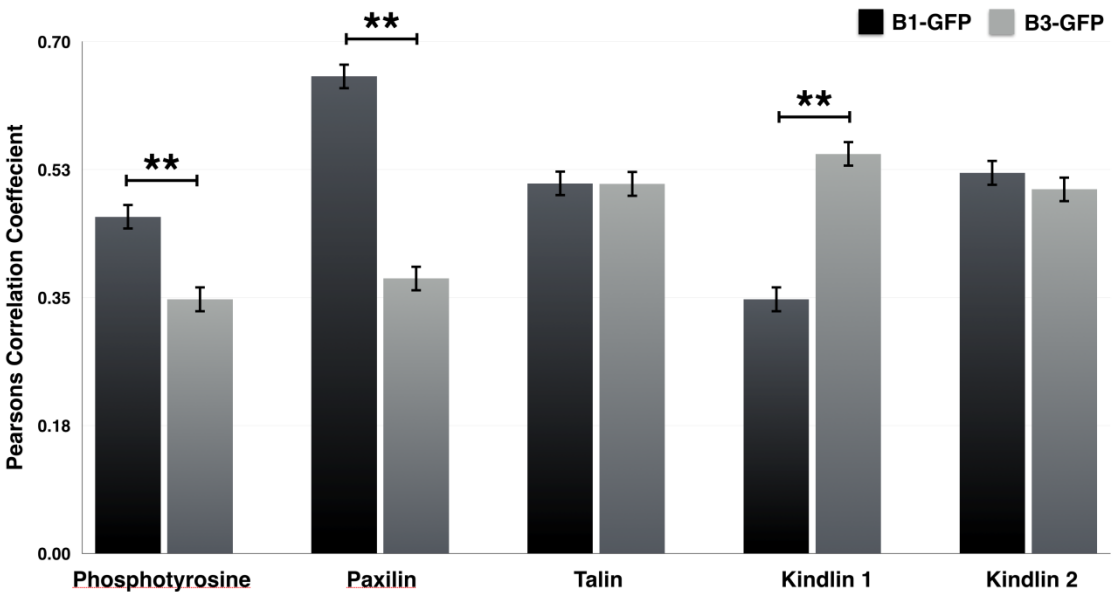

Figure 3.7: β1-GFP has higher co-localisation with phosphotyrosine and paxilin and lower co-localisation with kindlin 1 than integrin β3-GFP on CDM.

Quantification was performed on confocal images like that shown in figure 3.5 and 3.6 using Pearsons correlation coefficient analysis to determine the degree of correlation where 1.0 is perfectly correlation and 0.0 is no correlation. This analysis was performed on MEF cells on CDM expressing integrin β1-GFP or β3-GFP stained with antibodies against endogenous phosphotyrosine, paxilin, talin, kindlin 1 or kindlin 2 in the 568 channel. Error bars are S.E.M., n= >30 cells per condition and ~6 confocal slices per cell dependant upon cell size and orientation, graph is representative of three independent experiments, * = P<0.05, * * = P<0.001, * * * = P<0.0001

3.8 Characterisation of knockdown of integrins activators in fibroblasts

Talin, kindlin 1 and kindlin 2 are known activators of integrins and have been proposed to act together to promote integrin activation. In order to better understand and characterise the effects of each of these proteins within the context of adhesion and migration, it was important to knockdown each of these proteins specifically. Unvalidated shRNA constructs were used to generate lentivirus which was then used to infect NIH3T3 cells, with a scrambled shRNA being used as control. The efficiency of knockdown was assessed by western blot of cell lysates as seen in Figure 3.8. Two different lentiviral shRNA constructs were used for each protein to account for off-target effects.

Figure 3.8 shows efficient knockdown of talin by two different constructs. When compared with control cells, talin knockdown cells appeared to show an increase in the expression levels of paxillin. Kindlin 1 was seen to be efficiently reduced by infection with two separate lentiviral shRNA in Figure 3.8. Kindlin 1 knockdown cells were also seen to have reduced expression levels of paxillin compared with control cells. Kindlin 2 was effectively knocked down by two separate constructs seen in Figure 3.8. Knockdown cells were found to be largely stable in culture, although kindlin 2 knockdown cells grew much slower and tended to lose the shRNA over short culture periods. Cells were lysed and the knockdown efficiency was checked prior to using these cells in further experiments.

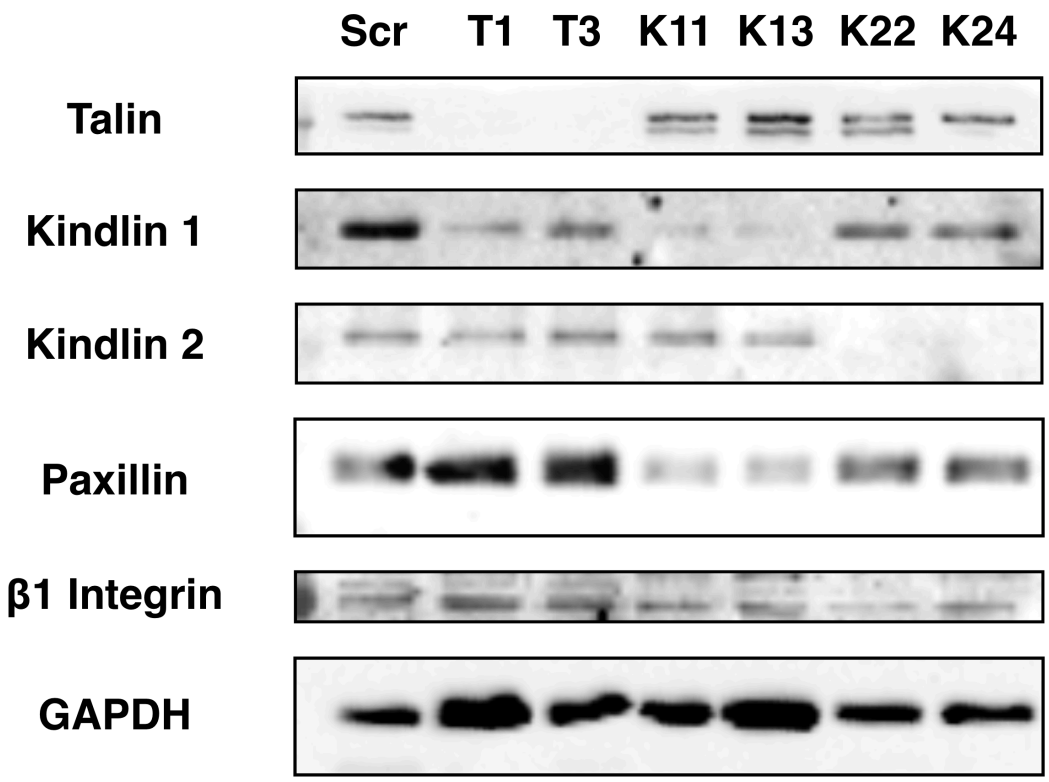

Figure 3.8. shRNA lentiviral constructs targeting integrin activators validated in fibroblasts.

Western blots of lysates from NIH3T3 fibroblasts expressing scrambled (Scr) shRNA or shRNA specifically targeting either talin (T1, T2), kindlin 1 (K11, K13) or kindlin 2 (K22, K24). Lysate concentration was equalised and were blotted for talin, kindlin 1 or kindlin 2 before also being probed for paxillin, β1 integrin and GAPDH as a loading control.

3.9 Knockdown of talin or kindlins in fibroblasts reduces random migration speed on 2D fibronectin

Data in Figures 3.3 and 3.7 showed that there were differences in the co-localisation between talin and kindlin 1 and integrin subunits. One of the main functions of adhesions and therefore integrin activators is to facilitate cell migration. In order to better understand the role of each integrin activation partner protein, talin, kindlin 1 and kindlin 2, in this process, each protein was knocked down and cell migration measured by time-lapse microscopy.

In order to do this the cell lines stably expressing lentiviral shRNA knockdown vectors were seeded sparsely on to a fibronectin coated plastic plate and random migration followed using phase contrast time-lapse microscopy. Cell nuclei were then tracked using the manual tracking plug-in in ImageJ over the entire imaging period and resultant tracks were plotted from a common origin (Figure 3.9a). As these trackplots clearly demonstrate, talin and kindlin 1 knockdowns did not migrate as efficiently as control cells, but kindlin 2 knockdown cells showed the greatest affect on migration.

The speed of cell migration in 2D was also quantified from the tracks obtained and all three knockdowns were found to have significantly reduced random migration speed when compared with control cells (Figure 3.9b). Fibroblasts with reduced kindlin 2 expression were seen to have a

trend towards the lowest migration speed although this was not significantly lower than the speed measured in talin or kindlin 1 knockdown cells. Migration persistence is defined as the displacement of the cell divided by the total path length e.g. if a cells initial position was A and final position was B, the distance between A and B would be the displacement, and the entire distance the cell actually travelled would be the total path length. Overall migration persistence was not affected in kindlin 1 and kindlin 2 knockdown cells, but knockdown of talin resulted in increased migration persistence on 2D fibronectin coated plastic (Figure 3.9C).

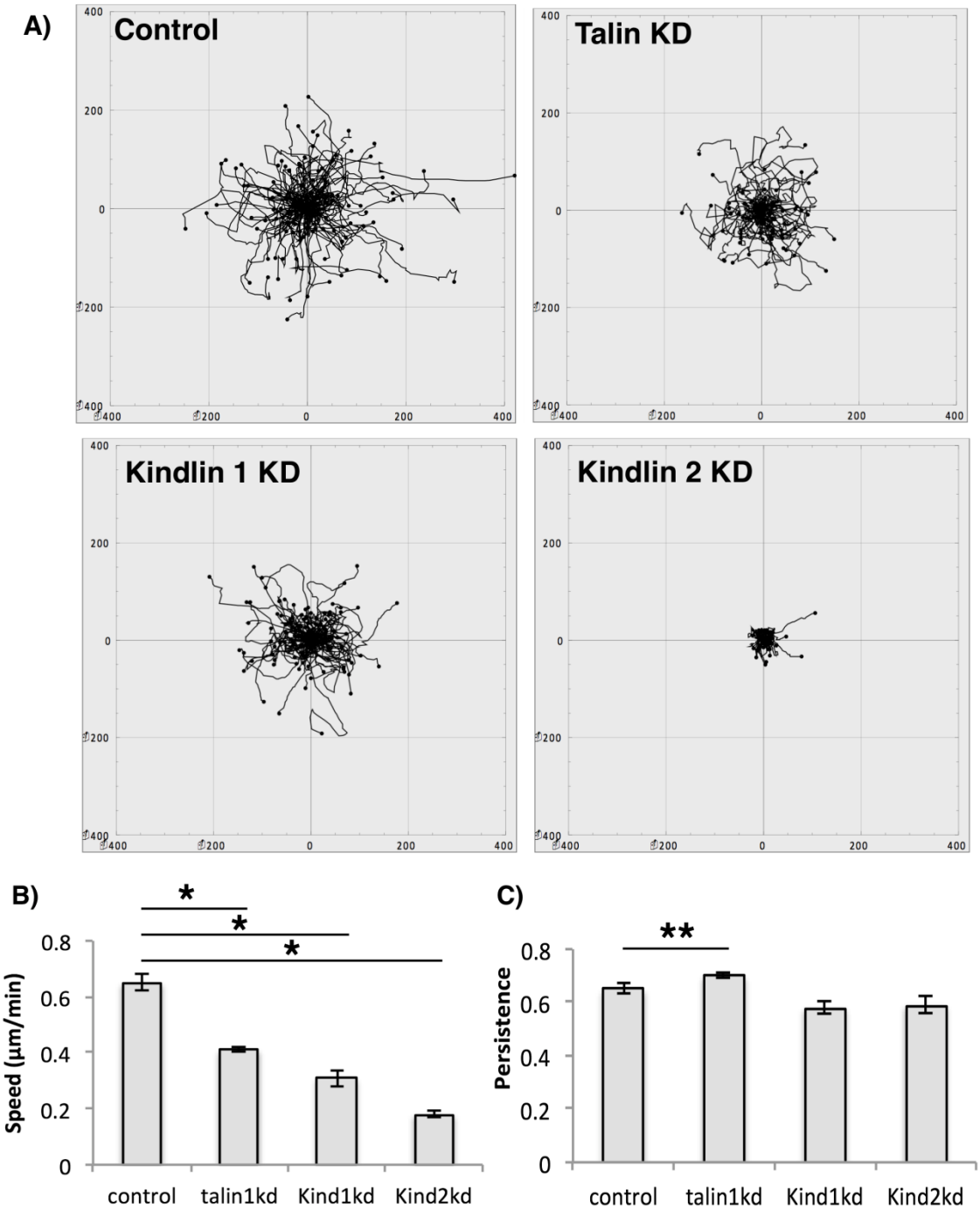

Figure 3.9. Knockdown of talin or kindlin in fibroblasts reduces random migration speed on 2D fibronectin.

A) Representative tracks of NIH3T3 control or specified knockdown cells seeded on fibronectin coated plastic and recorded randomly migrating over 8 hours with a frame taken every 10 minutes. Cells were tracked using the manual tracking ImageJ plugin and tracks analysed and plotted in Mathematica. **B)** Average speed of the cells tracked in A) over the entire imaging period. **C)** Mean persistence of cells tracked in A) using the chemotaxis mathematica notebook. Error bars are S.E.M., n= <70 over four independent experiments, * = P<0.05, * * = P<0.001.

3.10 Knockdown of kindlin but not talin reduces random migration speed in fibroblasts in CDM

Data presented in Figures 3.3 and 3.7 showed that there are differences in the co-localisation between integrin activators and different integrins in cells on 2D versus 3D ECM. It was therefore important to characterise the differences in migration between different integrin activator knockdowns in cells within a 3D CDM environment. The knockdown cell lines used in Figure 3.9 were plated onto CDM and were imaged by phase contrast time-lapse microscopy as for 2D surfaces. These cells were then tracked and analysed in the same manner as shown in Figure 3.9.

As seen in cells on 2D FN, Kindlin 2 knockdown again showed the largest effect on migration as shown in the rose plots in Figure 3.10a. Knockdown of talin, unlike in the 2D context (Figure 3.9b), did not result in a change in migration speed of cells in CDM when compared with control cells (Figure 3.10b). Kindlin 1 and kindlin 2 knockdown resulted in significant decreases in migration speed, and. Kindlin 2 again had the most significant effect on migration speed of any of the knockdowns. Analysis of migration persistence from the cell tracks demonstrated that talin and Kindlin 2 knockdown resulted in a significant reduction in migration persistence in fibroblasts in CDM, whereas Kindlin 1 knockdown did not affect migration persistence. The data shown in Figures 3.9 and 3.10 reveal that depletion of integrin activators can significantly alter migration speed and persistence and that kindlin 2 has the largest affect on migration speed.

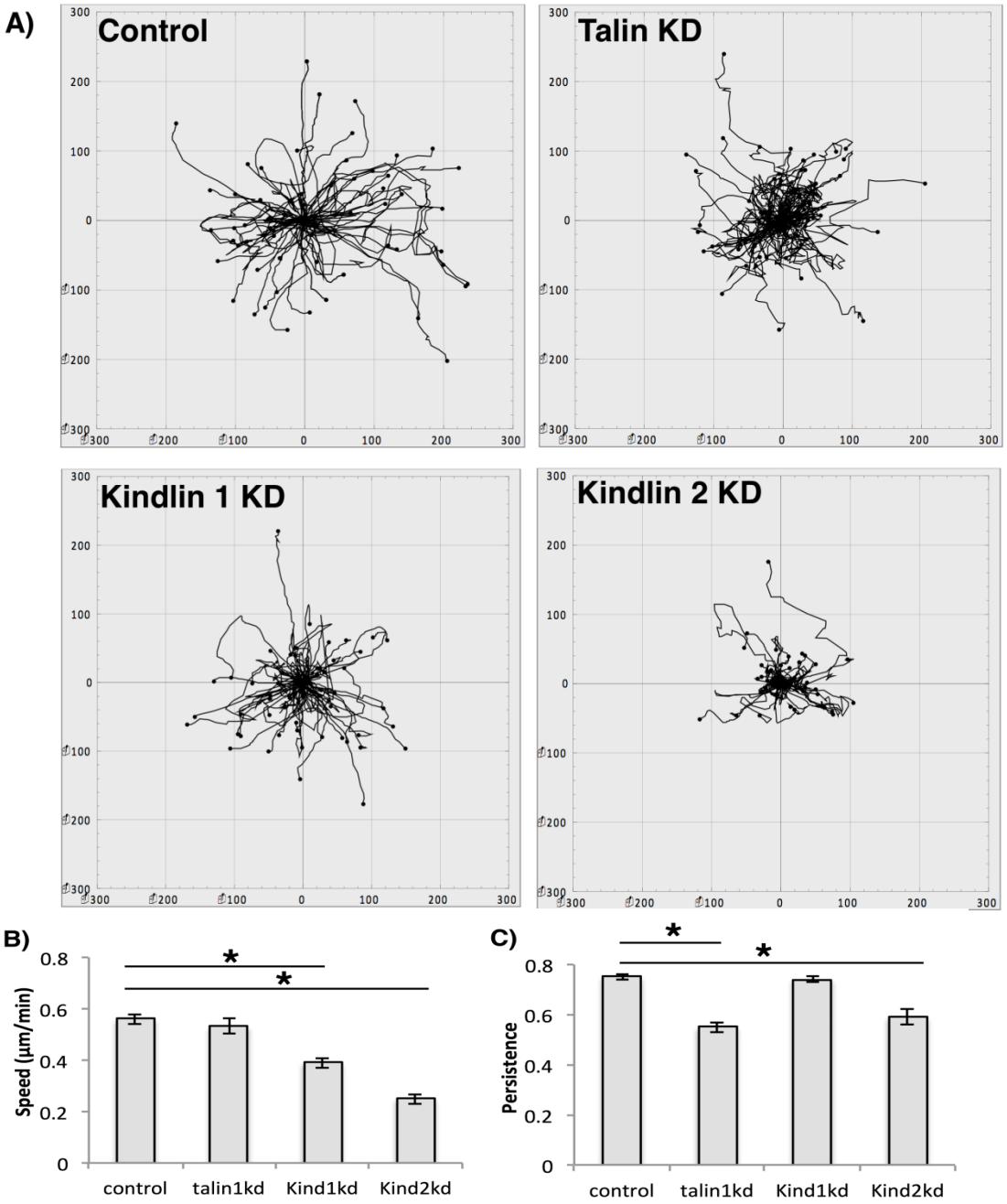

Figure 3.10. Knockdown of kindlin but not talin reduces random migration speed of fibroblasts in CDM.

A) Tracks of NIH3T3 control or lentiviral knockdown cells with reduced talin, kindlin 1 or kindlin 2 expression seeded on CDM made in plastic 8 well chambers and recorded randomly migrating over 8 hours with a frame taken every 10 minutes. Cells were tracked using the manual tracking ImageJ plugin and tracks produced using the chemotaxis mathematica notebook by G. Dunn. **B)** Average speed of the cells tracked in A) as calculated by the chemotaxis mathematica notebook by G. Dunn. **C)** Mean persistence of cells tracked in A) using the chemotaxis mathematica notebook. Minimum n= 60 cells over 4 independent experiments Error bars are S.E.M., * = P<0.05, * * = P<0.001

3.11 Knockdown of either talin or kindlin 2 decreases the number of total and active β1 integrin positive focal adhesions in fibroblasts on 2D fibronectin

Having demonstrated potentially different roles for talin, kindlin 1 and kindlin 2 in cell migration, the next important question to address was on the impact of depleting these molecules on integrin activation. Figure 3.11a shows control or knockdown cells stained with 9EG7 antibody, which recognises endogenous mouse active β1 integrin through binding to an epitope that is only available upon integrin binding to extracellular ligand. Paxillin was also co-stained for in these experiments to define focal adhesions. From these images a noticeable reduction in intensity and staining of the talin knockdown can be seen compared with control, with fewer 9EG7 and paxillin-positive adhesions being seen. Smaller reductions are noticeable for kindlin 1 and kindlin 2 knockdown.

The mean focal adhesion number per cell was analysed using ImageJ software by thresholding on the paxillin staining in multiple cells and values were calculated for all four cell lines and compared with control. As shown in Figure 3.11B, the mean number of paxillin-positive focal adhesions was significantly decreased for each of the knockdown cell lines analysed compared to controls. Kindlin 1 knockdown showed the smallest reduction in paxillin positive focal adhesion number when compared with

control. Talin and kindlin 2 knockdown cells had the most significant reduction in paxillin-positive focal adhesions.

Staining with 9EG7 recognised the active and extended conformation of β1 integrin and thus can be used to identify the effect of the knockdown of specific integrin activators on β1 integrin activation. Figure 3.11C shows the mean active-β1 integrin positive focal adhesion number per cell for control and knockdown cells. Knockdown of kindlin 1 did not significantly alter the number of active β1 integrin-positive focal adhesions per cell. However, kindlin 2 and talin knockdown resulted in a significant reduction in active-β1 integrin positive focal adhesions.

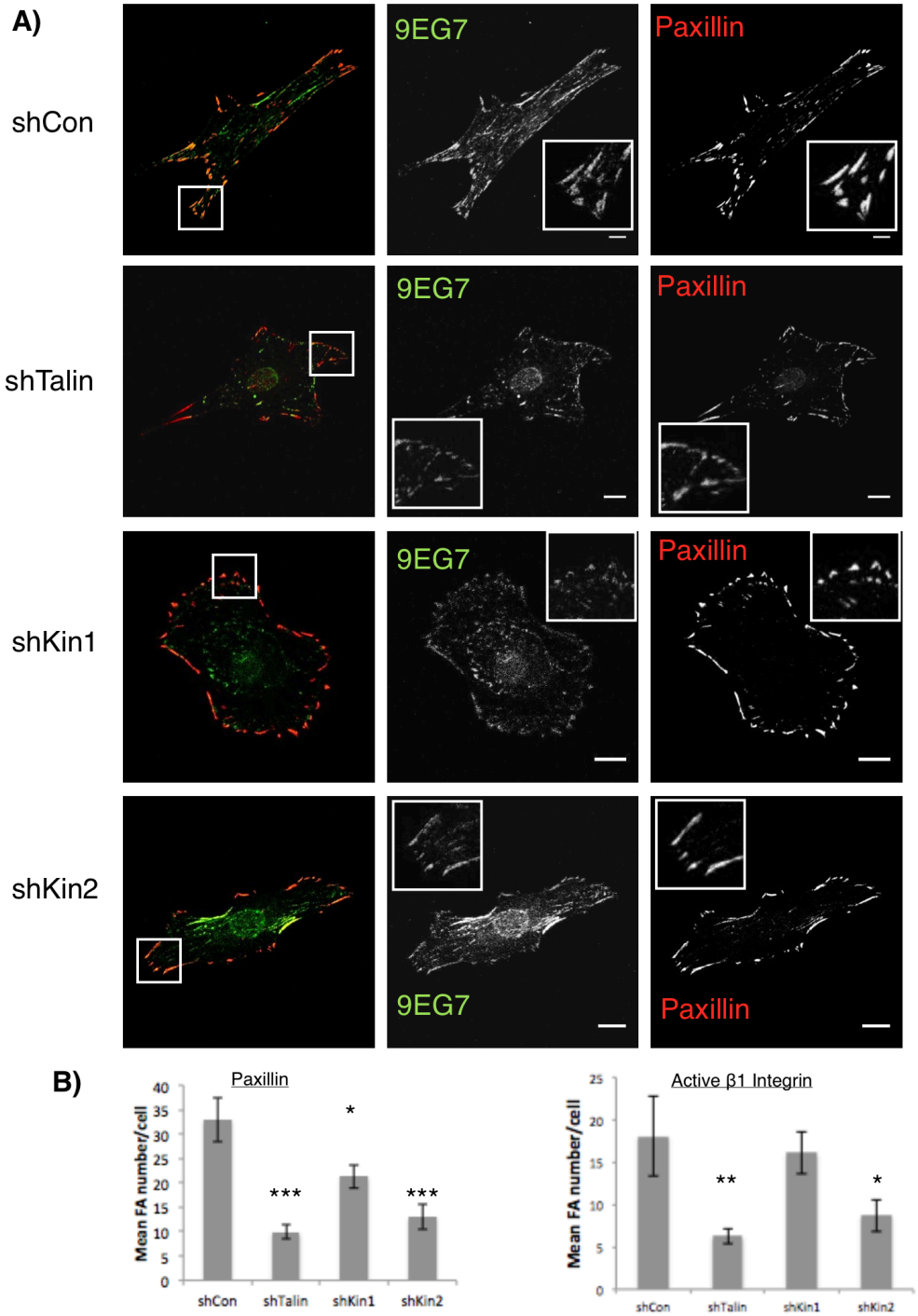

Figure 3.11. Knockdown of talin or kindlin 2 decreases the number of total and active β1 integrin positive focal adhesions on fibroblasts on 2D fibronectin.

A) Confocal images of fixed NIH cells infected with shRNA to knockdown either talin, kindlin 1, kindlin 2 or a control construct plated onto fibronectin coated coverslips. Endogenous active β1 integrin (9EG7) was stained for using FITC secondary antibody (green). Endogenous paxillin was stained using Alexa 568 secondary antibody (red). Scale bars = 10μm. Average number of either paxillin positive focal adhesions (B) or 9EG7 active β1 integrin positive focal adhesions (C) for cells infected with indicated shRNA. Error bars are S.E.M., * = P<0.05, ** = P<0.01, ***= P<0.001

3.12 Knockdown of either talin or kindlin 2 decreases the number of total and active β1 integrin positive focal adhesions on fibroblasts in CDM

Having seen that there are differences in the effects of integrin activator knockdown on migration between cells in CDM or on 2D substrates, it was important to next determine whether the differences shown in Figure 3.11 also occurred in cells within 3D CDM. Figure 3.12a shows representative example maximum intensity projections of confocal images of control or integrin activator knockdown cells in CDM stained for either paxillin or 9EG7. Analysis of the paxillin or 9EG7-positive focal adhesions was performed as in Figure 3.11.

Figure 3.12b shows the mean focal adhesion number per cell as determined from paxillin staining. When compared with control fibroblasts, talin, kindlin 1 and kindlin 2 knockdown cells all showed a significantly reduced number of focal adhesions per cell. This was also reflected by a decrease in the mean number of active β1-positive focal adhesions per cell for these cells lines as shown in Figure 3.12C.

Taken together it can be concluded that the knocking down any of the integrin activation proteins results in a more significant impact on adhesion assembly and integrin activation in cells within CDM environments compared to on 2D fibronectin.

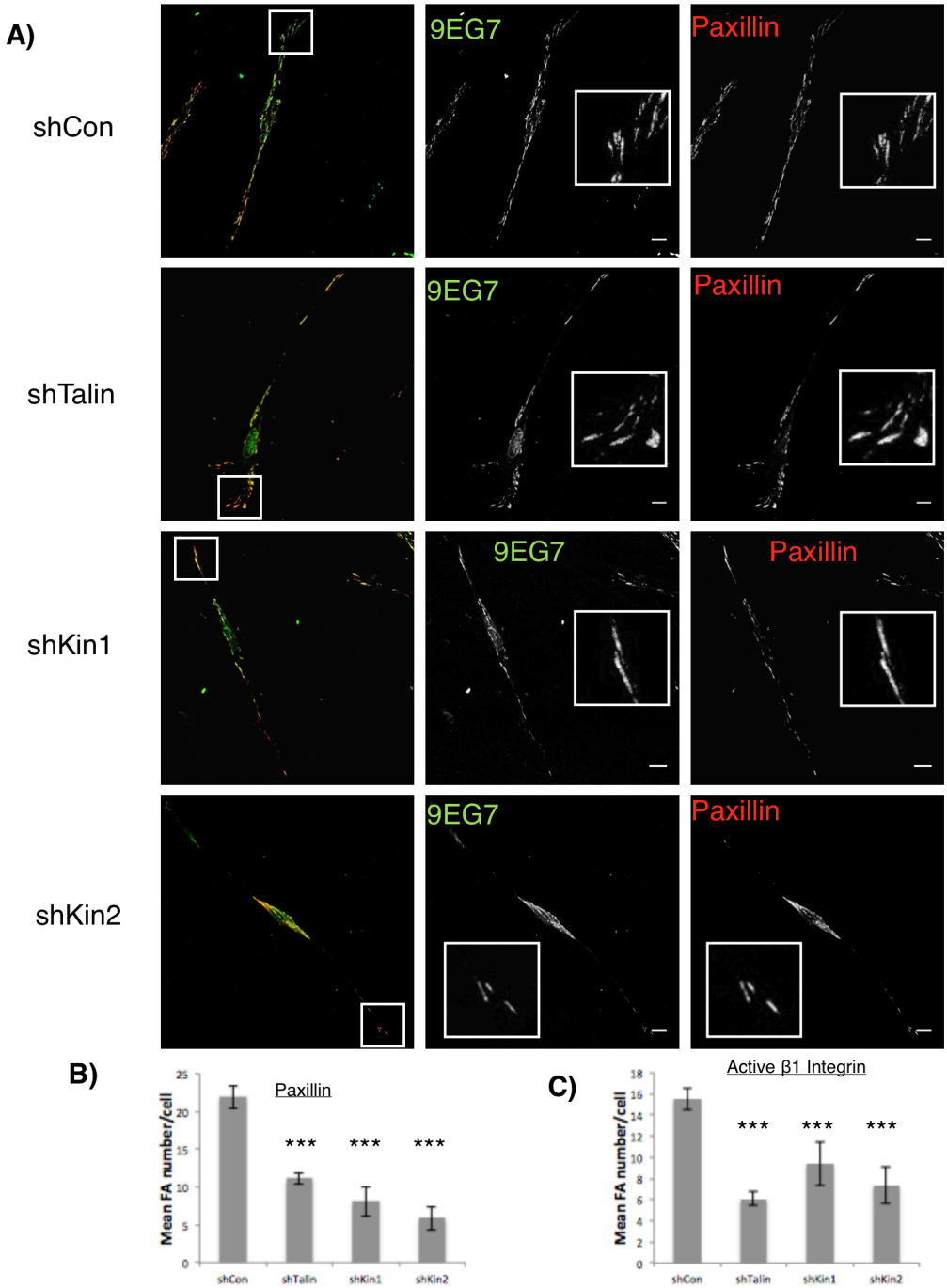

Figure 3.12. Knockdown of talin, kindlin 1 or kindlin 2 decreases the number of total and active β1 integrin positive focal adhesions in fibroblasts in cell derived matrix.

A) Confocal maximum intensity projections of images of fixed NIH cells infected with shRNA to knockdown either talin, kindlin 1, kindlin 2 or a control construct plated onto CDM. Endogenous active β1 integrin (9EG7) was stained for using FITC secondary antibody (green). Endogenous paxillin was stained using Alexa 568 secondary antibody (red). Scale bars = 10μm. Average number of either paxillin positive focal adhesions (B) or 9EG7 active β1 integrin positive focal adhesions (C) for cells infected with indicated shRNA. Error bars are S.E.M., ***= P<0.001

Discussion

The aim of the experiments in this chapter was to define whether differences exist between integrin partitioning, localisation or function of the three known integrin activation molecules, talin, kindlin 1 and kindlin 2, in fibroblasts. Data presented in this chapter showed that talin, kindlin 1 and kindlin 2 all colocalise to β1 and β3-GFP positive adhesions as has been previously shown by others (Tadokoro et al., 2003; Meves et al., 2009; Karaköse et al., 2010). However the degree of co-localisation to specific integrins had never been previously investigated. Data demonstrated that talin showed higher co-localisation with β1-GFP than β3-GFP with the reverse seen for kindlin 1. In cells on CDM, the kindlin 1 - β1-GFP colocalisation was seen to an even greater extent compared with cells on 2D fibronectin, again suggesting that kindlin 1 may play a role in differential activation of specific integrins and that this might be sensitive to the changes in ECM topology or mechanics in 3D matrices. Interestingly, there was no difference in the co-localisation of kindlin 2 to either β1 or β3-GFP integrin subunit in both 2D and 3D CDM assays, this suggests that kindlin 2 is playing an integral role in the integrin activation of both β1 and β3 integrins but is not sensitive to environmental changes or composition in the surrounding ECM. Due to the 3D nature of cells in CDM colocalisation analysis was performed on z-slices from acquired z-stacks of imaged cells, rather than being performed on maximum intensity projects in order to reduce false positives and increase reliability. CDM is

made up of a mixture of matrix proteins including collagen and fibronectin. To test whether the ECM composition or structure is impacting on the Kindlin-1-integrin association, CDM could be flattened such that the fibres were still present but the cells were no longer able to invade and fully cover themselves in the matrix. Another possibility would be to use combinations of soluble matrix proteins such as collagen and fibronectin and coat the glass or plastic with the mixtures to determine whether the same enhanced integrin association phenotype was observed for kindlin-1.

When talin was knocked down by shRNA, an increase in paxillin was observed (Figure 3.8), this may be explained by paxillin expression increasing to compensate for the loss of talin as both proteins play key roles in the architecture of adhesions. Kindlin 2 knockdown cells had the most severe phenotype in culture and cells were highly rounded, and slow-growing (data not shown). Due to the nature of the experimental set-up, shRNA knockdown efficiency was found to decrease over time and this effect was mitigated by checking protein levels by western blot with cell lysate samples taken from the day of the experiment from each cell line. Subsequent analysis demonstrated the kindlin 2 knockdown cells had the most significant reduction in migration speed in both 2D and CDM environments in addition to having the largest phenotypic change in cultured cell morphology. An interesting extension of this work would be to look and see if the same migration phenotypes were observed after introducing a chemotactic gradient or other migration queue to allow for

the separation of the affects on persistence from the affects on speed. Early studies into the role of kindlin 2 showed just how important it is, kindlin 2 knock-out was found to be embryonic lethal in mice (Dowling et al., 2008; Montanez et al., 2008), and conditional knockdown in zebrafish development was found to result in abnormal heart development (Dowling et al., 2008). Similarly, in a study where talin was knocked out in mice it was found to be embryonic lethal also, due to a large disorganisation at gastrulation suggested to be because of a defect in migration (Monkley et al., 2000). By comparison kindlin 1 knock-out in *C. elegans* embryos were found to be able to develop to hatching but then would die due to an inability to move from an impairment of muscle fibre formations (Rogalski et al., 2000). Combined with the data in this chapter a picture builds up of the importance of talin and kindlin 2 within cells especially within development and cellular migration.

The effect of knockdown of integrin activators on integrin activation was measured more directly in this chapter through the analysis and comparison of the number of 9EG7-positive focal adhesions in cells in both 2D and 3D CDM substrates. It was found that in cells on CDM, knockeddown in talin, kindlin 1 or kindlin 2 all resulted in a highly significant reduction in both the total number of focal adhesions and the number of active-β1 containing focal adhesions. Interestingly, kindlin 1 knockdown cells on 2D substrates showed only a small reduction in total

focal adhesion number and a non-significant reduction in the number of active-β1 containing focal adhesions.

Overall, within these experiments talin was seen to have the largest affect on both focal adhesion number and active-β1 containing focal adhesions, whereas kindlin 2 was seen to have a strong but slightly less severe affect on these two parameters. This is somewhat in contrast to the migration data in this chapter, where kindlin 2 was observed as having the largest affect on migration. Previous studies have shown that transient expression of either kindlin 1 or kindlin 2 can inhibit integrin α5β1 and αIIβ3 activation independent of kindlin-integrin binding in CHO cells (Harburger et al., 2009). However, when the talin head domain is co-expressed with both kindlin 1 and kindlin 2 they can activate αIIbβ3 in a integrin binding dependent manner but inhibit β1-integrin activation (Ma et al., 2008; Harburger et al., 2009). Furthermore, it has been shown that kindlin 2 is required for activation of integrins in mouse cells (Montanez et al., 2008).

Further to this it has been found that cellular migration can be inhibited by knock down or overexpression of kindlin 2 (Shi et al., 2007; Ma et al., 2008), further suggesting that kindlin 2 may be the key integrin activator from the kindlin family in fibroblasts. Since an interaction with the β tail is not required for inhibition of integrin activation by kindlin 1 or 2 (Ma et al., 2008), the absence of robust colocalisation between either β1 or β3 integrin and kindlin 1 at focal adhesions suggests that kindlin 1 may play more of a role

in keeping integrins inactive until talin and kindlin 2 can bind and fully activate the integrin, suggesting kindlin 1 may be acting as a scaffold protein. Alternatively, kindlin 1 may bind to other adhesion proteins at these sites to sequester them away from the integrin. Indeed, kindlins have been shown to bind to a number of other proteins, including integrin linked kinase (ILK,) migfilin and kindlins themselves (Lai-Cheong et al., 2010).

As these experiments used antibodies that recognised just one active β-integrin subunit, the effect of talin, kindlin 1 or kindlin 2 knockdown on activation on other integrins was not assessed. The experiment would have been enhanced by use of an antibody to recognise active-β3 integrin in mouse cells which is not currently available.

Finally, the data in this chapter have given us greater insight into the relative contribution of talin, kindlin 1 and kindlin 2 to integrin activation and cell migration and indicated the importance of studying these proteins effects together. However, there has long been a debate within the field as to the precise dynamics involved within the earliest stages of integrin activation and adhesion formation, particularly as to whether kindlins function as a recruitment factor for talin to integrin β tails or if talin activates the integrin directly, and kindlin functions as a recruiter of other proteins and strengthens the nascent adhesions (Montanez et al., 2008;

Moser et al., 2009; Calderwood et al., 2013; Ye et al., 2014). These questions will be addressed in the following chapters.

4. Recruitment of integrin activators at focal adhesions

Introduction

Talin is suggested to be the molecule whose binding activates the integrins, with kindlin functioning either to potentiate integrin-talin binding, as an adapter directly recruiting talin, or to play a role in relieving inhibition of integrin activation, as it has been shown that kindlins share an overlapping binding site with ICGAP and filamin, two inhibitors of integrin activation (Kiema et al., 2006; W. Liu et al., 2013). Both talin and kindlins have been shown to bind to two different NXXY motifs in the integrin β subunit cytoplasmic tails, talin binds to the membrane proximal NPXY motif (Calderwood et al., 2002) and kindlins bind to the membrane distal NPXY motif (Ma et al., 2008). The close proximity of these two motifs has led some to conclude that talin must bind first to potentiate the binding of kindlin (Kahner et al., 2012), or that kindlin must bind first to potentiate binding of talin (Moser, Legate, et al., 2009). While it is clear that kindlins play a role in integrin activation, it is not clear whether they also regulate talin-integrin binding. Moreover, the timeline of recruitment of each of these proteins to newly forming adhesion sites, and thus their potential sequential or combined effect on inside-out activation of integrins remains unclear.

Experiments in the previous chapter demonstrated differences in the levels of Kindlin proteins colocalising with integrins at focal adhesions. Kindlin-1 showed preferential colocalisation with β3 integrin over β1 in both 2D and

3D matrices. β3 has been proposed to predominantly reside within peripheral, transient adhesions rather than the more stable or fibrillar sites (Worth et al., 2010) suggesting Kindlins-1 and -2 may exhibit different recruitment to adhesions depending on integrin association.

The aim of the experiments in this chapter was to analyse the spatio-temporal recruitment of talin and kindlin 1 or talin and kindlin 2 to sites of forming focal adhesions within live cells. This would provide novel information regarding spatio- and temporal dynamics of each protein with respect to each other, and whether kindlin and talin molecules are co-recruited to support integrin activation and/or adhesion assembly or if this occurs sequentially. Furthermore, the effect of promoting integrin activation in contributing to formation or recruitment of talin or kindlins as adhesions will be tested. This will help to define whether integrins generate a positive feedback loop that alters the adhesion microenvironment and dictates recruitment of activating molecules to strengthen or promote receptor clustering. These experiments will provide important insight into the relationship between integrins activators and integrins during adhesion assembly.

4.1 Kindlin 1 is present at forming adhesions before talin in NIH3T3 fibroblasts

In order to determine the kinetics of recruitment of talin and kindlin 1 to forming focal adhesions, NIH3T3 fibroblasts were transfected with constructs encoding talin-GFP (from K. Yamada, NIH, USA) and kindlin 1-dsRed (from D. Calderwood, Yale University, USA). Fluorescently labeled proteins have been known to mislocalise or else stick to each other, both of these constructs have been shown to be able to localize correctly (Harburger et al., 2009; Worth et al., 2010). Transfected cells were then incubated for 24 hours before being plated onto a fibronectin coated imaging dish and live cell imaging was performed on a confocal microscope. The 488 channel was used to visualise talin-GFP, the 568 channel to visualise kindlin 1-dsRed, and interference reflection microscopy (IRM) was used to define the sites of adhesion formation to negate the requirement for a third transfected marker protein. Figure 4.1A shows representative stills from one of these movies, zoomed in on a region where an adhesion is forming. The top panels show the IRM channel where areas where the cell is making contact to the substrate are shown as dark regions. Kindlin 1 and talin channels are shown in the bottom two sets of panels. Arrows marked ‘A’ denote an adhesion starting to form in the reflectance channel; arrows marked ‘B’ and ‘C’ denotes kindlin-1 and talin arriving at the adhesion respectively. Images show a localised increase in kindlin 1-dsRed signal (arrow B) before there is a

similar increase in talin-GFP signal (arrow C). This was seen for forming adhesions in different cells from independently performed experiments.

Quantification of multiple movies acquired over separate days was performed as described in Materials and methods. Briefly, a thresholded mask was used to be able to partition just the regions where adhesions were, generated from a thresholded maximum intensity projection, this was applied to each of the channels and the integrated density of each channel, for each frame was measured per adhesion in ImageJ before then being normalised to the highest value for that particular adhesion. This data was then plotted over time to provide a normalised trace for the signals from each channel over time. A representative graph from one focal adhesion measurement is shown in figure 4.1B. The light grey trace shows the normalised integrated density for kindlin 1-dsRed and the black trace shows the normalised integrated density for talin-GFP. The light grey kindlin-1 trace can be seen to peak earlier than the black talin trace around frame 121. The integrated density and therefore the levels of kindlin-1 fall slightly after this peak before increasing again along with the talin trace. This characteristic early peak, fall, then rise was seen from other quantified movies. To enable statistical comparisons between multiple adhesions and cells, meta-analysis was performed to determine the average time to this first peak for each channel. The resulting averages are shown in the graph in Figure 4.1 C. Kindlin-1-dsRed arrived significantly earlier than talin-GFP in forming adhesions in fibroblasts.

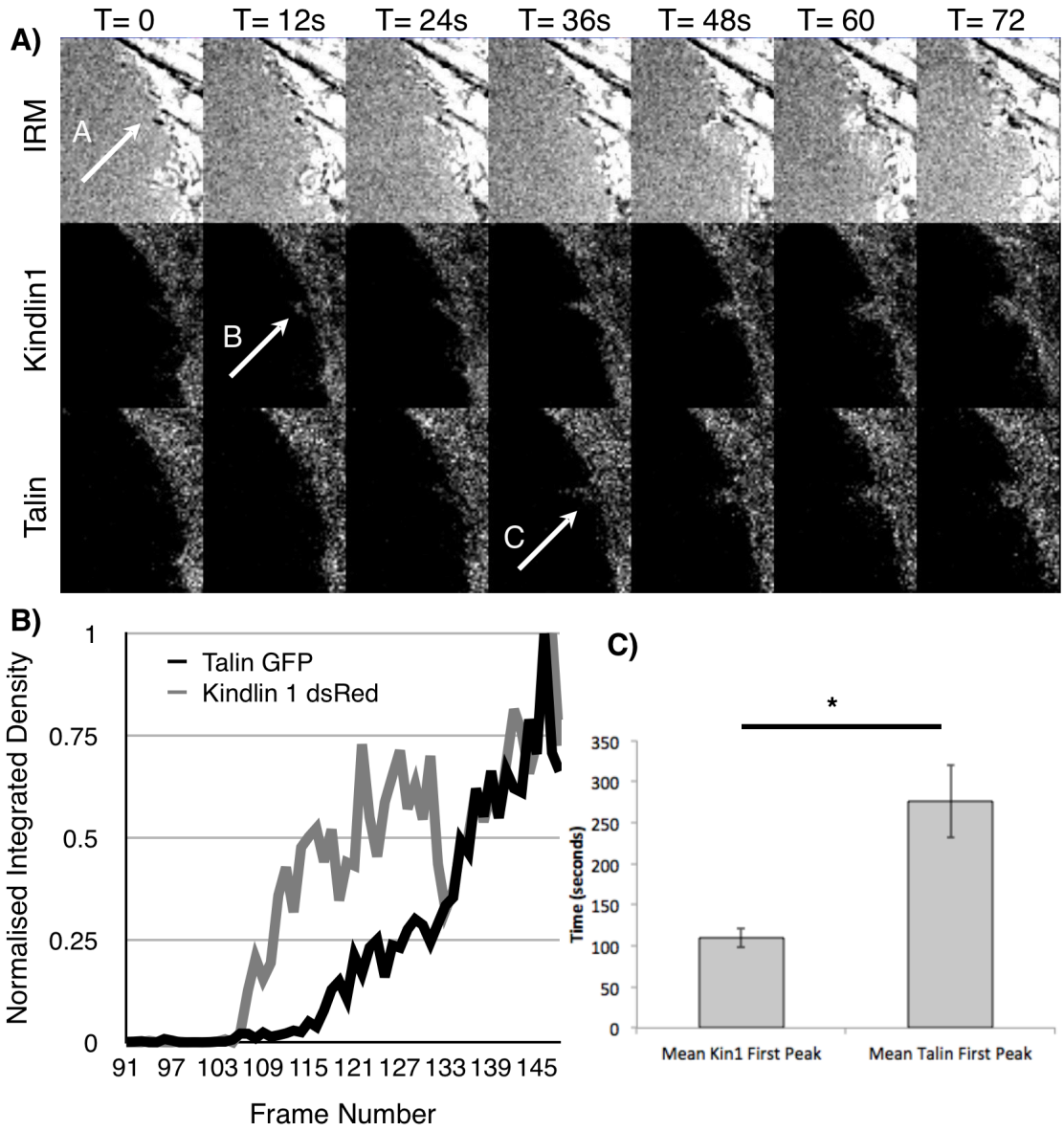

Figure 4.1. Kindlin 1 is present at forming adhesions before talin in NIH3T3 fibroblasts.

A) Confocal stills from time-lapse movies of NIH cells expressing kindlin 1-dsRed and talin-GFP. IRM channel shows contact sites between the cell and the substrate. Arrow A denotes adhesion formation, arrow B denotes kindlin arrival to this site and arrow C denotes talin arrival. Time in second is shown along the top of the image. B) A representative example of the normalised integrated density over time for either kindlin 1 dsRed or talin-GFP for a single focal adhesion. The frame rate is 1 frame every 12 seconds. C) Quantification of the mean time from adhesion initiation to the first normalised peak in either talin-GFP or kindlin 1 dsRed levels. n = >20 adhesions from >10 cells over minimum of 3 experiments. * = $P<0.05$.

4.2 Kindlin 2 is present at forming adhesions before talin in NIH3T3 fibroblasts

In order to determine whether the same trend of early arrival at adhesions was also evident for Kindlin-2, NIH3T3 fibroblasts were transfected with constructs encoding talin-GFP and kindlin 2-mCherry (S. King, PhD thesis 2009). Transfected cells were then incubated for 24 hours before being plated onto a fibronectin coated imaging dish and live cell imaging was performed on a confocal microscope. The 488 channel was used to visualise talin-GFP, the 568 channel to visualise kindlin 1-mCherry, and interference reflection microscopy was used to be able to determine the sites of adhesions without requiring a third transfected protein. Figure 4.2 A shows representative stills from one of these movies, zoomed in on a region where an adhesion is forming. The top panels show the IRM channel, showing areas where the cell is making contact to the substrate as dark regions. Kindlin 2 and talin channels are shown in the bottom two panels. Arrows in each panel denotes points at which the adhesion starts to form and are labeled ‘A’ in the reflectance channel, ’B’ in the talin channel ad ‘C’ in the kindlin-2 channel. Localised increase in kindlin 2-mCherry signal was observed before a similar increase in talin-GFP signal was seen.

Quantification of these movies was performed as in Figure 4.1. A representative sample is shown in figure 4.2 B. The light grey trace shows

the normalised integrated density for kindlin 2-mCherry and the black trace shows the normalised integrated density for talin-GFP. The light grey kindlin-2 trace can be seen to peak earlier than the black talin trace around frame 43. The integrated density and therefore the levels of kindlin-2 fall slightly after this peak. This was also seen for other graphs of different adhesions from many cells produced from this analysis. To be study the results as a group, a meta-analysis was performed to determine the average time to the first peak for either channel as in Figure 4.1. The resulting averages are shown in the graph in Figure 4.2 C. Kindlin 2-mCherry was seen arriving significantly earlier than talin-GFP in forming adhesions in fibroblasts. Taken together, data from Figures 4.1 and 4.2 conclude that both kindlin 1 and kindlin 2 arrive before talin at sites of forming focal adhesions.

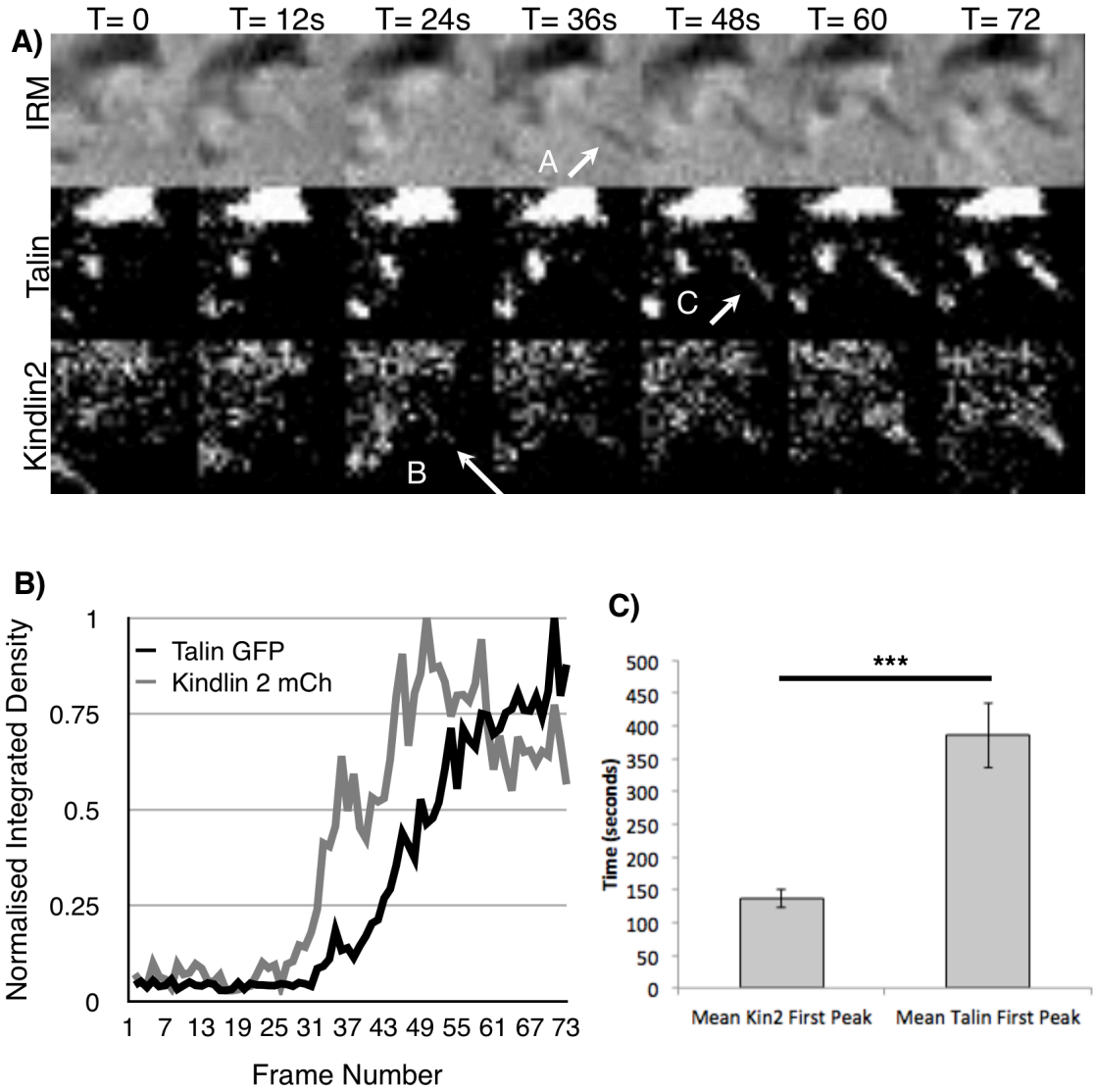

Figure 4.2. Kindlin 2 is present at forming adhesions before talin in NIH3T3 fibroblasts.

A) Confocal stills from time-lapse movies of NIH cells expressing kindlin 1-mCherry and talin-GFP. IRM channel shows contact sites between the cell and the substrate. Arrow A denotes adhesion formation, arrow B denotes kindlin arrival to this site and arrow C denotes talin arrival. Time in second is shown along the top of the image. B) A representative example of the normalised integrated density over time for either kindlin 1-mCherry or talin-GFP for a single focal adhesion. The frame rate is 1 frame every 12 seconds. C) Quantification of the mean time from adhesion initiation to the first normalised peak in either talin-GFP or kindlin 1-mCherry levels. n = >20 adhesions from >10 cells over minimum of 3 experiments. * = $P<0.05$.

4.3 Knockdown of kindlin 1 or kindlin 2 does not affect the amount of talin recruited to focal adhesions

The fact that kindlin 1 and kindlin 2 arrive at forming focal adhesions before talin might suggest that kindlins play a role in recruiting talin to adhesions. To analyse this, kindlin-1 and kindlin-2 shRNA knockdown cells used in Chapter 3 were used to dissect the effect of kindlin knockdown on the recruitment of talin to focal adhesions.

NIH3T3 fibroblasts infected with lentiviral shRNA constructs to knockdown either kindlin 1 or kindlin 2 or infected with a scrambled shRNA were seeded on fibronectin coated glass coverslips and left to adhere before being fixed and stained for endogenous talin followed by Alexa 488 secondary antibody. Representative images from these cells can be seen in figure 4.3 A. In the left panel control shRNA fibroblasts show characteristic talin staining with smaller talin-positive adhesions at the leading edge of a cell, and larger adhesions at the rear of the cell. Kindlin 1 knockdown cells stained for talin show fewer focal adhesions and lower talin localisation, with more talin signal in the perinuclear region. Kindlin 2 knockdown cells stained for talin are poorly spread and have very few talin-positive adhesions, as shown in these cells previously for paxillin and active integrin staining (Figure 3.11).

The talin-positive focal adhesions from these cells were quantified (size and number as described in chapter 3), and the integrated density (intensity) of endogenous talin at each adhesion was also quantified. The resultant graphs are shown in Figure 4.3 B. The number of talin-positive focal adhesions in kindlin 1 knockdown cells was unchanged compared to controls. However, Kindlin 2 depleted cells had a significant reduction in talin-positive focal adhesions. No significant differences were observed in the average size of talin-positive focal adhesions across the different cell lines. Kindlin 1 knockdown cells showed a trend towards increased talin integrated density, whereas kindlin 2 depleted cells tended towards lower talin integrated density. However, neither of these differences was statistically significant when compared to control cells.

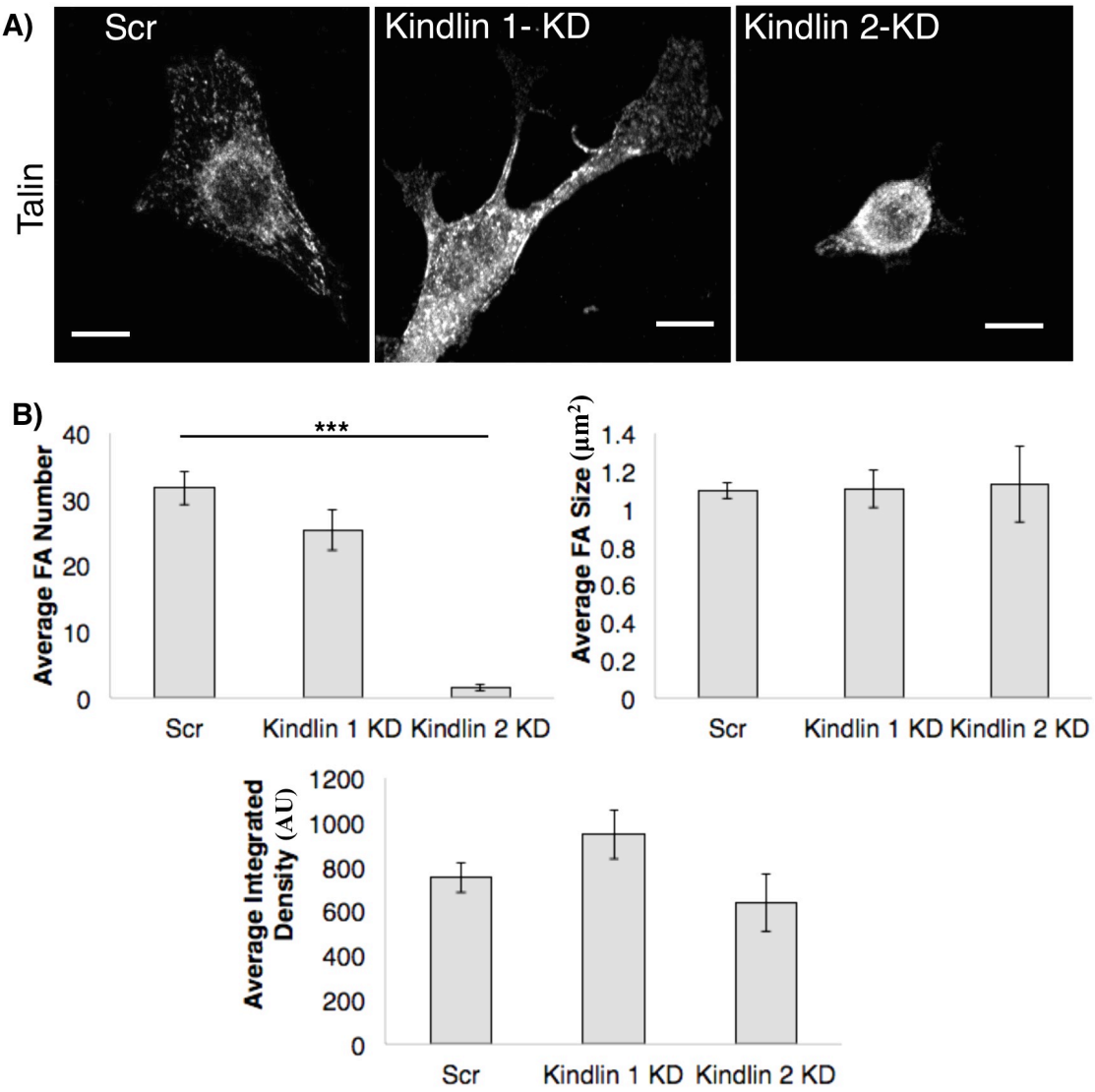

Figure 4.3. Knockdown of kindlin 1 or kindlin 2 does not affect the amount of talin recruited to focal adhesions.

A) Single slice confocal images of fixed NIH3T3 cells transfected with shRNA constructs against kindlin 1, kindlin 2 or a scrambled shRNA sequence on fibronectin coated glass coverslips. Cells were stained for endogenous talin followed by by Alexa 488 secondary antibody. B) Quantification was performed on confocal images of cells knocked down for kindlin 1, kindlin 2 or transfected with scrambled shRNA and stained for talin. Quantification determined average focal adhesion number, size and the average integrated density of proteins stained for in focal adhesions. Error bars are S.E.M. n= >13 cells per condition, graphs are representative of two independent experiments. *** = P<0.0001. Scale bar = 10µm.

4.4 Integrin activation increases talin density within focal adhesions

Data shown in Figure 4.3 suggests that depleting kindlin levels does not specifically alter the amount of talin recruited to focal adhesions, however, as also shown in Chapter 3, kindlin-2 depletion has a significant global effect on focal adhesion assembly and cell morphology. This data suggests that kindlins may not directly impact on the recruitment of talin to adhesion sites. However, the effect may be indirect, meaning that kindlin association with integrins may influence integrin-dependent recruitment of talin (and kindlins) to adhesions. In order to test this, the effects of integrin activation of inhibition on the recruitment of talin, kindlin 1 and kindlin 2 were assessed. Two different approaches were employed; treatment of cells with monoclonal antibodies that activate (9EG7) or inhibit (BMC5) β1 integrin function respectively or treatment of cells with small RGD peptides or Mn^{2+} to mimic outside-in inhibition or activation of integrins respectively. No function activating antibodies are available for mouse β3 integrins so these experiments could only be performed to test β1 functionally. Mn^{2+} ions acts to promote general integrin activation (β1 and β3) through binding to the MIDAS site in integrins and inducing a conformational change, whereas RGD peptides bind the ligand-binding site and mimic association of cells to RGD-containing ligands such as fibronectin (Ginsberg et al., 1985; Mould et al., 2002). Of note, RGD peptides have previously been shown to act as both agonists and antagonists for

integrins, and are recognised as inhibitors for β3 integrin (Caswell et al., 2008) but likely agonists for β1 integrins (M. Parsons et al., 2008).

NIH3T3 fibroblasts were transfected with talin-GFP and seeded onto fibronectin coated glass coverslips and left to adhere overnight. Expressed GFP-tagged proteins were used in these experiments in place of antibody staining for endogenous talin as antibody treatments precluded the use of staining with anti-talin antibodies raised in the same species. Cells were then washed and incubated for 30 minutes with either 9EG7 (10 μg/ml), BMC5 (10 μg/ml) or IgG (10 μg/ml) as a control, or treated with RGD peptide (100 μg/ml) or Mn^{2+} (1mM) for one hour. Cells were then fixed and imaged by confocal microscopy. Representative images of talin-GFP are shown in Figure 4.4 A. Talin-GFP localised to focal adhesions at the edge of the cell, larger focal adhesions and fibrillar adhesions under the cell body following treatment with control IgG antibody, as previously shown for endogenous talin in untreated cells (figure 4.3). After treatment with either 9EG7 or RGD the intensity of talin signal appeared reduced. BMC5, RGD or Mn^{2+} treatment appeared to induce larger talin-GFP positive adhesions than in the control images. Notably, Mn^{2+} treatment resulted in increased protrusion formation and apparent spread cell area compared to other treatments.

Talin-GFP-positive adhesions were quantified as previously described for Figure 4.3 and the average number and size of adhesions and integrated

density of talin-GFP at these adhesions was quantified. The resulting graphs are shown in Figure 4.4 B. There was a trend towards reduced average talin-GFP-positive focal adhesion number following 9EG7 treatment, although this was not statistically significant. However, BMC5, RGD and Mn^{2+} treatment resulted in an increase in talin-positive adhesion number that was statistically significant. Average talin-GFP-positive focal adhesions size was unaffected by most of the treatments, except following RGD treatment when focal adhesions were significantly larger. There was no increase in the talin-GFP integrated density at adhesions in 9EG7 or BMC5 treated cells compared to IgG treated control cells (Figure 4.4, bottom graph). However, there was a statistically significant increase in the talin-GFP integrated density levels at adhesions in both Mn^{2+} treated and RGD peptide treated cells. These experiments demonstrate that activating integrins through outside-in stimulation promotes recruitment of talin to focal adhesions.

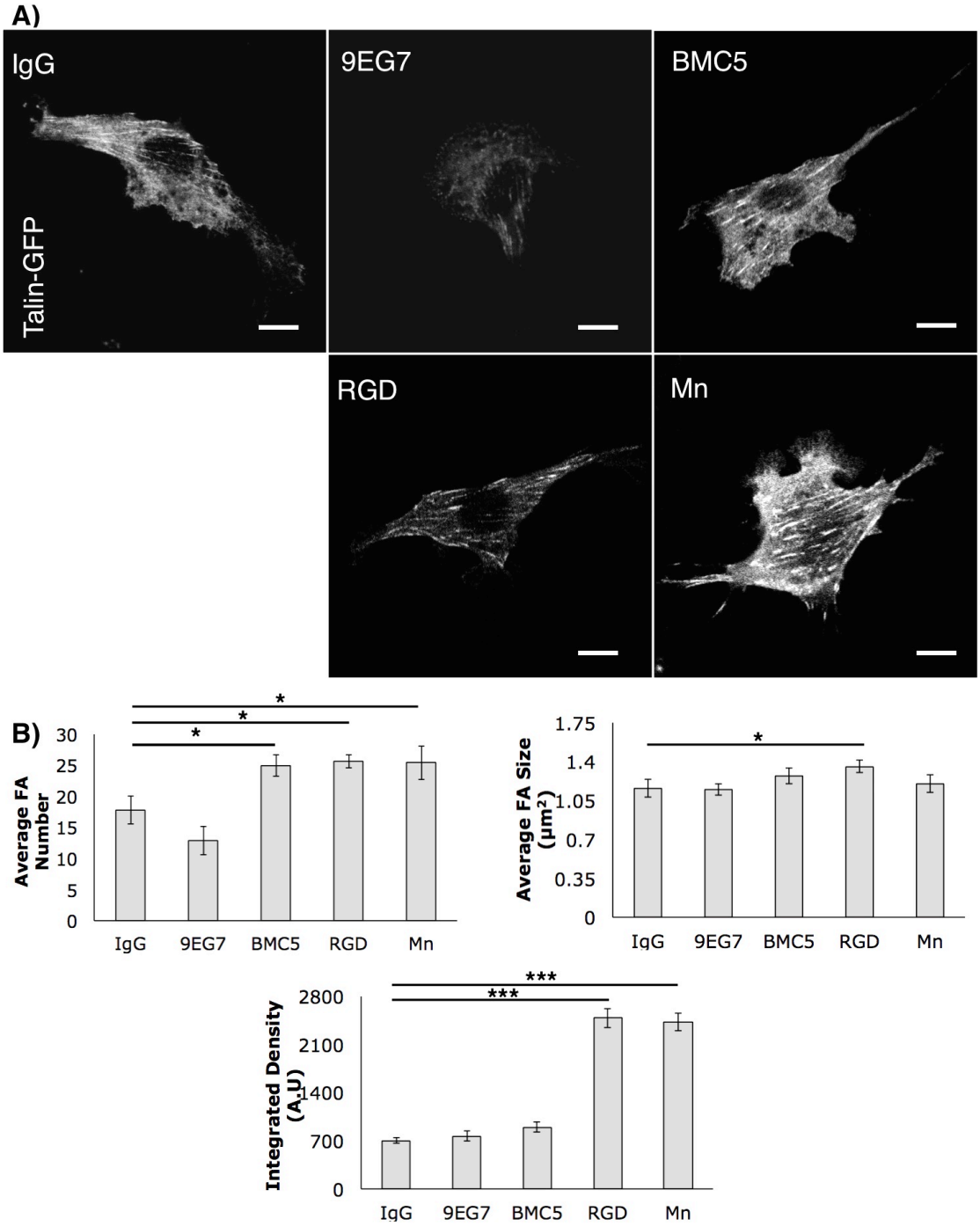

Figure 4.4. Integrin activation increases talin density within focal adhesions

A) Single slice confocal images of fixed NIH3T3 cells transfected with talin-GFP on fibronectin coated glass coverslips treated with IgG (10 µg/ml) as control, 9EG7 (10 µg/ml), BMC5 (10 µg/ml), RGD peptide (100 µg/ml) or manganese (1mM). B) Quantification was performed on confocal images of cells treated as in A. Quantification determined average focal adhesion number, size and the average integrated density of GFP-tagged proteins in focal adhesions. Error bars are S.E.M. n= >18 cells per condition, graphs are representative of two independent experiments. * = P<0.05, ** = P<0.001, *** = P<0.0001. Scale bar = 10 µm.

4.5 RGD treatment reduces the number of kindlin 1-GFP positive focal adhesions

NIH3T3 fibroblasts were transfected with kindlin 1-GFP and seeded onto fibronectin coated glass coverslips and left to adhere overnight. Cells were then washed and incubated with either 9EG7 (10 µg/ml), BMC5 (10 µg/ml), IgG (10 µg/ml) as control or with RGD peptide (100 µg/ml) or Mn2+ (1mM). The cells were then fixed and imaged by confocal microscopy. Representative images of kindlin-1 GFP are shown in Figure 4.5 A. Kindlin 1- localised to focal adhesions at the edge of the cell, and a few larger more mature adhesions beneath the cell body following treatment with control IgG antibody as seen for endogenous kindlin-1 staining (Figures 3.1, 3.2). Treatment of cells with either 9EG7 or BMC5 antibodies or RGD peptide resulted in kindlin 1-GFP localised to adhesions (centre panels,figure 4.5 A). Treatment with Mn^{2+} led to an increase in the number of smaller kindlin1-GFP-positive focal adhesions and an apparent increase in membrane protrusion, as also shown in Figure 4.5.

Kindlin 1-GFP-positive adhesions were quantified as previously described (Figure 4.4), and the average number and size of adhesions and integrated density of GFP-kindlin-1 at these adhesions was quantified. The resulting graphs are shown in Figure 4.5B. Of all the conditions analysed, only RGD treatment resulted in a significantly reduced number of kindlin-1-positive focal adhesions, as shown in the left graph of Figure 4.5B. The

size of kindlin-1-GFP positive adhesions was unaffected by any of the treatments, but the levels of kindlin-1-GFP at adhesion sites was significantly reduced following treatment of cells with RGD peptide (bottom graph, Figure 4.5B).

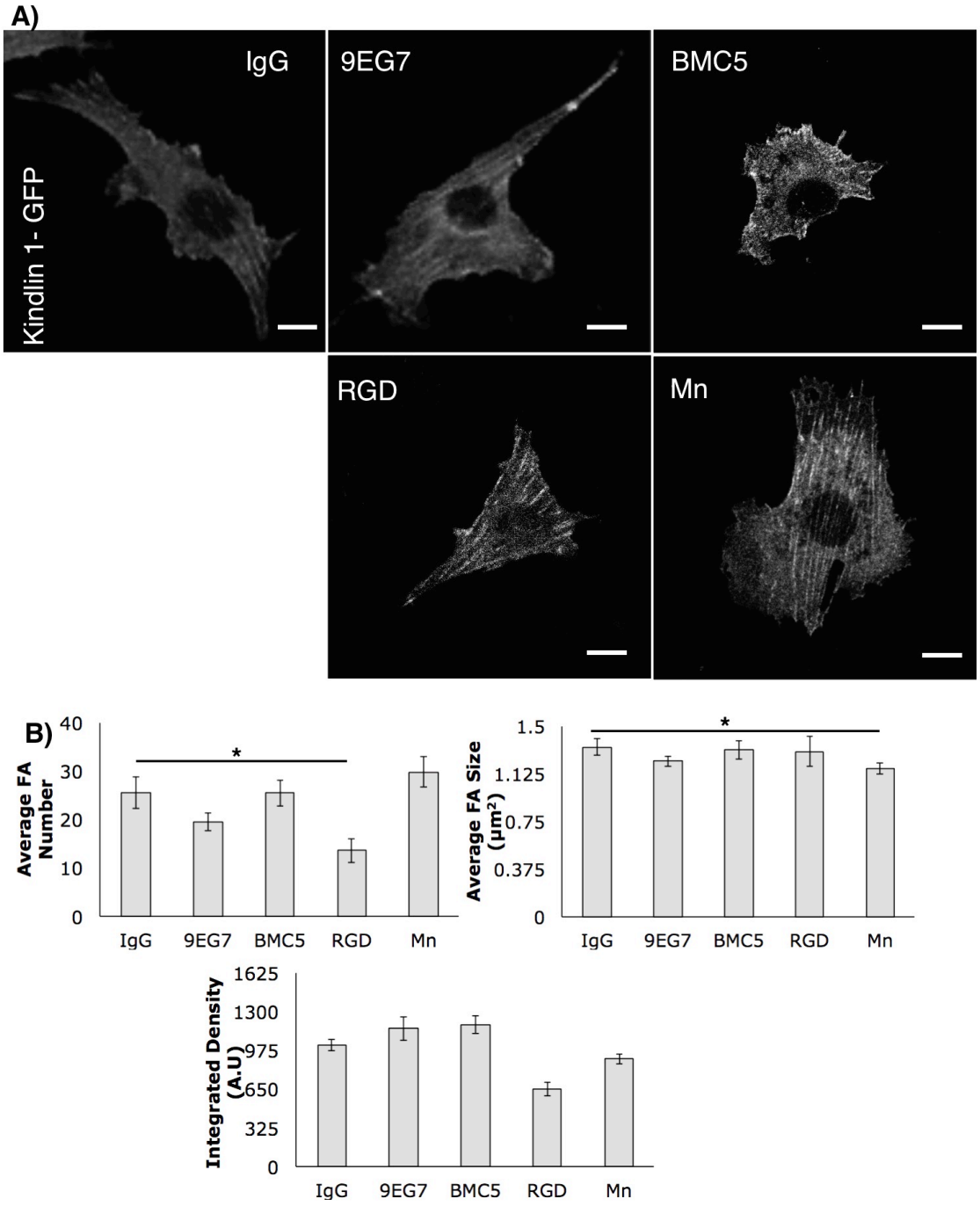

Figure 4.5. RGD treatment reduces the number of kindlin 1-GFP positive focal adhesions.

A) Single slice confocal images of fixed NIH3T3 cells transfected with kindlin 1-GFP on fibronectin coated glass coverslips treated with IgG (10 μg/ml) as control, 9EG7 (10 μg/ml), BMC5 (10 μg/ml), RGD peptide (100 μg/ml) or Mn^{2+} (1mM). B) Quantification was performed on confocal images of cells treated as in A. Quantification determined average focal adhesion number, size and the average integrated density of proteins stained for in focal adhesions. Error bars are S.E.M. n= >18 cells per condition, graphs are representative of two independent experiments. * = $P<0.05$. Scale bar = 10 μm.

4.6 Kindlin 2 at focal adhesions is unaffected by Mn^{2+} or RGD treatments

To determine whether Kindlin-2 also showed reduced recruitment to adhesions following integrin activation manipulation, NIH3T3 fibroblasts were seeded onto fibronectin coated glass coverslips and left to adhere overnight. Cells were then washed and incubated with RGD peptide (100 µg/ml) or Mn^{2+} (1mM) or untreated as control. The cells were then fixed and stained for endogenous kindlin 2 followed by Alexa 488 secondary antibody and imaged by confocal microscopy. Endogenous kindlin-2 was analysed in these experiments due to technical difficulties in expressing sufficient levels of kindlin-2-GFP. Due to this issue, only experiments using RGD or Mn2+ treatment could be performed as treatment with antibodies results in cross-reaction when staining for endogenous proteins.

Representative images of kindlin-2 are shown in Figure 4.6 A. In the top left panel kindlin 2 shows localisation to focal adhesions at the edge of the cell and some, larger focal adhesions beneath the cell body as previously shown in Chapter 3. Treatment with RGD or Mn^{2+} resulted in an apparent shift of Kindlin-2-positive adhesions to the periphery of the cells.

Quantification of the average number and size of adhesions and integrated density of endogenous kindlin-2 was performed as for previous figures. Resulting graphs are shown in Figure 4.6B. There were no significant

differences observed for mean FA number, size or levels of Kindlin-2 at focal adhesions following treatment with either RGD peptide or Mn^{2+}. This data suggests that Kindlin-1 and -2 show differential responses to integrin activation and that Kindlin-1 and talin are more sensitive to changes in outside-in integrin activation in terms of adhesion residence compared to Kindlin-2.

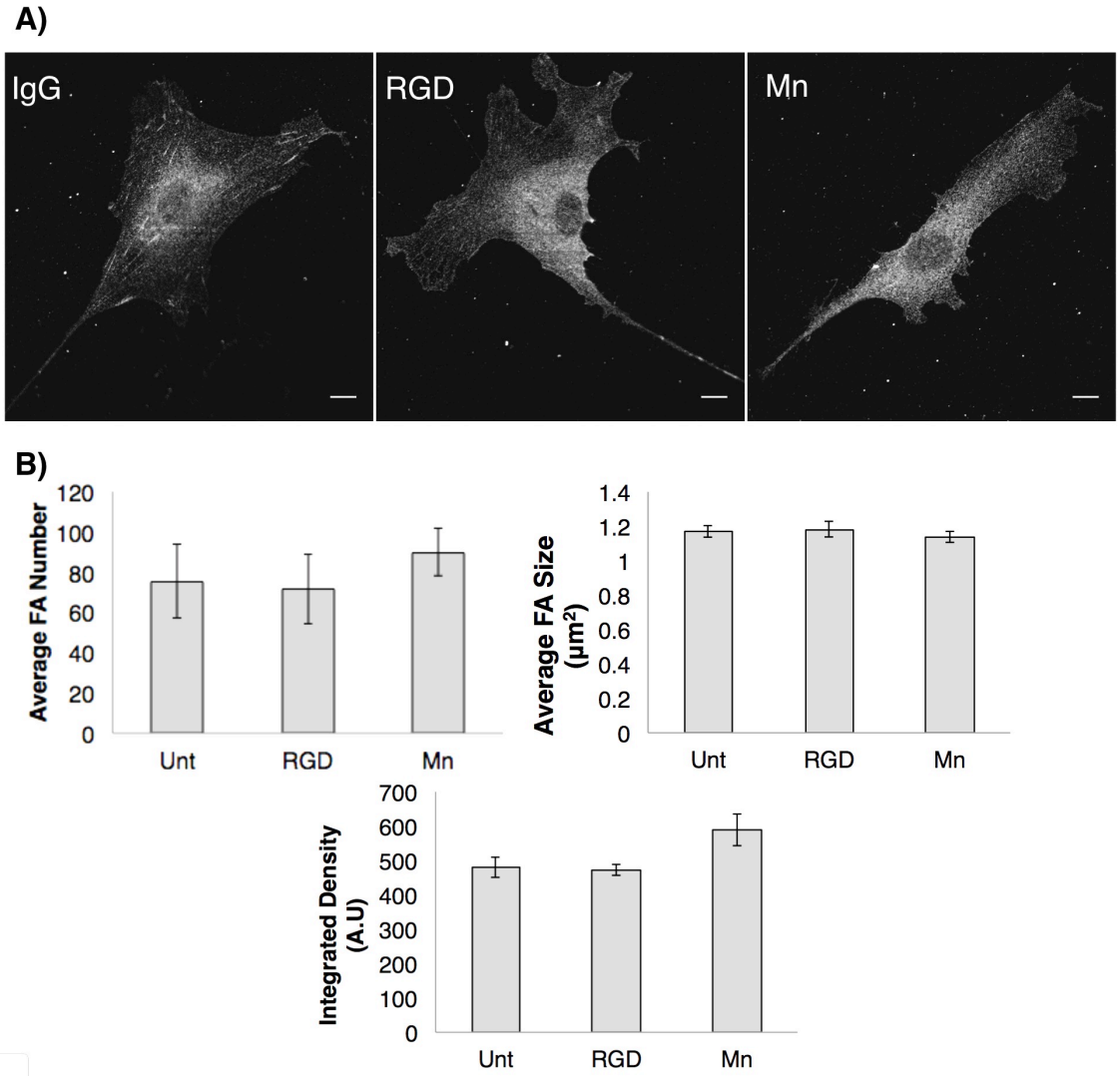

Figure 4.6. Kindlin 2 at focal adhesions is unaffected by Mn^{2+} or RGD treatments.

A) Single slice confocal images of fixed NIH3T3 cells on fibronectin coated glass coverslips treated with RGD peptide (100 μg/ml), Mn^{2+} (1mM) or untreated as control. Cells were stained for endogenous kindlin 2 followed by Alexa 488 secondary antibody. B) Quantification was performed on confocal images of cells treated as in A. Quantification determined average focal adhesion number, size and the average integrated density of proteins stained for in focal adhesions. Error bars are S.E.M. n= >18 cells per condition, graphs are representative of two independent experiments. Scale bar = 10 μm.

4.7 Inhibiting integrin activation results in increased talin binding to integrin β1 and β3 subunits

Previous figures showed that outside-in manipulation of integrin activation using RGD peptides or Mn^{2+} increased density of talin at adhesions. However, it was important to determine whether this result was also seen using a biochemical approach. Previous studies have shown that immunoprecipitation between integrins and talin is not reliably achieved in the absence of chemical crosslinking reagents (Klockenbusch and Kast, 2010; Hirata et al., 2014). In order to determine whether this was also the case in NIH3T3 cells, adherent cells plated onto fibronectin coated dishes were left untreated or treated with the membrane permeable chemical crosslinking compound DSP and subjected to immunoprecipitation using IgG control antibodies or those against β1 or β3 integrin subunits. Complexes were then analysed by western blotting and probed for talin. Representative blots shown in Figure 4.7A demonstrate that no detectable endogenous talin was precipitated with either integrin in the absence of crosslinking reagents. However, treatment with crosslinking reagent resulted in a significant level of talin in both β1 and β3 integrin IP lanes compared to IgG alone control.

In order to determine whether RGD or Mn^{2+} biochemically altered integrin-talin complex formation, adherent cells plated onto fibronectin coated dishes were treated with RGD peptide (100 μg/ml), Mn^{2+} (1mM) or

untreated as control before being cross-linked and lysed. These lysates were cleared of cytoskeletal components and incubated with IgG beads bound with antibodies against integrin β1 or integrin β3 or IgG only as control. After allowing for the binding of the integrin to the antibody bound beads for 2 hours, the beads were washed and samples run on SDS-PAGE gels and probed for talin or kindlin-2.

Figure 4.7 B shows a representative example blots of IPs performed with β1- integrin antibody beads. Talin was associated to similar levels in untreated and RGD-treated cells following IP with β1-integrin antibody beads. Surprisingly, treatment of cells with Mn2+ resulted in reduced levels of talin in complex with β1 integrin (Figure 4.7B). Kindlin-2 levels did not change across the treatments. Analysis of β3 integrin IP's demonstrated a small increase in the level of integrin-associated talin following treatment with RGD and a reduction in cells treated with Mn^{2+} but no clear change in Kindlin-2 levels (Figure 4.7C). Kindlin-1 was not identified in IP complexes under the conditions used, and this is possibly due to the relatively low expression levels in fibroblasts and lower affinity of the antibody for this protein by western blotting.

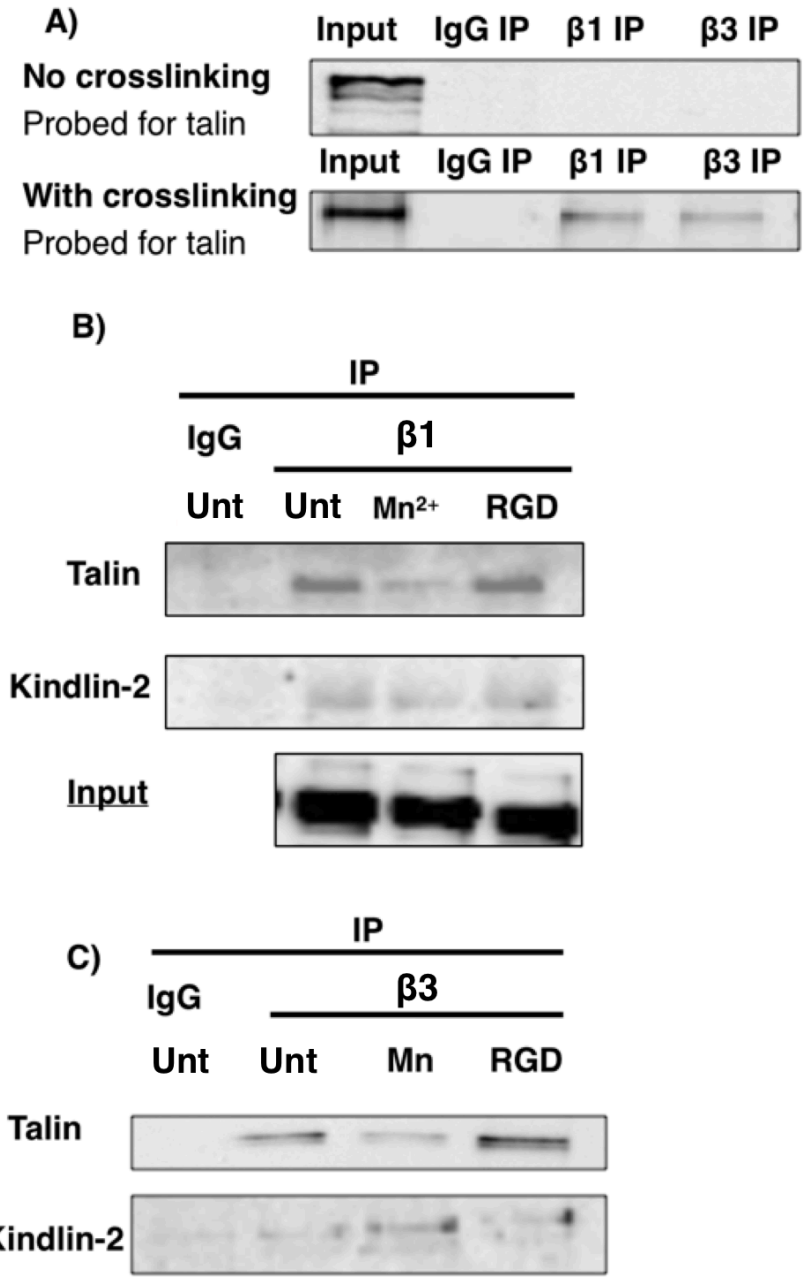

Figure 4.7. Outside-in integrin activation results in reduced talin binding to integrin β1 and β3 integrin subunits.

A) Immunoprecipitation of talin with integrin β1 antibody, integrin β3 antibody or IgG control antibody with lysates either not crosslinked or crosslinked with DSP. Total lysate input is shown in the first lane as control. B) Immunoprecipitation of talin or kindlin-2 with integrin β1 antibody or IgG as control in NIH 3T3 cells treated with manganese, RGD peptide or untreated. Input lysates used for immunoprecipitation were blotted for talin as control. C) Immunoprecipitation of talin or kindlin-2 with integrin β3 antibody or IgG as control in NIH 3T3 cells treated with manganese, RGD peptide or untreated. Blots are representative of three independent experiments.

Discussion

The aim of the experiments in this chapter was to analyse the spatio-temporal recruitment of talin, kindlin 1 and kindlin 2 to sites of forming focal adhesions within live cells and determine whether integrin activation may act as a positive feedback mechanism to recruit talin or kindlin molecules to adhesions. Both kindlin 1 and kindlin 2 were shown to arrive significantly earlier than talin at forming adhesions. This data would agree with the previously proposed model of integrin activation whereby kindlins play a role in potentiating the β subunit cytoplasmic tail of the integrin for talin to bind and fully activate the integrin (Moser, Legate, et al., 2009). Expression of fluorescently labeled proteins carry with them the caveat that in order to provide enough visibility, the proteins must be overexpressed to an extent. Expression of kindlin 1 and kindlin 2 have been previously shown to result in reduced integrin activation independently of being able to bind integrin in CHO cells (Harburger et al., 2009). However, it was also shown that co-expression of the talin head domain with kindlin 1 or kindlin 2 results in increased activation of integrins (Ma et al., 2008; Harburger et al., 2009). In this thesis, expression of kindlin 1 and kindlin 2 was conducted alongside expression of talin in mouse cells which, based on the data in the field, suggests that the observed focal adhesion formation events may have been contributed to by artificial levels of expression of these proteins in that there may have been an increase in activation of integrins. However, the question being asked was which protein arrives at forming

adhesions first therefore the experimental setup was appropriate, albeit with caveats. Recently, in migrating CHO cells, it was published that kindlin 2 is present at forming adhesions before talin is, and a rise in kindlin 2 correlates with a rise in α5 integrin suggesting that they may exist in a complex (Bachir et al., 2014). This study used fluorescence fluctuation methods in order to answer similar questions to that proposed in this thesis and despite using different experimental and analytical methods came to conclusions supporting the data in this thesis. However, the authors did not directly compare the recruitment times of both talin and kindlin 2 within the same cell, and did not look at kindlin 1 at all. As both kindlin 1 and kindlin 2 are known to be able to bind to phospholipids, phospholipids may be recruiting kindlins to adhesions, leading to talin recruitment. The role of phospholipids in adhesion will be explored further in Chapter 5. Alternatively, as other focal adhesion proteins are known to be able to bind kindlins, they could be recruiting kindlins to forming adhesions before talin, independent of kindlin-integrin binding. Possible proteins that are shown to be able to bind to and could recruit kindlins to adhesions are ILK, migfilin or even other kindlins (Mackinnon et al., 2002; Lai-Cheong et al., 2008).

Interestingly, knockdown of kindlin 1 did not significantly reduce the amount of talin at adhesions, but a small reduction was seen. This data suggests that a small amount can compensate for a large reduction in total levels of kindlin 1 or that kindlin 2 can compensate for kindlin 1 loss of

function. Kindlin 2 knockdown, as seen in previous chapters, has a very large effect on the phenotype of the cells, and therefore on the localisation of proteins within it. The poor spreading phenotype explains the significantly lower number of talin positive focal adhesions in these cells. Importantly, there was not a significant reduction in the integrated density of talin following knockdown of either kindlin, suggesting that either a small amount of kindlin is required to recruit talin or that kindlin does not play a role in stabilising talin at focal adhesions. Due to the static nature of these studies on the effect of kindlin knockdown on talin localisation to adhesions, details on the effect on recruitment of talin can not be concluded. Previous biochemical work in CHO cells has suggested that depletion of kindlin 2 does not affect talin recruitment to the plasma membrane, and that over-expression or depletion does not affect the interaction between talin and integrin αIIbβ3 in cells (Kahner et al., 2012). Contradicting this, earlier work in mouse and CHO cells has shown that kindlin-2 is required for talin induced integrin activation of αIIbβ3 and impairs αvβ3-mediated adhesion and migration (Montanez et al., 2008; Ma et al., 2008). Kindlin 1 and 2 clearly have a key role in integrin activation, but this may not be through direct recruitment of talin.

In this chapter RGD and manganese treatement was chosen in order to allow for antibody staining of cells, additionally where antibodies were not used integrin inhibitory or activating anitbodies were used. This was done in order to have two experimental approaches to answer the same

question in order to produce robust data. Cells were treated with the antibodies or treatment while being attached to coverslips prior to being fixed and stained or imaged. Another way of approaching this experiement would be start treatment while cells are in suspension and seed them onto the coverslips directly, this was not done here in order to be able to examine the effects of the treatments on mature adhesions and not just on forming adhesions. Due to time constraints kindlin 2 experiments (Figure 4.6) were performed via staining rather than expression of flouresently labeled kindlin 2. In order to further validate this approach, similar experiments could have been carried out on endogenous talin and kindlin 1 which would also serve to verify the results of data shown in figures 4.4 and 4.5. It was shown in this chapter that RGD and manganese treatment increased the amount of talin recruited to focal adhesions, and the overall number of talin-positive adhesions, but reduced the levels of kindlin 1-positive focal adhesions with no effect seen on kindlin 2. It has been shown that RGD can act to both inhibit and stimulate different types of integrins (Caswell et al., 2008; M. Parsons et al., 2008). Given the similarity in staining and the results between manganese treated and RGD treated cells, it would suggested that RGD is acting as an agonist, activating integrins rather than inhibiting their activation. The data in this chapter would suggest that integrin binding to its extracellular ligand promotes retention of talin at these sites, most likely to maintain linkage between the adhesion and the actin cytoskeleton, yielding two possibilities.

Firstly, kindlin-1 may be displaced either by talin binding to F-actin or through another protein being recruited and specifically displacing kindlin-1 but not kindlin-2 from adhesions. This may be ICAP1 or filamin as both have been shown to be able to bind to integrin β tails at the same membrane distal NPXY motif as kindlin (Y. Liu et al., 2012; Kiema et al., 2006). However, these proteins are thought to inhibit integrin activation. ILK has been shown to be able to bind to kindlin-2 and to further enhance integrin activation (Mackinnon et al., 2002; Montanez et al., 2008) and has also been shown to be able to bind to kindlin 1 as previously shown in mass spectrometry data from our group (Begum, PhD Thesis, 2013). Kindlin 2 may stay at focal adhesions as it has been shown to be required for migfilin targeting to and stability at adhesions and is thought to form part of a link between integrins, kindlins and actin via migfilin and filamin (Brahme et al., 2013).

Secondly, integrin activation and clustering may promote a change in the phospholipid composition of the membranes, releasing kindlin 1 from the membrane at adhesions. The kindlin-1 PH-domain has been shown to be able to bind to negatively charged phospholipids (Yates et al., 2012) and kindlin 2 has been shown to specifically bind to PIP3 (J. Liu et al., 2011). This will be explored further in Chapter 5 of this thesis.

In this chapter it was shown by immunoprecipitation that talin has increased binding with integrins β1 and β3 following RGD treatment, which

is in agreement with the immunofluorescence images and quantification in this chapter. However, manganese treatment resulted in less talin binding to β1 or β3 integrins which is contradictory to the immunofluorescence images and quantification in this chapter. As the immunofluorescence does not analyse direct talin-integrin interactions, the signal may be due to talin recruitment to adhesions no longer being dependant upon integrin binding. FAK is a very well studied protein that is known to be able to bind to PI(4,5)P2, talin and to integrins following activation (Lawson et al., 2012). FAK has been shown to be able to localise to adhesion independently of talin and has been shown to directly bind to talin (Lawson et al., 2012). It has been proposed that FAK may recruit talin to adhesions at adhesion initiation, for talin to be later transferred to integrins to facilitate adhesion maturation (Lawson and Schlaepfer, 2012). Another possibility is that talins proven ability to bind to phospholipids allows it to remain tethered at adhesions binding both to a lipid raft and to actin, thus not needing to be tethered to a transmembrane protein such as integrin. Data in this chapter has frequently raised the question of the role of phospholipids in the recruitment of talin and kindlin to adhesions, this will be explored further in Chapter 5.

5. Defining the requirement of phospholipids for talin and kindlin recruitment

Introduction

Integrin activators are known to be able to bind to specific phospholipids in the membrane via the talin head domain, or the PH domain and the conserved F1-loop domain in kindlins (Elliott et al., 2010; Bouaouina et al., 2012; J. Liu et al., 2011). Kindlins have a PH domain that is known to be required for kindlins to be able to promote integrin activation. Deletion of this domain has been shown to impair kindlin 2-dependent activation of β1 and β3 integrins (Ma et al., 2008; J. Liu et al., 2011). It has been shown biochemically that kindlin 2 PH-domain can bind to PIP3 (J. Liu et al., 2011) and that kindlin 1 PH-domain can also bind to phospholipids (Yates et al., 2012).

Talin is thought to be auto-inhibited as a dimer until near an acidic phospholipid micro-domain such as a PI(4,5)P2 micro-domain, which is thought to relieve this auto-inhibition and allow for binding to integrin β subunit cytoplasmic tails (Elliott et al., 2010). In addition focal adhesions have been shown to be rich in PI(4,5)P2 (Ling et al., 2002). It is not clear if this is true for all focal adhesions and for all cell types, or indeed if this is the case in cells within a more physiologically relevant 3D ECM model. The phospholipids PI(3,4)P2 and PI(4,5)P2 are also both known to be important second messengers and the products of PI3Kinases. PI(3,4)P2 has additionally been shown to regulate recruitment of Akt to the plasma membrane (Franke et al., 1997). It was important to be able to study two

species of PIP2 as well as PIP3 in order to be able to elucidate the specific roles they play in adhesion, potentially in regulating integrin activation through talin and kindlin recruitment, and how integrins contribute to local changes in membrane phospholipid content or distribution.

The aims of this chapter are to assess the effect of inhibition of phospholipid synthesis on the localisation of talin and kindlins and the impact on β1 integrin activation status in 2D and 3D ECM environments. The role of integrins in generating micro domains of specific phospholipids within fibroblasts will also be analysed, as well as the effect of integrin activation on membrane order. The aim is to understand the role of integrins in assembling distinct microenvironments that subsequently may act to recruit specific talin or kindlin proteins to result in maximum integrin activation.

5.1 Quercetin treatment of fibroblasts inhibits PI(3,4)P2 and PI(4,5)P2 localisation to focal adhesions

Phospholipids have previously been indicated to play a role in recruiting a number of key adhesion proteins to focal adhesions. In order to be able to study further the effects of phospholipids on focal adhesion proteins it was important to characterise a tool that inhibits the normal phospholipid cycle. Quercetin is a flavanoid that has previously been shown to act as a pan-inhibitor for kinases involved in both PIP2 and PIP3 generation (Singhal et al., 1995; Walker et al., 2000). This inhibitor was used in preference to other PI3K specific inhibitors as it is able to block both PIP2 and PIP3 production and allows for the assessment of the role of both phospholipids in integrin behavior. NIH 3T3 cells were treated with either 100µM of quercetin or an equal volume of DMSO as a vehicle control. The effect of quercetin treatment on the localisation of specific PIP species was then assessed by immunostaining. Cells were co-stained for paxillin to provide a general marker for focal adhesions.

Endogenous PI(3,4)P2 was seen to localise to the periphery in DMSO-treated NIH fibroblasts, with highest signal near protrusions and focal adhesions (denoted by paxillin staining in the top panels; figure 5.1). Treatment with quercetin resulted in a reduction in overall and peripheral PI(3,4)P2 signal but with some signal still present in vesicles around the peri-nuclear region. PI(4,5)P2 showed similar localization to the cell

periphery in DMSO treated cells and this was significantly reduced following quercetin treatment (middle panels, figure 5.1). Endogenous PIP3 did not show clear localisation to the cell periphery or focal adhesions in untreated cells but rather was seen in small vesicles within the cytoplasm. Quercetin treatment did not result in any change in PIP3 localisation, although overall levels were reduced (Figure 5.1). In all cases, paxillin staining was present at focal adhesions.

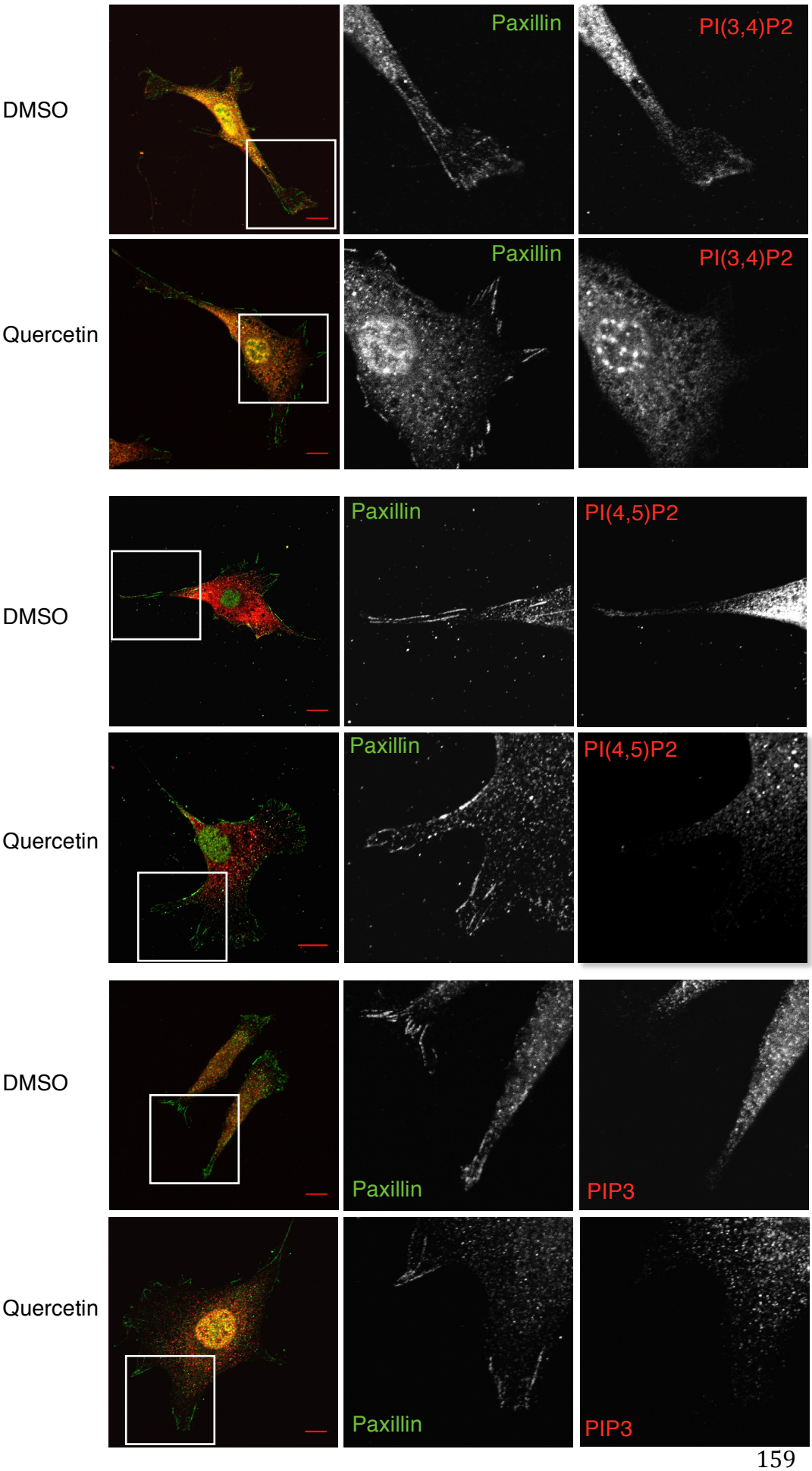
DMSO
Paxillin
PI(3,4)P2
Quercetin
Paxillin
PI(3,4)P2
DMSO
Paxillin
PI(4,5)P2
Quercetin
Paxillin
PI(4,5)P2
DMSO
Paxillin
PIP3
Quercetin
Paxillin
PIP3

Figure 5.1. Quercetin treatment of fibroblasts inhibits PI(3,4)P2 and PI(4,5)P2 localisation to focal adhesions.

Single focal plane confocal images of fixed NIH cells plated on fibronectin coated glass coverslips and treated with either 100μM Quercetin or the same volume of DMSO. Endogenous PI(3,4)P2, PI(4,5)P2 and PIP3 were stained for followed by Alexa 568 secondary antibodies (red). Endogenous paxillin was stained for followed by Alexa 488 secondary antibody (green) Zoomed in images of the highlighted areas are shown as individual channels. Scale bar = 10μm. Representative of ~30 cells per condition from three independent experiments.

5.2 Quercetin treatment alters talin recruitment to adhesions but not kindlin 1 or kindlin 2

Talin and kindlin family proteins contain domains which have been shown to be able to associate with specific phospholipids (Yates et al., 2012; J. Liu et al., 2011; Bouaouina et al., 2012; Moore et al., 2012; Elliott et al., 2010). It was therefore important to quantify the impact of inhibition of phospholipid production on the size, number and localisation of talin, kindlin 1 or kindlin 2 positive adhesions and subsequent integrin activation. NIH 3T3 fibroblasts were plated onto fibronectin-covered coverslips and left to adhere overnight before being treated with either 100μM quercetin or an equal volume of DMSO for an hour. Coverslips were then fixed and immunostained with 9EG7 to detect active-β1 integrin or antibodies against endogenous talin, kindlin 1 or kindlin 2. Cells were then imaged by confocal microscopy and example images are shown in figure 5.2.

Quercetin-treated cells showed reduced peripheral staining for talin and active-β1 integrin compared to control cells (top panels, Figure 5.2). However, no differences were seen in kindlin1 or kindlin2 staining between control and quercetin treated cells (Figure 5.2, middle and bottom panels).

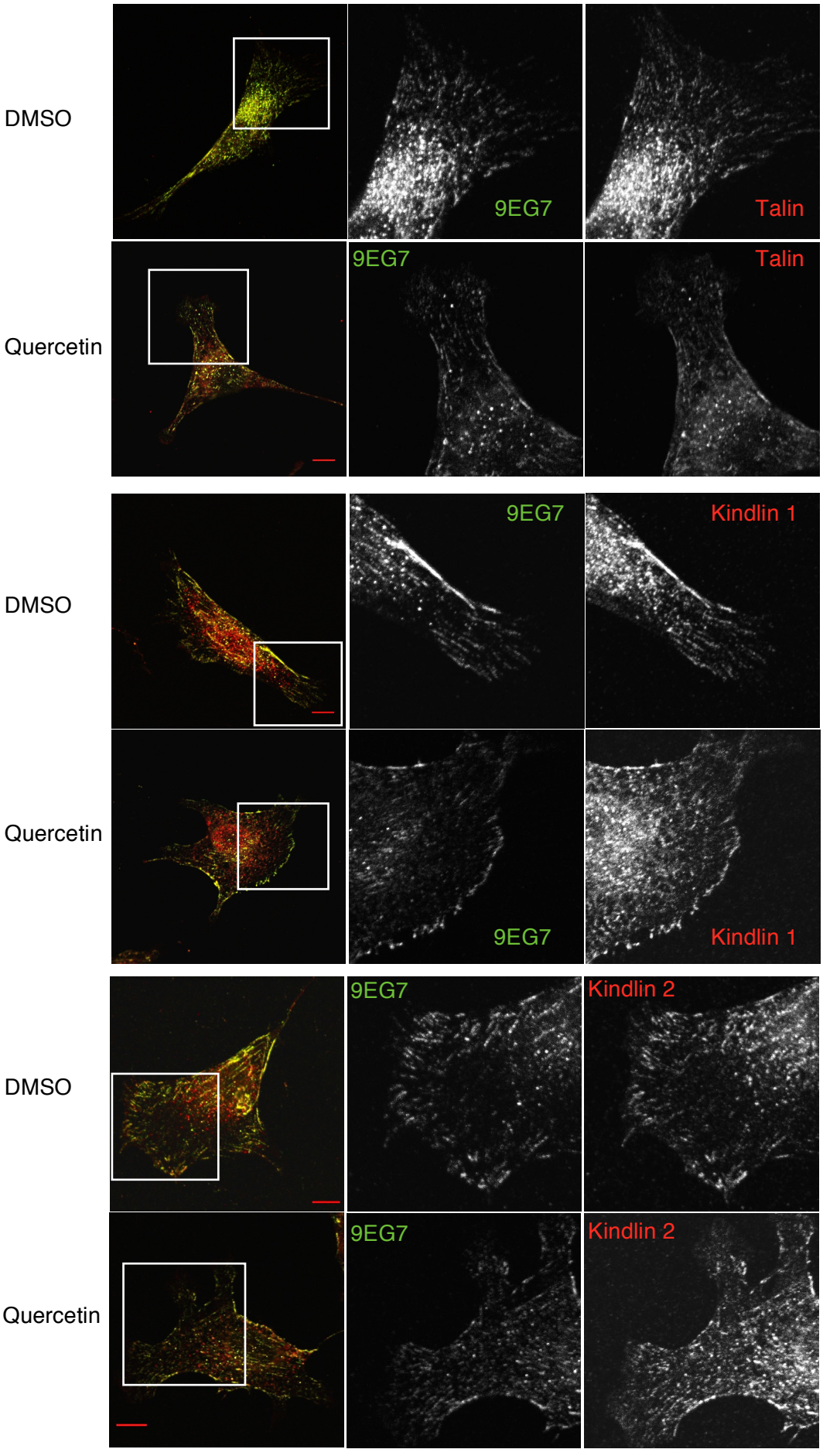
DMSO
9EG7
Talin
Quercetin
9EG7
Talin
DMSO
9EG7
Kindlin 1
Quercetin
9EG7
Kindlin 1
DMSO
9EG7
Kindlin 2
Quercetin
9EG7
Kindlin 2

Figure 5.2. Quercetin treatment reduces adhesion localisation of talin, but not kindlin 1 or kindlin 2.

Single slice confocal images of fixed NIH cells plated on fibronectin coated glass coverslips and treated with either 100μM Quercetin or the same volume of DMSO. Endogenous talin, kindlin 1 or kindlin 2 were stained for followed by Alexa 568 secondary antibodies (red). Active-β1 integrin was stained for by using 9EG7 antibody followed by Alexa 488 secondary antibody (green) Zoomed in images of the highlighted areas are shown as individual channels. Scale bar = 10μm. Representative of ~30 cells per condition from three independent experiments.

5.3 Inhibiting phospholipid production with quercetin results in reduced number of focal adhesions containing talin and active-β1 integrin

Confocal images of quercetin or DMSO-treated cells stained for talin, kindlin 1, kindlin 2 or 9EG7 as shown in figure 5.2 were quantified to determine the average number, size and area of talin, kindlin 1, kindlin 2 or 9EG7-positive focal adhesions. The integrated density was also measured as this reports on the concentration of signal and therefore the density of staining for each protein within adhesions.

The quantification, shown in figure 5.3, showed that following quercetin inhibition of phospholipid production there was a significant reduction in the number and area of talin-positive focal adhesions. Similarly, 9EG7-positive focal adhesion number and area decreased significantly following treatment with quercetin. However, there was no significant effect of quercetin treatment on average focal adhesion size, area, number or integrated density for kindlin 1 or kindlin 2 positive adhesions. There was also no significant effect of quercetin treatment on talin or 9EG7 positive focal adhesion size or integrated density.

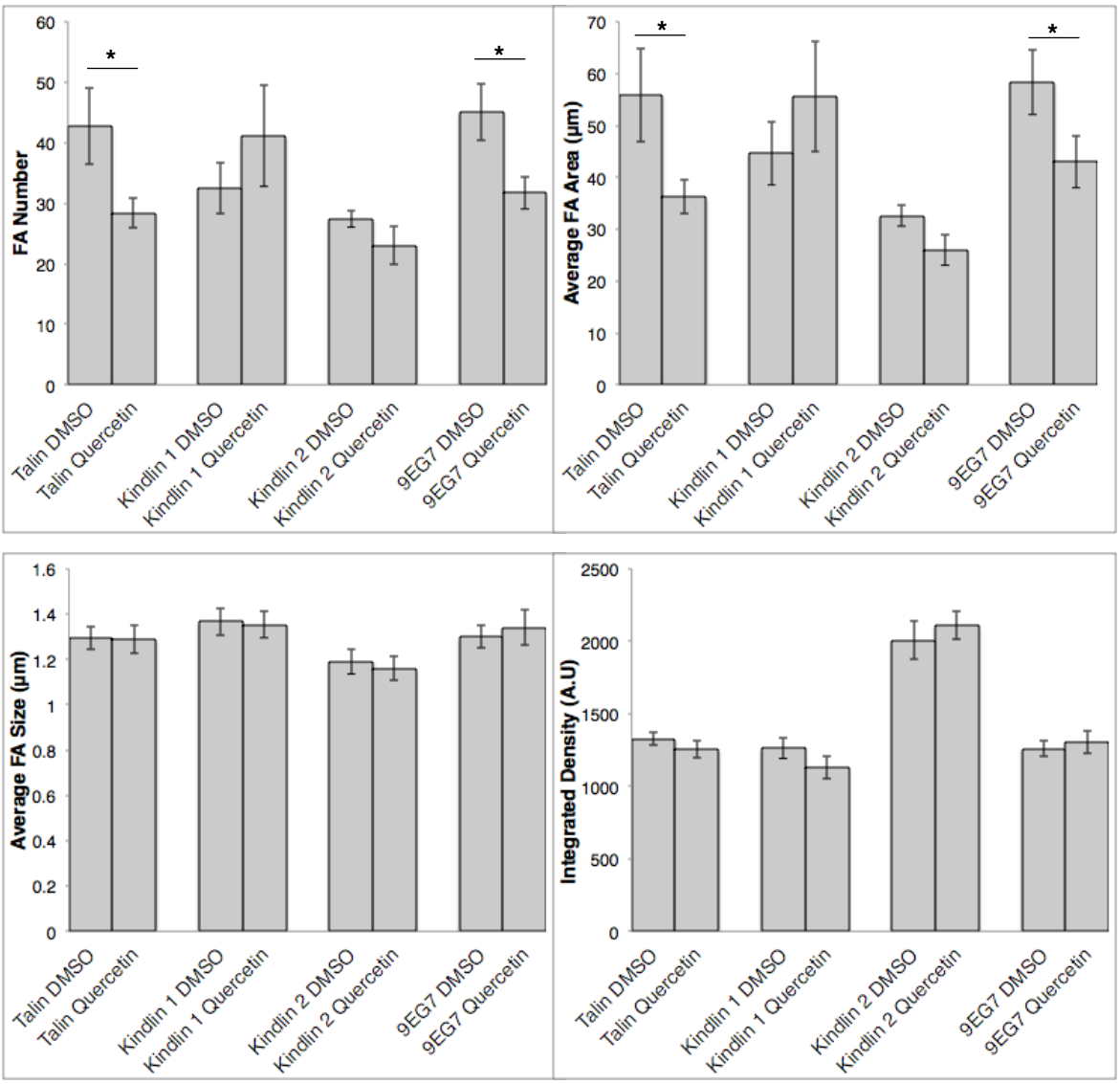

Figure 5.3. Inhibiting phospholipid production with quercetin results in reduced number of focal adhesions containing talin and active-β1 integrin.

Quantification was performed on confocal images of DMSO or quercetin treated NIH cells stained for talin, kindlin 1, kindlin 2 or 9EG7 as shown in figure 5.2. The quantification determined average focal adhesion number, size, total area, and the integrated density of the proteins stained for in focal adhesions. Error bars are S.E.M., n= >25 cells per condition, graphs are representative of three independent experiments, * = P<0.05.

5.4 Quercetin treatment increases talin binding to β1 and β3 integrins in NIH3T3 cells

Data shown in this chapter demonstrated that quercetin treatment inhibited the levels and recruitment of both PI(3,4)P2 and PI(4,5)P2 at adhesion sites (Figure 5.1) and this correlated with a reduction in levels of talin, but not kindlins, at focal adhesions and a reduction in active β1 integrins (Figures 5.2, 5.3). In order to determine whether the apparent decrease in talin lcoalisation to adhesions also resulted in reduced talin-integrin association, co-IP's were performed using antibodies against either β1 or β3 integrins. In order to retain association between integrin and talin, cells were pre-treated with the membrane permeable crosslinker DSP prior to lysis, as previously shown in Chapter 4. Cells were also treated with DMSO or 100μM quercetin for an hour before being cross linked and incubated with IgG beads bounds with antibodies against integrin β1 or integrin β3 or IgG only as control. After allowing for the binding of the integrin to the antibody bound beads for 2 hours, the beads were washed and analysed by western blotting.

Figure 5.4 A shows a representative example of results from β1 integrin IP experiments however, equal levels of β1 and β3 integrin in the materials used for the IP has not been shown here. Also, ideally the amount of protein being used would have been quantified and equalied prior to each experiment. Data shown here demonstrated that both talin and kindlin 2

were associated with β1 integrin under control conditions, and levels of both complexes increased following incubation of cells with quercetin (Figure 5.4A). Talin and kindlin 2 were not precipitated with IgG alone. Similar results were found for β3 integrin complexes, where both talin and kindlin 2 levels increased in the complex following quercetin treatment (Figure 5.4B). This data suggests that PIP2 inhibition may lead to reduced integrin-talin association at adhesion sites, but enhanced binding outside adhesion structures, potentially to maintain the integrins in an inactive conformation.

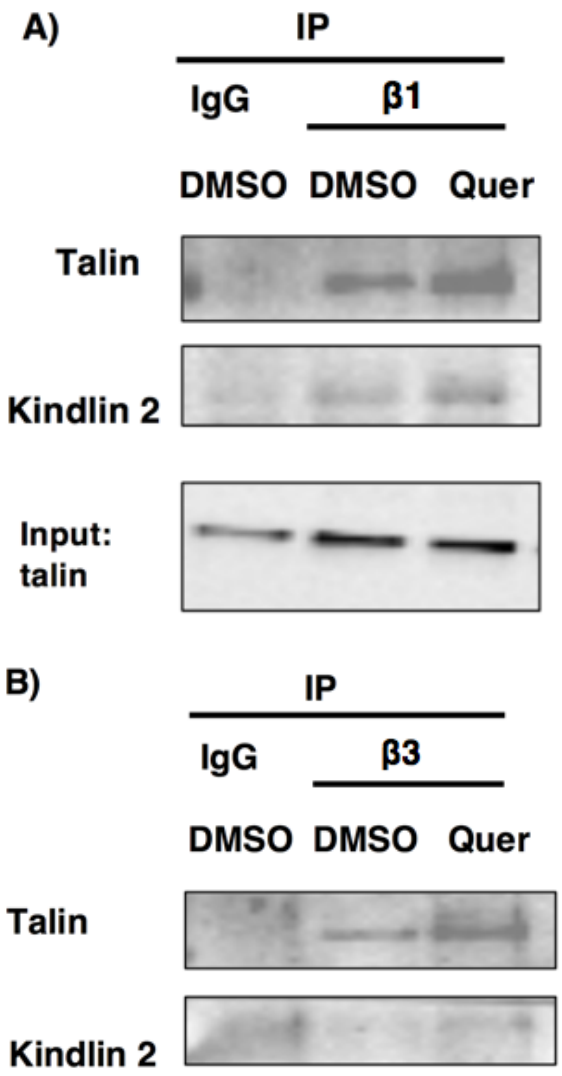

Figure 5.4 Quercetin treatment increases talin binding to β1 and β3 integrin in NIH3T3 cells.

A) Immunoprecipitation of talin or kindlin 2 with integrin β1 antibody or IgG as control in NIH cells treated with DMSO or quercetin. IgG heavy chain is shown as control for antibody concentration. B) Immunoprecipitation of talin or kindlin 2 with integrin β3 antibody or IgG as control in NIH cells treated with DMSO or quercetin. C) Input lysates used for immunoprecipitation were blotted for talin as control. Blots are representative of three independent experiments.

5.5 ECM dimensionality and integrin expression do not affect global levels of PI(3,4)P2 or PIP3

As shown in Chapter 3, the dimensionality of the substrate that cells are in changes the nature of cell adhesions. It was therefore important to establish whether cells in 2D vs. 3D environments showed changes in their phospholipid content. NIH cells were allowed to adhere to either fibronectin or to CDM before being lysed and analysed by dot blot for PIP2, PIP3 or GAPDH as a loading control (Figure 5.5A). Results showed no observable differences between the amount of detected PIP2 or PIP3 in cell lysates from cells in CDM or on fibronectin.

It was also important to determine if specific integrins play a role in production of phospholipids and thus potentially influence recruitment of adhesion proteins. . Figure 5.4 B shows levels of PIP2 or PIP3 from β1 integrin or β3 integrin knock-out (KO) MEFs compared with NIH 3T3 cells. Again, data showed no observable changes in the levels of PIP2 or PIP3 between control cells and integrin KO cells. Together these data show that different ECM environments or integrin subunits do not significantly alter phospholipid levels in fibroblasts.

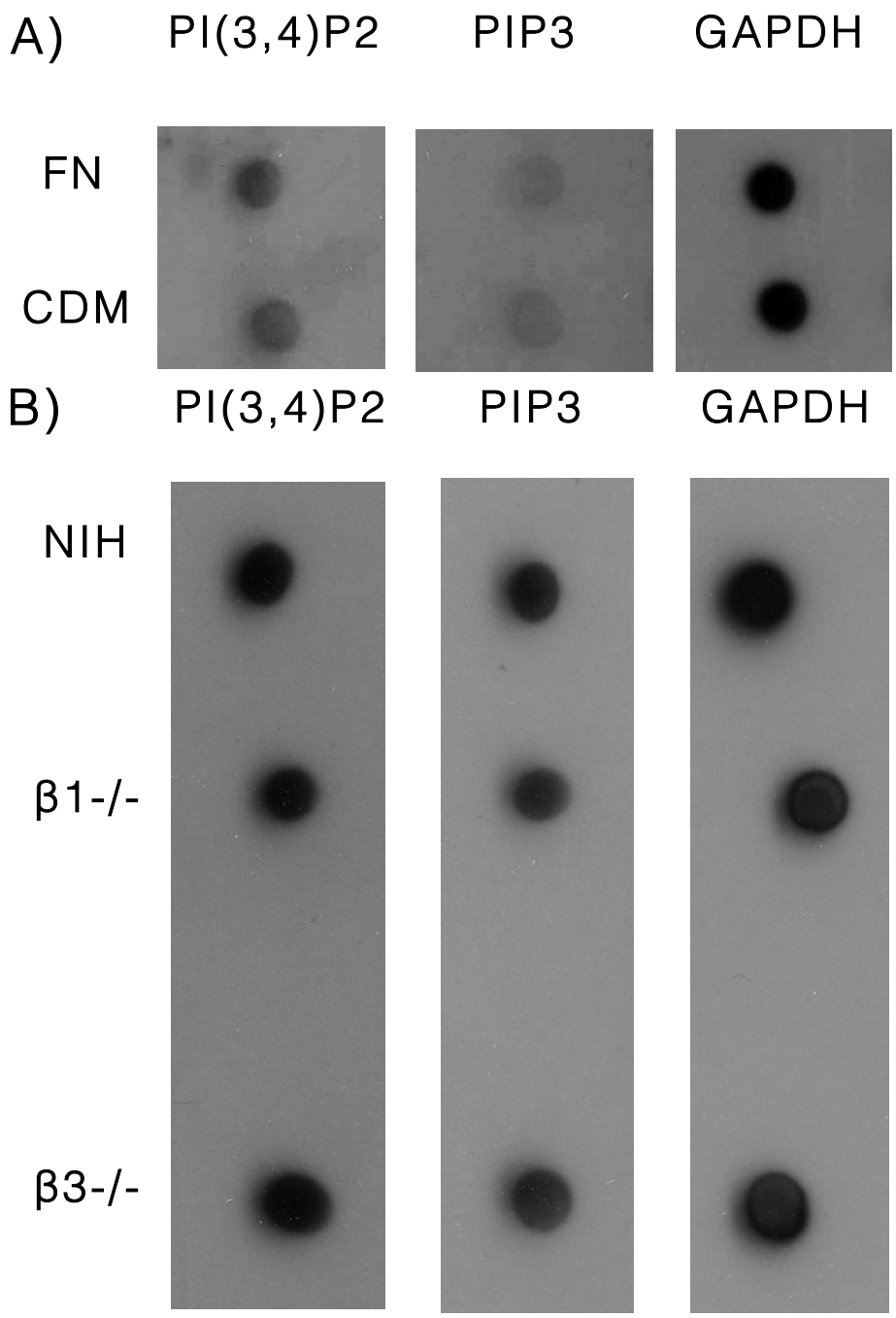

Figure 5.5. ECM dimensionality and integrin expression do not affect global levels of PI(3,4)P2 or PIP3.

A) Dot blot of NIH cell lysates plated onto either FN or CDM and blotted for either PI(3,4)P2, PIP3 or GAPDH as a loading control. B) Dot blot of NIH, β1-/- KO MEF or β3-/- KO MEF cell lysates blotted by use of antibody for either PI(3,4)P2, PIP3 or GAPDH as a loading control. Representative of three independent experiments.

5.6 PIP2 levels increase prior to adhesion assembly in NIH3T3 cells

Cell adhesion and migration is a dynamic process and as such it was important to analyse adhesion formation and assembly in live cells to complement fixed analysis and quantification. A number of phospholipid biosensors have been characterised to enable the study of phospholipid localisation in live cells. The PH domain-GFP sensors are the most commonly used, and these localise to sites of high concentrations of specific phospholipids depending upon the PH domain used. PLCδ1-PH-GFP is one such construct which uses the phospholipid binding PH-domain of PLCδ which is known to associate specifically with PI(4,5)P2 and enable visualisation of PIP2 dynamics over time (Zhang et al., 2004; Murata and Okamura, 2007, Source: B.J. Eickholt (KCL)).

NIH 3T3 cells were transfected with PLCδ1-PH-GFP and 24 hours later were plated onto fibronectin-coated imaging plates before live cell imaging was performed using a confocal microscope. The 488nm channel was used to visualise GFP, and interference reflection microscopy (IRM) was also performed at the same time to enable the interface between cell and coverslip where adhesions are formed to be assessed simultaneously. Figure 5.6 shows representative frames from a preliminary recording of an NIH cell transfected with PLCδ1-PH-GFP forming an adhesive protrusion. PH-GFP is seen increasing in the protrusion prior to the reflectance channel showing new adhesions being made (arrows in Figure 5.6).

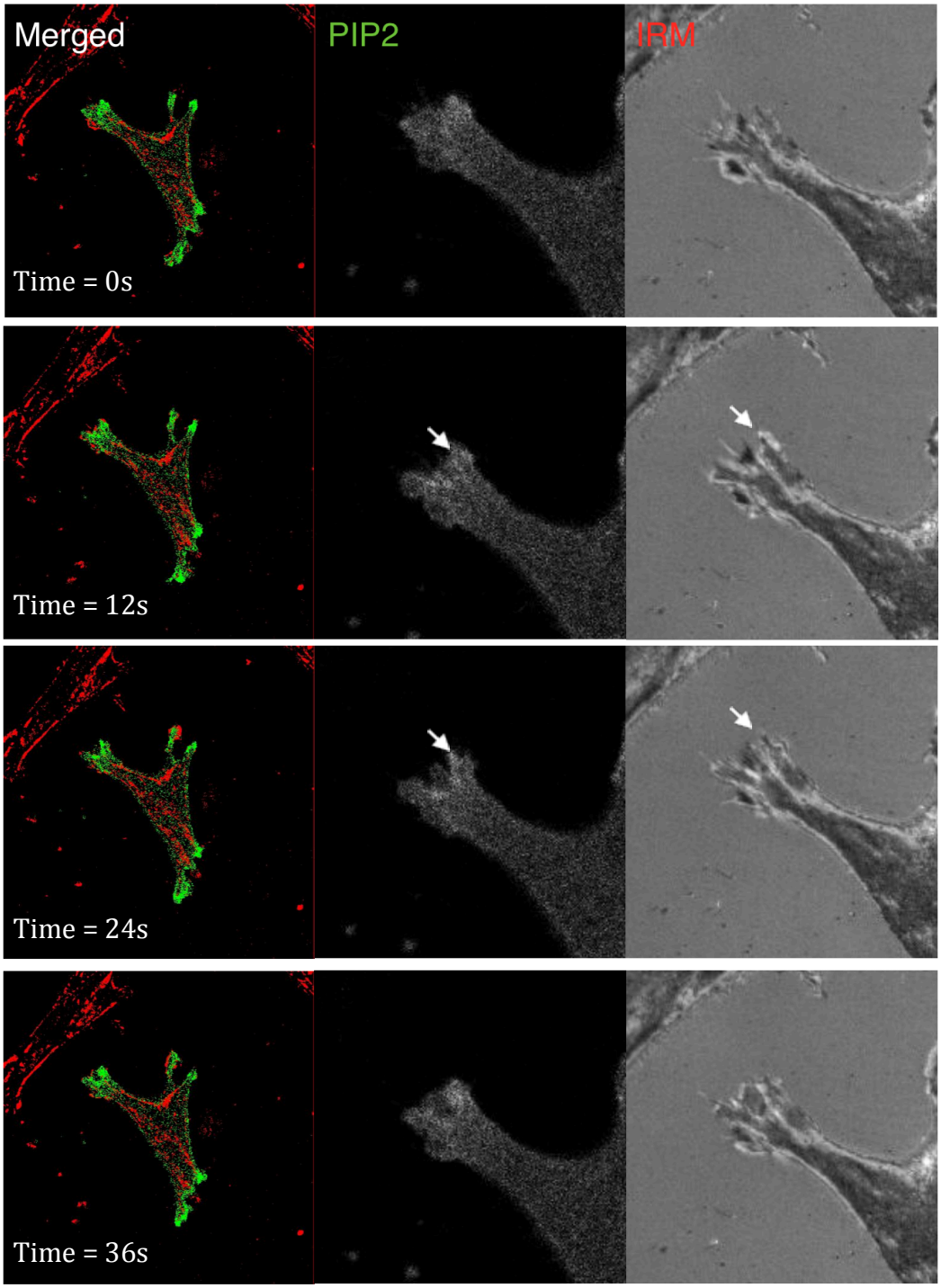

Figure 5.6. PIP2 levels increase prior to adhesion assembly in NIH3T3 cells.
Confocal stills from time-lapse movies of NIH cells expressing the PIP2 domain sensor, PLCδ1-PH-GFP. IRM channel shows contact sites between the cell and the substrate and is shown in the merged image as a thresholded channel (pseudocoloured in red). Localisation of PIP2 is indicated by an increase in PLCδ1-PH-GFP (green). Representative of 12 cells from two independent experiments.

5.7 PIP3 levels do not correlate with formation of new adhesions or protrusions in NIH 3T3 cells

In order to determine whether the changes in PIP2 localisation prior to adhesion assembly also occurred with PIP3, similar preliminary experiments were performed using the PH domain of the lipid kinase Akt tagged to GFP, which is a known reporter of localized PIP3 in cells (Várnai et al., 2005, Source: B.J. Eickholt (KCL)).

NIH 3T3 cells were transfected with Akt-PH-GFP and 24 hours later were plated onto fibronectin coated imaging plates before live cell time-lapse imaging was performed using confocal microscopy. The 488 channel was used to visualise GFP, and IRM was also performed at the same time. Figure 5.7 shows representative frames from a recording of a preliminary experiment of an NIH cell transfected with Akt-PH-GFP forming an adhesive protrusion. Akt-PH-GFP localises to the plasma membrane and is enriched at some membrane regions, but does not accumulate at sites immediately prior to protrusion or adhesion formation (arrows and insets).

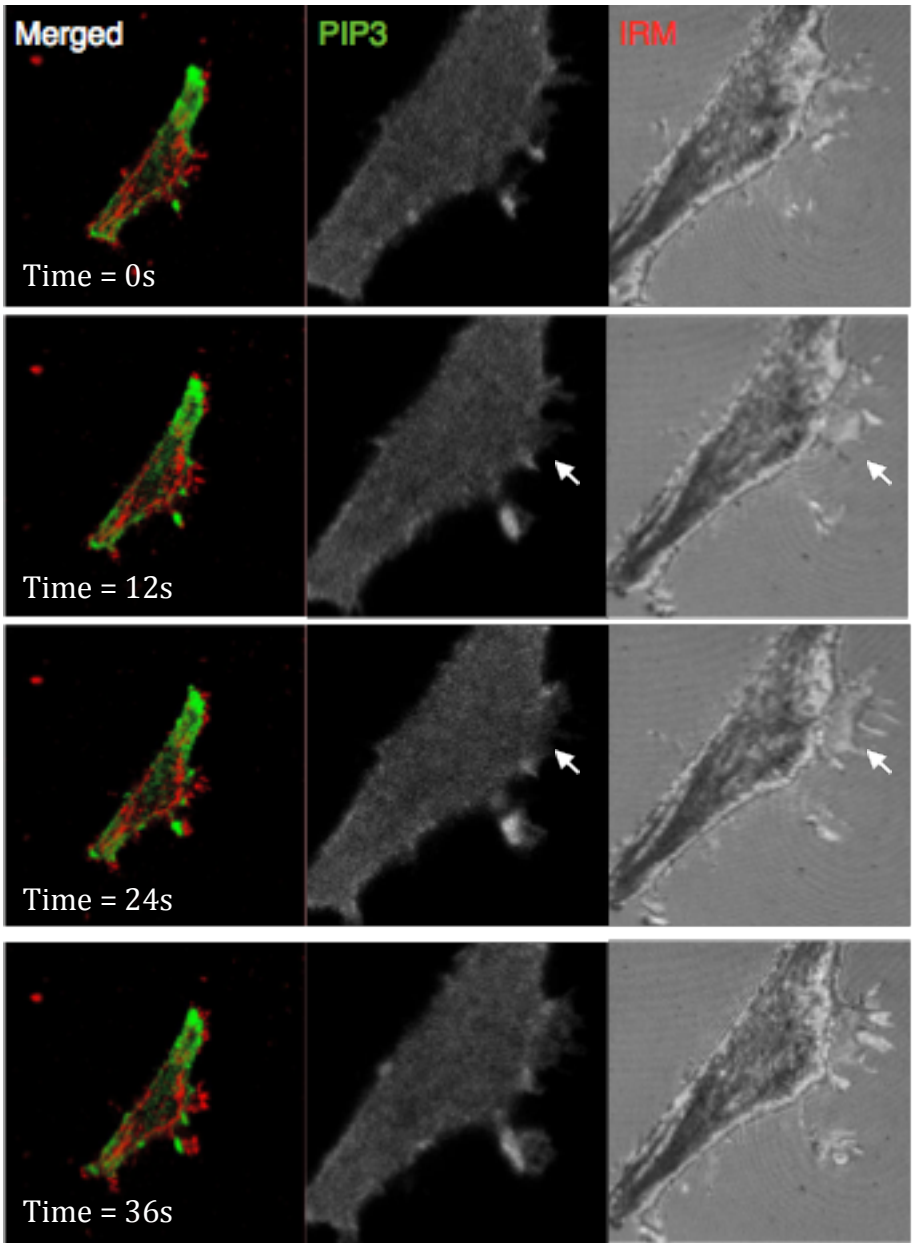

Figure 5.7. PIP3 levels to not correlate with formation of new adhesions or protrusions in NIH3T3 cells.

Confocal stills from time-lapse movies of NIH cells expressing the PIP3 domain sensor, Akt-PH-GFP. IRM channel shows contact sites between the cell and the substrate and is shown in the merged image as a thresholded channel (pseudocoloured in red). Increase in PIP3 is indicated by an increase in Akt-PH-GFP (green). Representative of 11 cells from two independent experiments.

5.8 PI(3,4)P2 does not localise to focal adhesions in β1 integrin knockout cells

Having shown that there are no global differences in the levels of phospholipids between NIH integrin knockout cells (Figure 5.5), but that PIP2 is locally recruited to new protrusion/adhesion sites (Figures 5.6 and 5.7) it was important to determine whether specific integrins may dictate local accumulation of different phospholipid species.

In order to asses this question, NIH 3T3, β1-/- or β3-/- fibroblasts were seeded onto fibronectin coated coverslips and fixed before being stained for endogenous PI(3,4)P2 and paxillin as a marker for focal adhesions. IRM was again used to further identify overall regions where cells were in contact with the glass. In NIH and β3-/- cells, PI(3,4)P2 was seen at the ends of protrusions overlapping with both paxillin-positive focal adhesions and IRM signals showed contact to the substrate (figure 5.8 top and bottom panels). However in β1-/- cells, PI(3,4)P2 was not seen at the cell periphery or to overlap with paxillin staining or IRM signals (Figure 5.8 middle panels) suggesting that β1 integrin may specifically control localization of PI(3,4)P2.

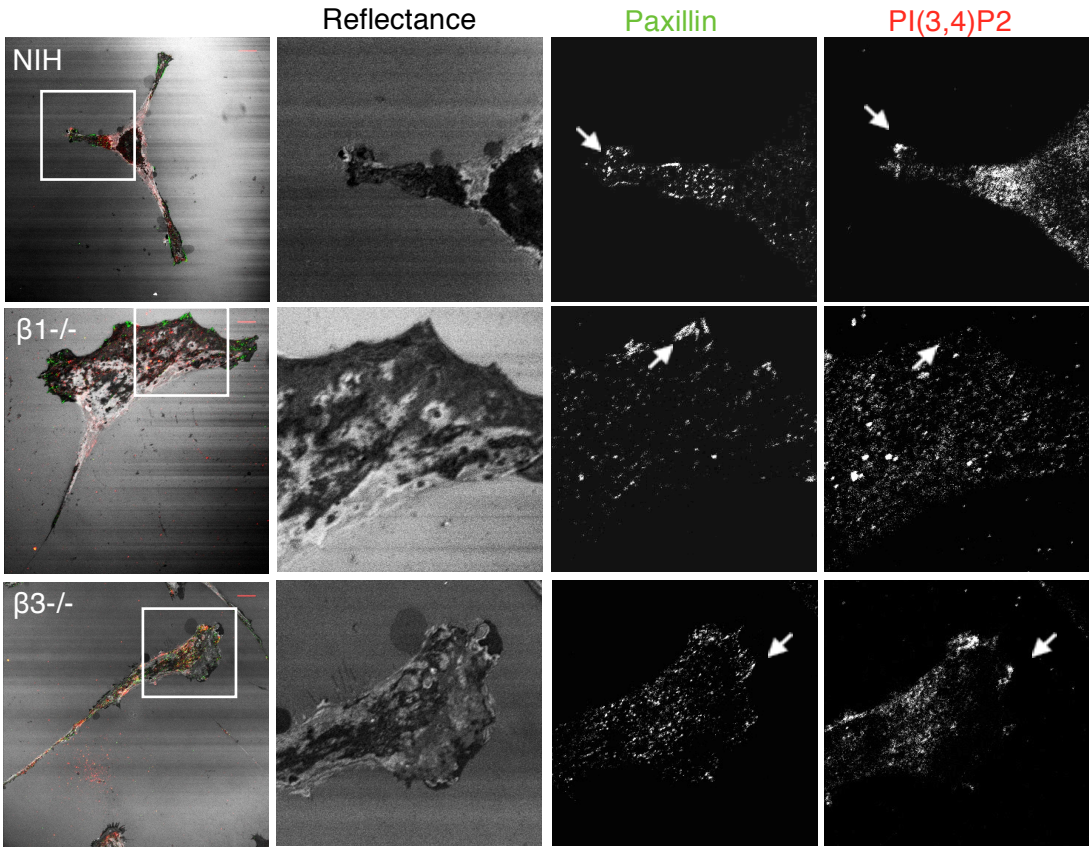

Figure 5.8. PI(3,4)P2 does not localise to focal adhesions in β1 integrin knockout cells.

Single slice confocal images of fixed NIH 3T3, β1-/- or β3-/- cells plated on fibronectin coated glass coverslips. Endogenous PI(3,4)P2 was stained for followed by Alexa 568 secondary antibodies (red). Endogenous paxillin was stained for followed by Alexa 488 secondary antibody (green). Interference reflection microscopy was used to show contact between the cells and the substrate (grey). Zoomed in images of the highlighted areas are shown as individual channels. Scale bar = 10μm. Representative of ~30 cells per condition from three independent experiments.

5.9 PI(4,5)P2 localises to focal adhesions in 2D and does not require β1 integrin

In order to determine whether the changes in localisation of PI(3,4)P2 at β1-/- adhesions was also the case for PI(4,5)P2, NIH 3T3, β1-/- or β3-/- fibroblasts were seeded onto fibronectin coated coverslips and fixed before being stained for endogenous PI(4,5)P2 and paxillin as a marker for focal adhesions. IRM was used to further identify where cells were in contact with the glass. NIH 3T3, β1-/- and β3-/- cells all showed PI(4,5)P2 localization at the ends of protrusions broadly overlapping with both paxillin-based focal adhesions and where the IRM channel showed contacts (Figure 5.9). Overall, this suggests that β1-/- can contribute specifically to recruitment or generation of PI(3,4)P2 at focal adhesions.

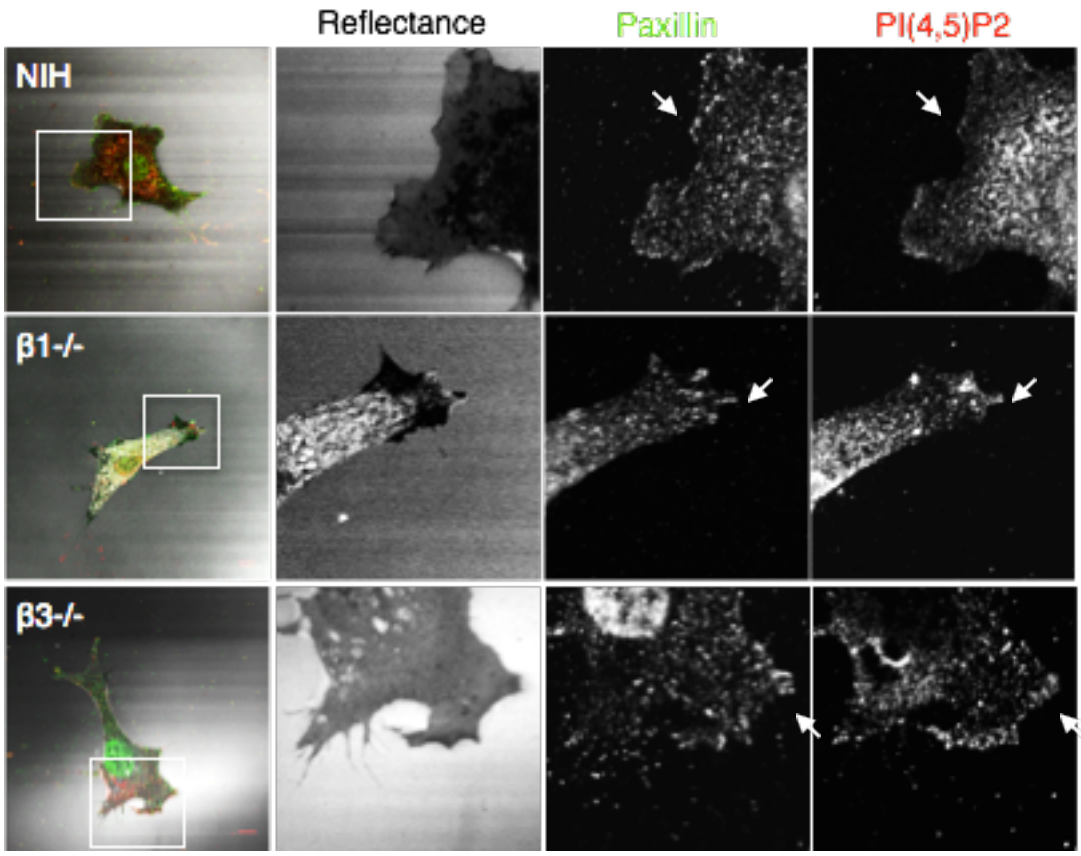

Figure 5.9. PI(4,5)P2 localises to focal adhesions in 2D and does not require β1 integrin.

Single slice confocal images of fixed NIH, β1-/- or β3-/- cells plated on fibronectin coated glass coverslips. Endogenous PI(4,5)P2 was stained for followed by Alexa 568 secondary antibodies (red). Endogenous paxillin was stained for followed by Alexa 488 secondary antibody (green). Interference reflection microscopy was used to show contact between the cells and the substrate (grey). Zoomed in images of the highlighted areas are shown as individual channels. Scale bar = 10μm. Representative of ~30 cells per condition from three independent experiments.

5.10 PIP3 does not localise to focal adhesions in control, β1-/- or β3-/- fibroblasts

PIP3 can be produced downstream of both PI(3,4)P2 and PI(4,5)P2 lipid species and previous figures have shown PIP2 PH domain reporters and endogenous PIP2, but not PIP3 PH domain reporters localize to focal adhesions. It was therefore important to analyse PIP3 localisation in fibroblasts. NIH 3T3, β1-/- or β3-/- cells were seeded onto fibronectin-coated coverslips and fixed before being stained for endogenous PIP3 and paxillin. IRM was used to further identify where cells were in contact with the glass. Images shown in Figure 5.10 demonstrate that PIP3 localised within small vesicular or endosomal structures within the cytoplasm, but was not enriched at the plasma membrane in NIH 3T3, β1-/- or β3-/- cells. There was no clear overlap with paxillin or IRM channels in any of the cells, and the localisation did not appear to be altered in either integrin -/- cell line.

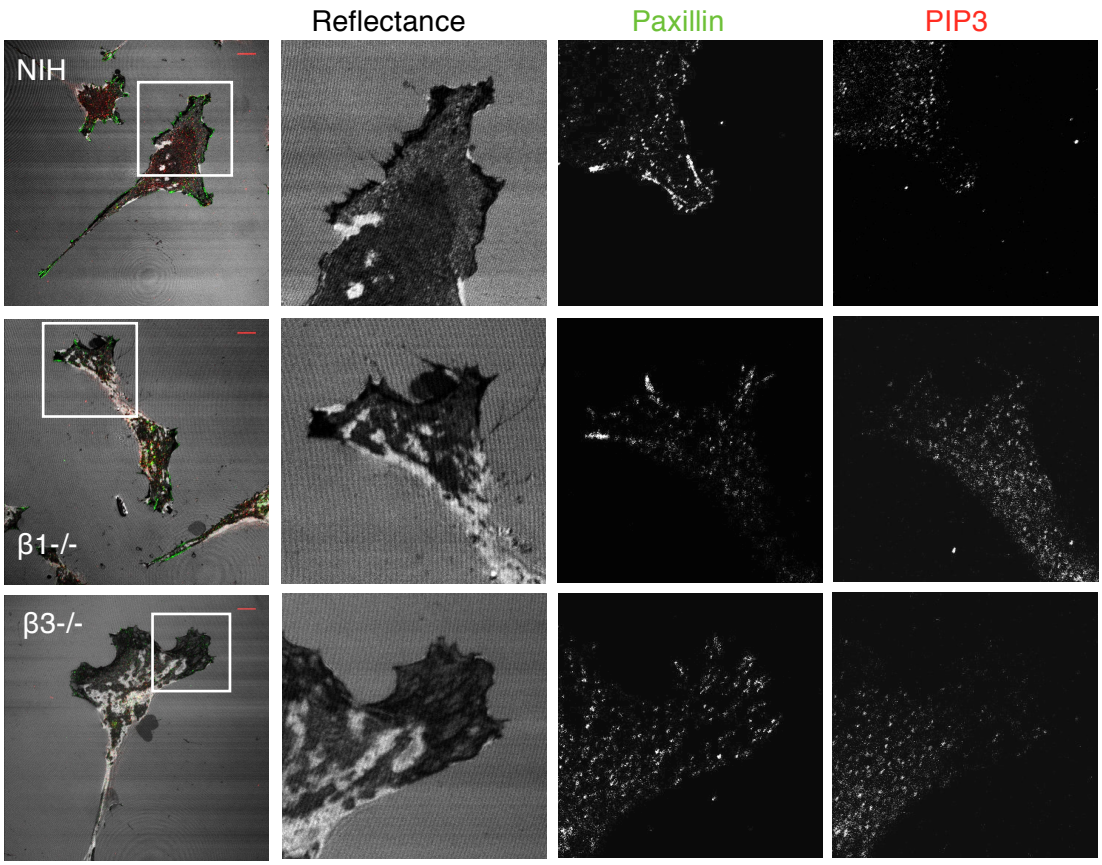

Figure 5.10. PIP3 does not localise to focal adhesions in control, β1-/- or β3-/- cell lines.

Single slice confocal images of fixed NIH, β1-/- or β3-/- cells plated on fibronectin coated glass coverslips. Endogenous PIP3 was stained for followed by Alexa 568 secondary antibodies (red). Endogenous paxillin was stained for followed by Alexa 488 secondary antibody (green). Interference reflection microscopy was used to show contact between the cells and the substrate (grey). Zoomed in images of the highlighted areas are shown as individual channels. Scale bar = 10μm. Representative of ~30 cells per condition from three independent experiments.

5.11 PI(3,4)P2 localises to focal adhesions in cells in CDM

Data shown in Figure 5.4 demonstrated that cells on CDM showed no global change in phospholipid composition compared to cells plated on 2D fibronectin. However, the absence of β1 integrin specifically reduced localisation of PI(3,4)P2 at adhesions in cells on 2D (figure 5.8). In order to address whether there was a localised change in phospholipids in fibroblasts in CDM, NIH 3T3, β1-/- or β3-/- cells were plated onto CDM coverslips and allowed to invade into the ECM for 24 hours. Cells were then fixed and immunostained for PI(3,4)P2 and co-stained for paxillin. Confocal images were then acquired.

PI(3,4)P2 staining in NIH 3T3 cells showed increased intensity adjacent to paxillin positive focal adhesions (top panels, figure 5.11) and as previously shown in Chapter 3, cells on CDM assembled fewer paxillin-containing focal adhesions compared to those on 2D FN. PI(3,4)P2 showed accumulation in specific protrusions and overlapping with paxillin staining in β1-/- and β3-/- cells but also showed higher perinuclear staining in these cells compared to NIH 3T3(Figure 5.11). This is in contrast to reduced adhesion-associated PI(3,4)P2 staining in β1-/- cells on 2D FN (Figure 5.8) and suggests that integrin specific recruitment of phospholipids may be sensitive to the local ECM environment.

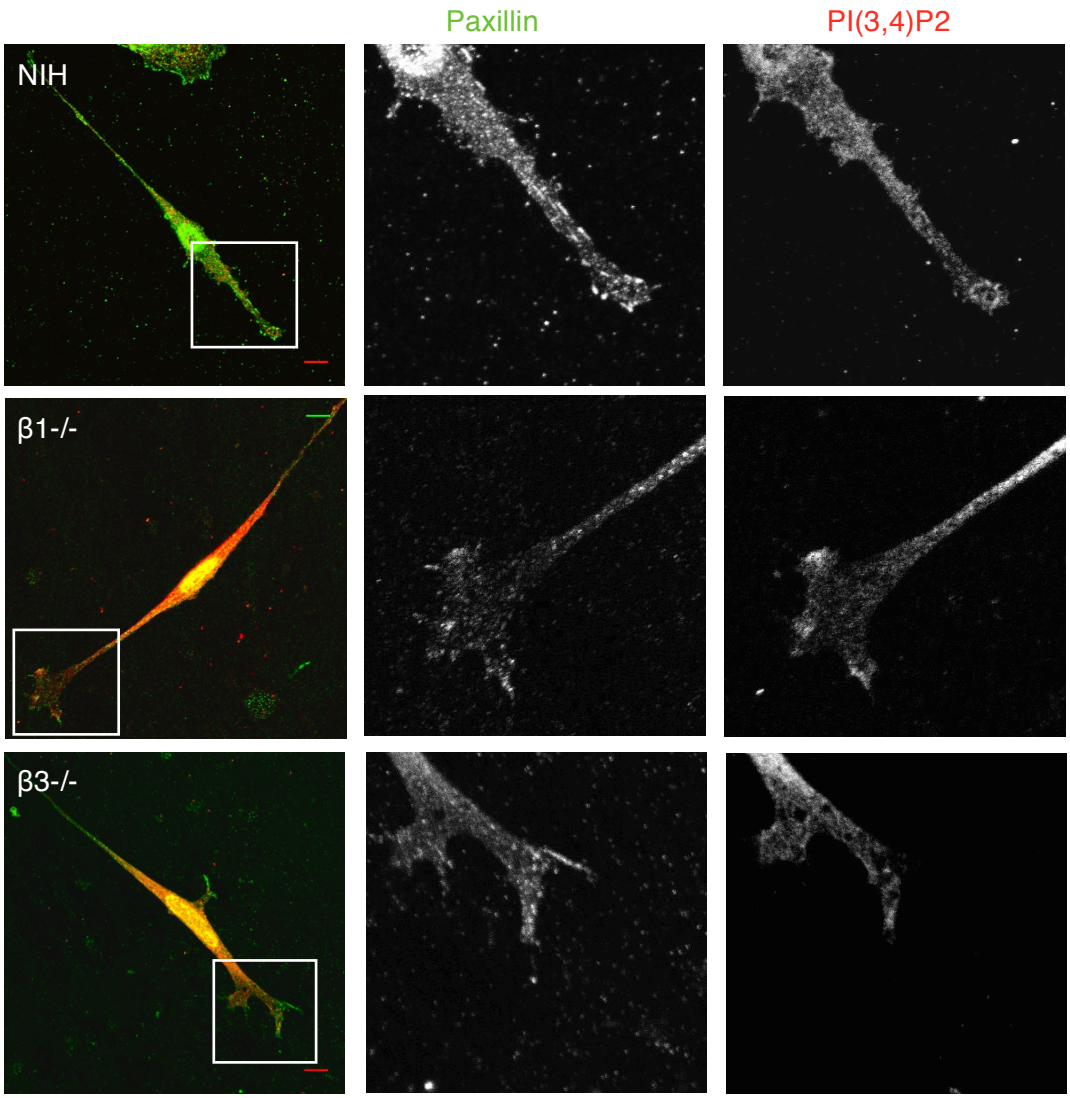

Figure 5.11. PI(3,4)P2 localises to focal adhesions in cells in CDM.

Maximum intensity projections from confocal images of fixed NIH, β1-/- or β3-/- cells plated on CDM. Endogenous PI(3,4)P2 was stained for followed by Alexa 568 secondary antibodies (red). Endogenous paxillin was stained for followed by Alexa 488 secondary antibody (green). Zoomed in images of the highlighted areas are shown as individual channels. Scale bar = 10μm. Representative of ~30 cells per condition from three independent experiments.

5.12 PI(4,5)P2 localises to focal adhesions in cells in CDM

In order to determine whether 3D ECM influenced PI(4,5)P2 localisation, NIH 3T3, β1-/- and β3-/- fibroblasts were plated onto CDM coverslips as in Figure 5.11, fixed and immunostained for PI(4,5)P2 and paxillin. Confocal images demonstrated that PI(4,5)P2 localised to membrane and protrusive regions around paxillin positive focal adhesions in NIH 3T3, β1-/- and β3-/- cells (Figure 5.12) and showed similar distribution in all cell types. Some background fluorescence can be seen in some of the images in Figure 5.12.

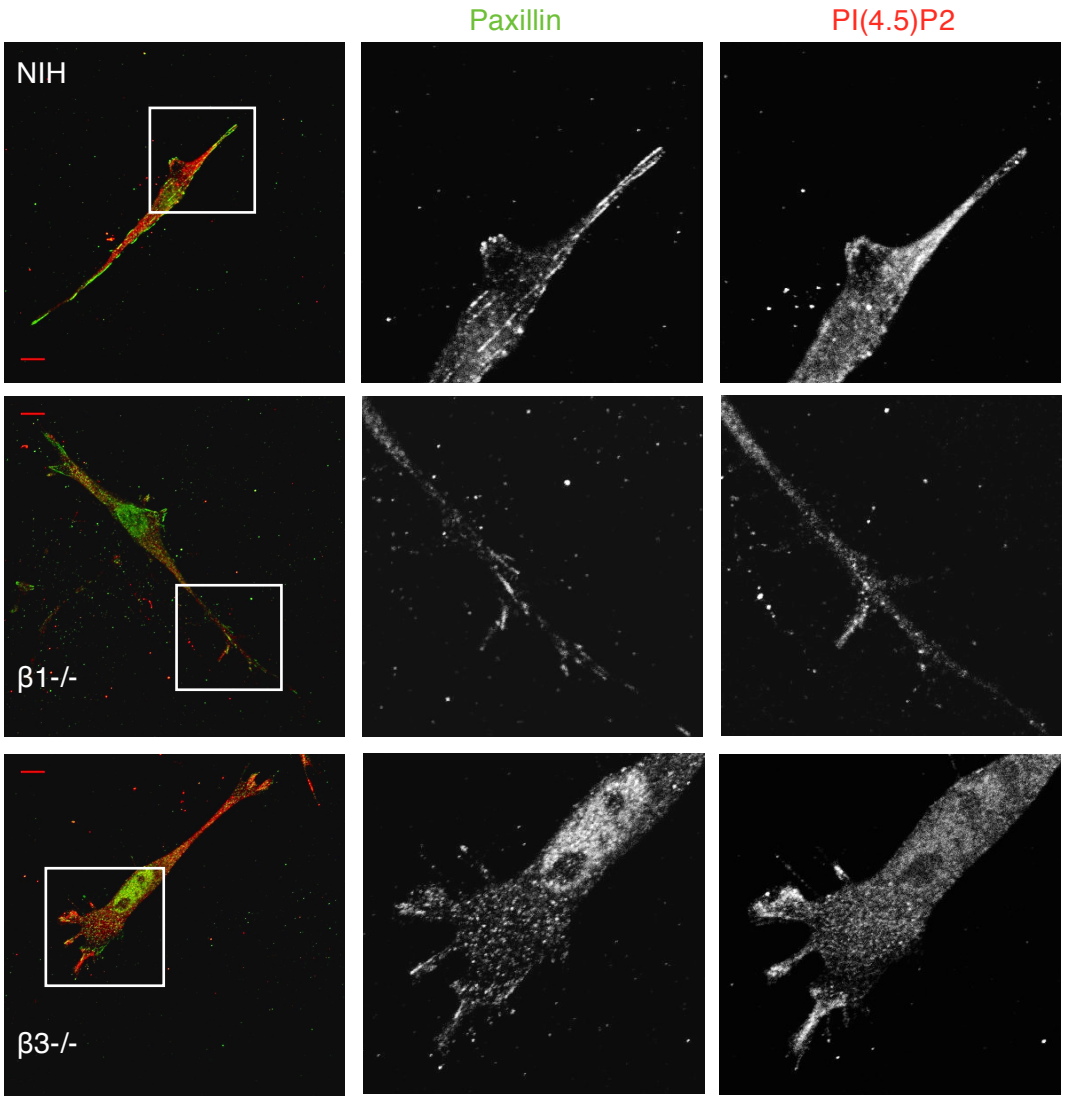

Figure 5.12. PI(4,5)P2 localises to focal adhesions in cells in CDM.

Maximum intensity projections from confocal images of fixed NIH, β1-/- or β3-/- cells plated on CDM. Endogenous PI(4,5)P2 was stained for followed by Alexa 568 secondary antibodies (red). Endogenous paxillin was stained for followed by Alexa 488 secondary antibody (green). Zoomed in images of the highlighted areas are shown as individual channels. Scale bar = 10μm. Representative of ~30 cells per condition from three independent experiments.

5.13 PIP3 does not localise to focal adhesions in cells in CDM

Previous data demonstrated that PIP3 did not show localisation to adhesion sites or membrane protrusions in cells plated on 2D FN. In order to determine whether this was altered in cells in 3D ECM, NIH 3T3, β1-/- or β3-/- cells were plated onto CDM, fixed and immunostained for PIP3 and paxillin as in Figures 5.11 and 5.12. Confocal images demonstrated that PIP3 predominantly localized within vesicles in the cytoplasm and did not accumulate at protrusions or near to paxillin positive focal adhesions in any of the cell lines analysed (Figure 5.13). This suggests that PIP3 does not accumulate at adhesions or protrusions in fibroblasts irrespective of the ECM environment. Some background fluorescence can be seen in some of the images in Figure 5.13.

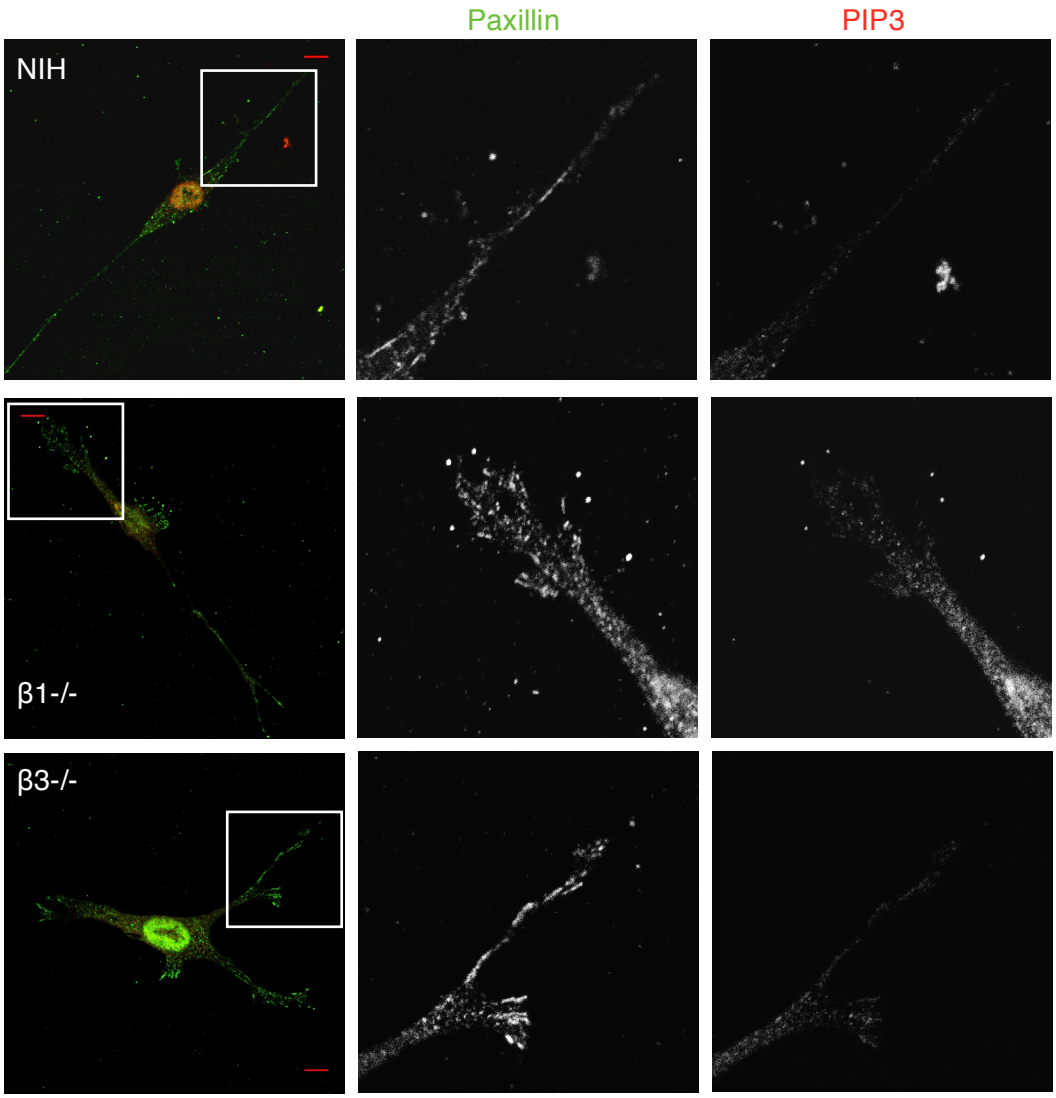

Figure 5.13. PIP3 does not localise to focal adhesions in cells in CDM.

Maximum intensity projections from confocal images of fixed NIH, β1-/- or β3-/- cells plated on CDM. Endogenous PIP3 was stained for followed by Alexa 568 secondary antibodies (red). Endogenous paxillin was stained for followed by Alexa 488 secondary antibody (green). Zoomed in images of the highlighted areas are shown as individual channels. Scale bar = 10μm. Representative of ~30 cells per condition from three independent experiments.

5.14 Integrin β3 -/- cells have less ordered membranes than control fibroblasts

Lipid rafts have been suggested to be membrane microdomains enriched in cholesterol and glycosphingolipids that act to organise groups of related proteins, glycoproteins, and other molecules and promote localised signaling responses (Simons and Gerl, 2010). Lipid rafts are also proposed to be involved in adhesion and integrin signaling (Gaus et al., 2006). Higher ordering of lipid acyl chains has been shown to be a marker for lipid rafts through use of membrane order dyes. Membrane order dyes change their emission spectra depending upon their conformation, which is directly modulated by the local packing of the lipids within the membrane. Integrins may play a role in distribution of lipid rafts and therefore may have an effect on local control of membrane order. Di-4-ANEPPDHQ is a well-characterized membrane order dye and has previously been shown to report on local changes in lipid packing and organization in a range of cell types (Kwiatek et al., 2013).

In order to determine whether integrins may dictate local changes in membrane order, NIH 3T3, β1-/- or β3-/- cells were seeded onto fibronectin-coated 2D imaging dishes and allowed to adhere. Cells were then incubated with the membrane dye for 30 mins before being washed and images of live cells were acquired by confocal microscopy. Di-4-

ANEPPDHQ membrane order analysis was then carried out on the resultant images as described in Materials and Methods.

Higher order membranes were seen predominantly towards the periphery of all cell lines (shown in red), and a lower ordered membrane (blue) towards the centre of the cell as seen in the false coloured images (figure 5.14 A). The grey values for each pixel were normalised and plotted as histograms next to representative images (5.14 A). NIH 3T3, β1-/- and β3-/- cells all showed a high proportions of ordered vs disordered membrane partitioning (skewed to the right of the Y-origin in all three cases), suggesting a high degree of lipid raft content in fibroblasts. β3-/- cells showed lower overall levels of ordered membranes compared to the other two cell types as indicated by the shift in curve to the left of the histogram in Fig 5.14 A, bottom panels.

The mean of the values derived from the histograms from 20 cells for each genotype was plotted and compared for each cell line (figure 5.14 B). There was no significant difference in the membrane order between NIH 3T3 and β1-/- cells. However, β3-/- cells showed a significantly lower degree of membrane order than NIH 3T3 and β1-/- cells (Figure 5.14 B).

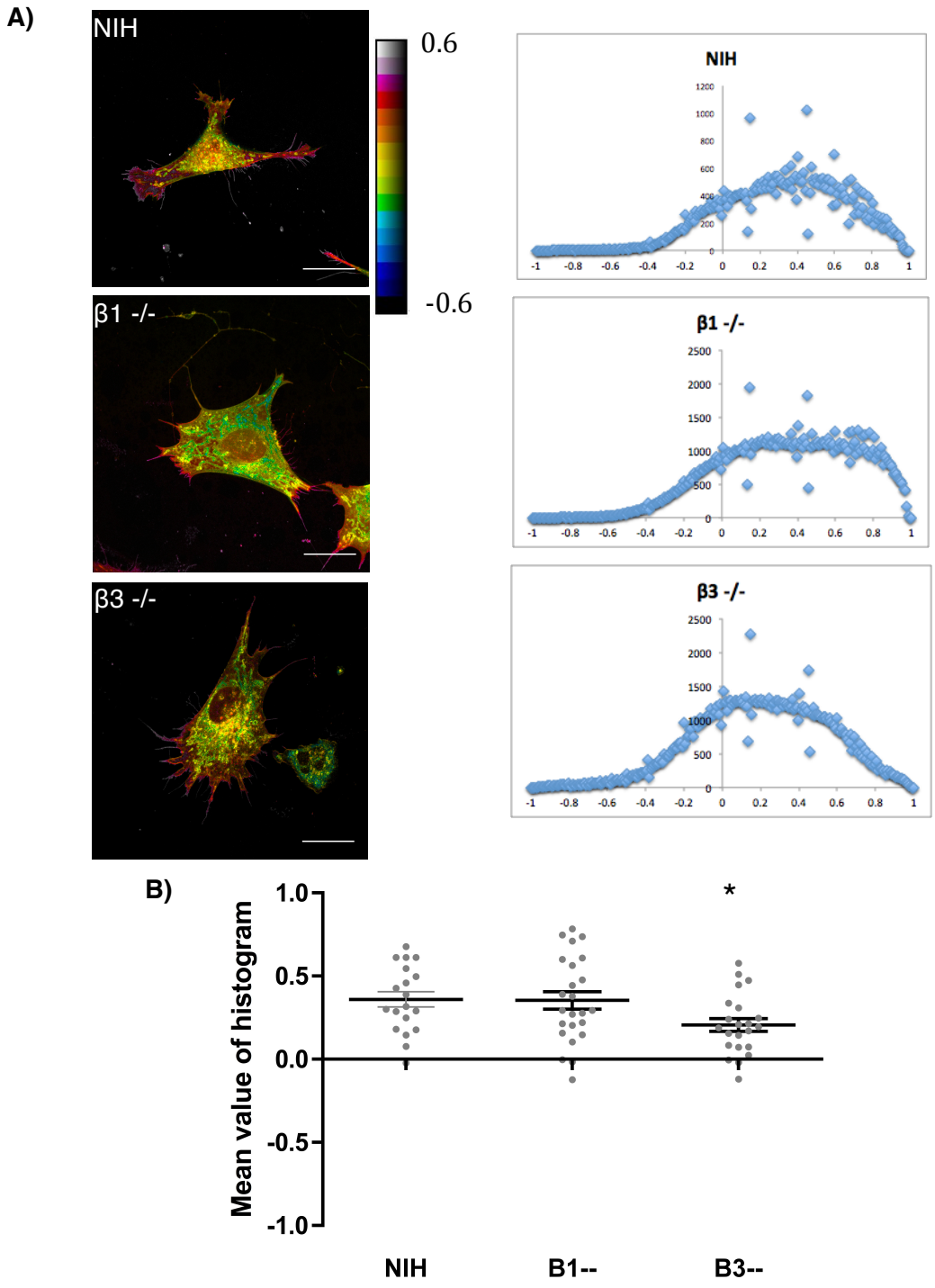

Figure 5.14. Integrin β3 -/- cells have less ordered membranes than control fibroblasts.
A) False coloured HSB images (with scale) from confocal images of live NIH or integrin knockout MEF cells after incubation with Di-4-ANEPPDHQ membrane order dye. Red indicates higher membrane order and blue indicates lower membrane order. Grey value of each pixel was quantified and histograms of grey value (x-axis) against average total number of pixels (y-axis) was produced. Scale bar = 20um n=20, from 3 independent experiments. B) Scattergraph of mean of the histogram data for each cell line, each point is the mean of the histogram produced from an individual cell. Error bars = SEM, * = P<0.05.

5.15 Treatment of cells with RGD peptide reduces local PI(3,4)P2 and PI(4,5)P2 accumulation

Integrin activation from the outside-in can be modulated using a number of different small molecules, as described in Chapter 4. Manganese ions (Mn^{2+}) can activate integrins through binding to a metal ion binding site in the β-subunit extracellular region resulting in a conformational change in the a1-helix (Mould et al., 2002; Chen et al., 2003). Soluble RGD peptide can bind to and block integrins from being activated by occupying the binding site between integrins and fibronectin (Ginsberg et al., 1985). Data in Chapter 4 demonstrated that both RGD and Mn^{2+} were likely acting as β1 integrin agonists, and resulted in high talin accumulation at adhesions, but lower Kindlin 1-positive focal adhesions. Given the known binding of both of these proteins to phospholipids, RGD and Mn^{2+} were used to study the effects of integrin activation status on the localisation of specific phospholipids.

NIH 3T3 cells were seeded on fibronectin coated glass coverslips and treated with 1mM Mn^{2+} for an hour or 100 μg/ml of RGD peptide for 30 minutes. After treatment, cells were briefly washed and fixed before being stained for PI(3,4)P2, PI(4,5)P2 or PIP3 and paxillin as a marker of focal adhesions. Confocal images were then acquired for all conditions and are shown in figure 5.15.

PI(3,4)P2 localised at paxillin positive focal adhesions at the ends of protrusions as shown in previous figures, and this was the case for both the untreated and Mn^{2+-} treated cells. Mn^{2+} treated cells showed higher numbers of membrane protrusions and smaller paxillin-positive adhesions (Figure 5.15, top panels). RGD treatment resulted in more diffuse PI(3,4)P2 staining across the cell but with some remaining associated PI(3,4)P2 overlapping with paxillin staining. Paxillin positive focal adhesions also appeared to be larger following RGD treatment (Figure 5.15, top left panel). Similar effects were seen in cells stained for PI(4,5)P2 (Figure 5.15, middle panels). PI(4,5)P2 localised with paxillin-positive focal adhesions in cellular protrusions in all cells, with increased accumulation in Mn^{2+} treated cells and more diffuse staining in RGD-treated cells.
PIP3 did not localise to paxillin positive focal adhesions or membrane protrusions under any of the treatment conditions and was seen to be largely peri-nuclear (bottom panels, Figure 5.15), as also shown in previous figures (Chapter 3).

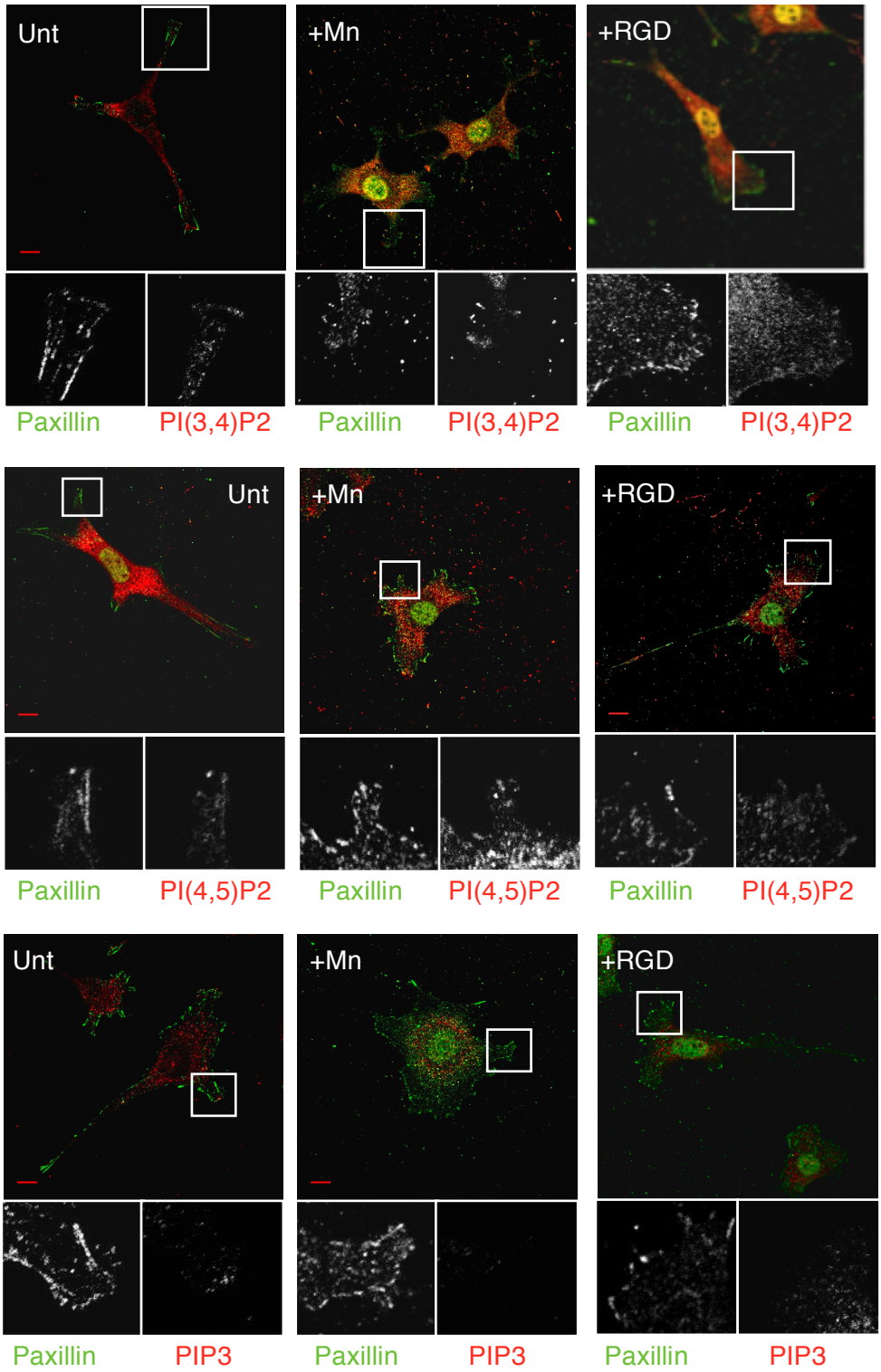

Figure 5.15. Treatment of cells with RGD peptide reduces local PI(3,4)P2 and PI(4,5)P2 accumulation.
Single slice confocal images of NIH cells either untreated or treated with 1mM manganese (Mn) or 100µg/ml RGD peptide. Endogenous PI(3,4)P2, PI(4,5)P2 and PIP3 were stained for followed by Alexa 568 secondary antibodies (red). Endogenous paxillin was stained for followed by Alexa 488 secondary antibody (green) Zoomed in images of the highlighted areas are shown as individual channels below the merged images. Scale bar = 10µm. Representative of ~30 cells per condition from three independent experiments.

5.16 Treatment of cells with Mn^{2+} or RGD-peptide does not alter membrane order

Having shown a role for integrin activation and inhibition on endogenous phospholipid localisation and intensity it was important to next determine whether this correlated with altered membrane order of cells following Mn^{2+} or RGD treatment. NIH 3T3 cells were seeded onto fibronectin coated imaging dishes and allowed to adhere. They were then treated with 1mM Mn^{2+} or 100 µg/ml RGD peptide along with the membrane dye (Di-4-ANEPPDHQ) for 30 minutes before being washed and images of live cells were acquired by confocal microscopy as in Figure 5.13. Di-4-ANEPPDHQ membrane order analysis was then carried out as described in Chapter 2.

As shown in Figure 5.14, all cells showed higher order membranes at the periphery of the cell (shown in red), and a lower ordered membrane (blue) towards the centre of the cell as seen in the false coloured images in Figure 5.16 A. The grey values for each pixel were normalised and were plotted as histograms as in Figure 5.14. These are shown alongside corresponding example images in Figure 5.16A. As shown in Figure 5.14, NIH 3T3 cells showed a higher proportion of ordered vs disordered membranes in control and treated cells. The mean of the histograms for 20 cells was plotted and treated cells were compared to untreated cells as shown in figure 5.16 B. There was no significant difference in the

membrane order of Mn^{2+} treated or RGD peptide treated NIH cells when compared to untreated control cells.

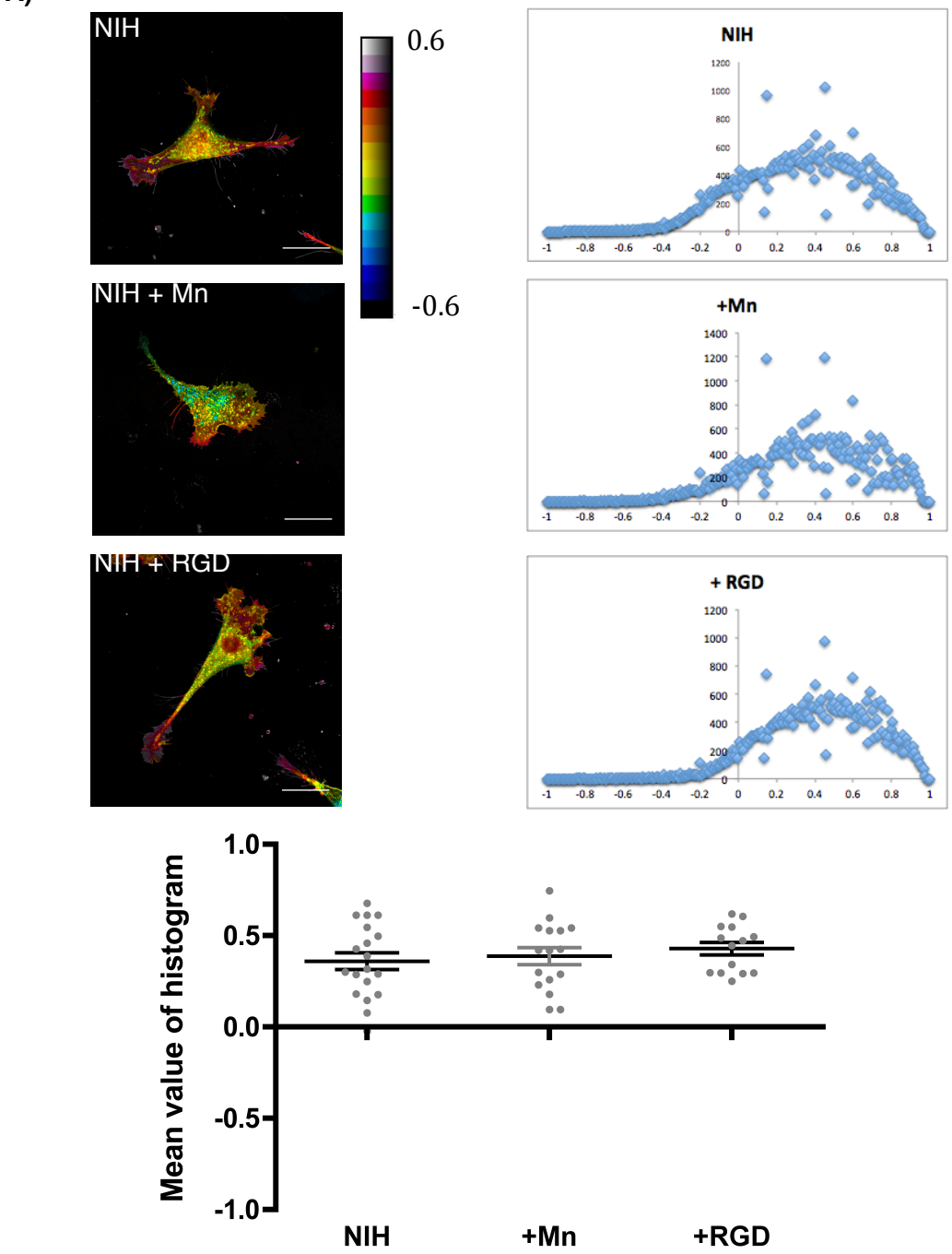

Figure 5.16. Treatment of cells with Mn^{2+} or RGD-peptide does not alter membrane order.
A) False coloured HSB images (with scale) from confocal images of live NIH cells untreated or treated with manganese or RGD-peptide after incubation with Di-4-ANEPPDHQ membrane order dye. Red indicates higher membrane order and blue indicates lower membrane order. Grey value of each pixel was quantified and histograms of grey value (x-axis) against average total number of pixels (y-axis) was produced. Scale bar = 20um n=20, from 3 independent experiments. B) Scattergraph of mean of the histogram data for each cell line, each point is the mean of the histogram produced from an individual cell. Error bars = SEM, * = P<0.05.

Discussion

Data shown in this chapter has demonstrated that PI(3,4)P2 and PI(4,5)P2 but not PIP3 are localized at focal adhesions. PI(4,5)P2 has previously been shown to be present in focal adhesions (Ling et al., 2002) and data in this chapter shows that quercetin treatment acts to reduce both total levels and localization of PIP2 species at adhesions. Moreover, RGD treatment leads to a decrease in the amount of PI(4,5)P2 at focal adhesions and conversely, inhibition of PIP production leads to fewer talin and active-integrin β1containing adhesions, but the size and density of proteins appears unaffected.

This data suggests that talin recruitment to newly formed focal adhesions is reduced following quercetin treatment. This is in agreement with the hypothesis that PI(4,5)P2 is required to relieve talin of its auto-inhibition and to bind to integrins (Elliott et al., 2010). The similar reduction in the number of active integrin-β1 containing adhesions and talin-positive adhesions following quercetin treatment suggests that talin, and PI(4,5)P2, may be required to activate and promote new β1 integrin containing adhesions. This would be in agreement with other studies indicating that talin is absolutely required for integrin activation and that kindlins function as adapter proteins to enhance talin-integrin binding (Ma et al., 2008; Harburger et al., 2009). This conclusion is further supported by other data in this chapter showing an increase in PIP2, but not PIP3, before adhesions

are formed in fibroblasts. To further confirm this increase before adhesion, use of a FRET probe could be utilised in the future to show when and where specific phospholipids are being made and to see if this happens immediately prior to adhesion assembly (Kemp-O'Brien and Parsons, 2013).

Interestingly, and somewhat counter-intuitively, quercetin treatment resulted in higher levels of talin-integrin complex formation as shown by co-immunoprecipitation. This may be due to either changes in stability of integrins within adhesions or associations between integrins and talin outside of the localised focal adhesions plaque. Previous studies have shown that both integrins and talin can occupy non-adhesions associated domains at the plasma membrane but whether integrins are able to co-associate with talin is currently unknown (Galbraith et al., 2007; Rossier et al., 2012). The requirement of phospholipids for sustained talin-integrin binding once the two proteins are bound is also not known, so it is possible that the pre-assembled complexes formed prior to quercetin treatment remain assembled with less mobile integrins and this results in a higher proportion of interacting talin.

The data in this chapter also suggests that kindlin 1 and kindlin 2 do not require PI(3,4)P2 or PI(4,5)P2 production in order to remain at focal adhesions. Kindlins have been shown to contain several regions for binding to lipids including the PH-domain and F1 loop (Bouaouina et al., 2012; Y. Liu et al., 2012) so may have more phospholipid-associated regions

than talin. No global changes in PI(3,4)P2, PI(4,5)P2 or PIP3 were observed by cells in CDM or by β1 or β3 integrin knockout cells but confocal analysis revealed that β1 -/- cells had an absence of PI(3,4)P2 at focal adhesions in 2D. Moreover, treatment of cells with RGD peptides resulted in a reduction in PIP2 levels at focal adhesions. This data suggests that β1 may play a role in setting up increased PI(3,4)P2 conditions in order to potentially facilitate recruitment of membrane associated proteins. Interestingly, β3 but not β1 integrin knockout cells were shown to have a lower membrane order than control cells suggesting that the remaining β1 integrin in β3null cells may be disorganized or incorrectly activated such that local membrane order is disrupted. Indeed, our lab and others have previously shown that β3 knockout cells exhibit higher levels of active β1 integrins but smaller and more peripherally located focal adhesions (Worth and Parsons, 2010), suggesting this may influence local membrane order either directly through adhesion protein disruption or indirectly through PI3kinase signaling.

6. Discussion

6.1 The role of membrane microdomains in integrin-based adhesion

In 1997, Simons and Ikonen suggested the existence of lipid rafts. These were then described as the partitioning of an area of the membrane by the presence of a high amount of sphingolipids, phospholipids and cholesterol (also called liquid ordered phase) with tight packing of lipids that can move within the membrane and serve as a platform for protein recruitment (Simons and Ikonen, 1997). They postulated that proteins exhibit a preference for partitioning within either an ordered or disordered phase, hence they would then be included or excluded from lipid rafts. These lipid rafts, it was suggested, would then serve as sites of signal transduction with increased rates of protein-protein interactions.

Given that cell adhesion to the ECM occurs at the plasma membrane, lipid rafts have been postulated to play a role in forming and maintaining adhesion signaling platforms. Initial studies suggested integrins were not present in lipid rafts (Fra et al., 1994) however, it was discussed that integrins could undergo crosstalk with other receptors forming membrane complexes (Porter and Hogg, 1998). Data started to emerge that showed LFA-1, a leukocyte integrin, could be activated via clustering of lipid rafts (Krauss and Altevogt, 1999) showing evidence in favour of lipid rafts playing a role in regulation of adhesion. Further evidence to support this was also found in the role of caveolin in integrin β1 signaling (Wei et al., 1999). It was shown that signaling for integrin function was dependent upon uPAR

regulation of caveolin that was believed to function through organising lipid domains near to integrins to facilitate signaling. Further work showed that both LFA-1 and α5β1 integrin adhesion was dependent upon lipid raft integrity (Leitinger and Hogg, 2002) and later studies went on to show that focal adhesions were regions with a high membrane order (Gaus et al., 2006). A high membrane order is the result of the tight packing of sphingolipids, cholesterol and proteins in addition to phospholipids and as such, high membrane order has been postulated to represent lipid rafts. Data in this thesis has examined the roles of specific phospholipids and integrins that we hypothesized may be involved in coalescing lipid rafts to act as adhesion signaling platforms. Live imaging demonstrated that PIP2 levels were increased immediately before adhesion formation and this enrichment of PI(3,4)P2 depended on β1 integrins. This is in agreement with previous work that suggested that β1 integrin is important for generation of plasma membrane domains (Singh et al., 2010). Following siRNA knockdown of β1 integrin, two different domain sensors (Bodipy-LacCer, a fluorescent form of lactosylceramide or AF647 PEG–Chol) were no longer correctly localised in comparison to high clustering in control cells. Furthermore, treatment of cells with the peptide RGD reduced local levels of PI(3,4)P2 and PI(4,5)P2 at adhesions, in support of the notion that β1 integrin can regulate local phospholipid synthesis and lipid raft composition. However, data presented in this thesis has shown that β3 integrins are not required to regulate phospholipid composition at adhesions, although β3-/- cells exhibited lower membrane order than

either control or β1-/- cells. This suggests that β3 integrin could still play a role in maintaining the membrane order or lipid rafts in fibroblasts, but not specifically phospholipids within focal adhesions. This may be due to changes in membrane protein packing or potentially the organization of the underlying actin cytoskeleton, which has also been proposed to regulate membrane order.

Data in chapter 5 demonstrated that PI(4,5)P2 was localised at focal adhesions but unlike PI(3,4)P2, this was not dependent upon either β1 or β3 integrins. Moreover, analysis in live and fixed cells demonstrated that PIP3 either is not localised to adhesion-related lipid rafts or that it is rapidly dephosphorylated so as not to be detectable by the methods used. It is possible that PIP3 may be transiently increased at adhesion sites but detection methods used here were not sensitive enough to detect a rapid spike in phospholipid levels. PIP3 can be dephosphorylated to either PI(3,4)P2 by SHIP2 or PI(4,5)P2 by PTEN. SHIP2 has been shown to be recruited to the plasma membrane following EGF or serum stimulation of cells (Erneux et al., 2011) and has also been shown to interact with known focal adhesion proteins p130Cas, filamin and lamellipodin (Prasad et al., 2001; Dyson et al., 2001; Yoshinaga et al., 2012). On the other hand, PTEN is known to be able to dephosphorylate PIP3 to produce PI(4,5)P2 and to also play a key role in promoting cell polarization (Leslie et al., 2008). Early studies showed a role for PTEN in regulating integrin-mediated cell spreading, focal adhesion formation and the down-regulation of FAK

phosphorylation (Tamura et al., 1998; 1999). Together, PTEN and SHIP2 provide a mechanism for the cell to control phospholipid-dependent signaling pathways and potentially the rapid removal of any potential pools of PIP3 present in adhesions.

6.2 Dynamics of talin and kindlins at adhesions

Data in this thesis has shown that both kindlin 1 and kindlin 2 arrive at sites of forming focal adhesions before talin. Kindlin binding to phospholipids has been shown to be important for kindlin function and for activation of integrins, and kindlin PH domains have been shown to bind to PIP3 (Ma et al., 2008; J. Liu et al., 2011; Yates et al., 2012; Elliott et al., 2010; Bouaouina et al., 2012). However, further studies demonstrated that the kindlin F0 loop shows a strong affinity for PI(4,5)P2, but that PIP3 showed preferential binding (Perera et al., 2011). Furthermore, kindlin 1 and 2 were shown to contain an F1-loop which is a poly-lysine non-structured motif that was shown to be required for targeting kindlins to phospholipids and was also shown to be required for kindlin-mediated integrin co-activation (Bouaouina et al., 2012). It was hypothesised that the interaction between kindlin and phospholipids via the PH domain, F0 domain and F1 loop region is required to tether kindlin to the membrane, and stabilise or orientate kindlin to facilitate interactions with integrin β tails and contribute to activation of integrins (Bouaouina et al., 2012). Data in this thesis showed

that inhibition of phospholipid synthesis, specifically reducing levels of PI(3,4)P2 and PI(4,5)P2 at adhesions, did not affect the ability of kindlin 2 to form a biochemical complex with β1 or β3 integrins. This supports previous work showing that when local PI(4,5)P2 synthesis is perturbed, kindlins are still able to be recruited to new adhesions (Legate et al., 2011). This data suggests that both PIP3 and PIP2 can allow for recruitment of kindlins to adhesions, but a deletion in kindlin lipid binding sites prevents normal kindlin function which is most likely due to a lack of targeting to the plasma membrane.

Previous publications have shown that when kindlins are over-expressed with the talin head domain this led to activation of β3 but not β1 integrins; indeed kindlin expression was seen to inhibit talin-induced β1 integrin activation in this model (Ma et al., 2008; Harburger et al., 2009). However, this study analysed integrin activation in suspended CHO cells using overexpression models and FACs analysis, hence the interpretation of this data in the context of adherent migratory cells remains unclear. Data presented in this thesis demonstrated that knockdown of kindlin 2 resulted in less focal adhesions and a reduction in active β1 integrin positive adhesions. The effect on the number of focal adhesions was in agreement with earlier work (Harburger et al., 2009) but the reduced β1 activation was contrary to the CHO cell data in the same study. One difference may be that kindlins play different roles in different cell lines, Harburger, *et al.* used CHO cells whereas this thesis utilised mouse fibroblasts. Indeed data

presented in this thesis shows that Kindlin-1 exhibited higher colocalisation with β3 integrins than with β1 integrins which supports the idea that kindlins may play a role in differential integrin activation. Integrin activation or inhibition through use of RGD peptide or manganese ions did not to affect the ability of kindlins to bind to β1 or β3 by co-immunoprecipitation (Chapter 5). In addition, kindlin 2 colocalised equally well with both GFP tagged β1 and β3 integrins (Chapter 3). Together this data is suggestive that kindlin 2 may play a more general role in integrin activation than kindlin 1, whose role in fibroblasts may be in facilitating activation of specific integrins.

It has been suggested that kindlins main role in adhesion and integrin activation, is to increase integrin clustering rather than directly activating integrins as talin has been shown to do (Ye et al., 2013; Kahner et al., 2012). It is a possibility that the increase in kindlin levels at early points during adhesion formation, that occurred before talin recruitment is required for pre-clustering of integrins in order to facilitate adhesion maturation.

Data in this thesis confirms the importance of phospholipids on talin recruitment. Inhibition of phospholipid synthesis in cells by quercetin treatment resulted in a reduction in the number of talin-positive focal adhesions and the number of active β1 integrin-positive focal adhesions (Chapter 5). This data is in agreement with other work showing that phospholipids enhance talin binding to β3 integrins (Moore et al., 2012).

Specifically, talin has been shown to exhibit highest affinity for PI(4,5)P2 (Moore et al., 2012). It is therefore interesting that data in this thesis shows that following quercetin treatment, talin binding to both β1 and β3 integrins is increased in co-IP's and whilst there are several possibilities to explain this (as discussed in Chapter 5), collectively the data currently suggests that a change in lipid raft composition could modulate integrin-talin binding through binding to either the F0F1 or F2F3 talin head domains (Moore et al., 2012).

6.3 Integrin specificity in adhesion assembly

Data in this thesis has also shown that talin colocalises with β1 integrins more than β3 integrins in fibroblasts. This could be due to the role of β1 integrins (but not β3) in generating higher local PIP2, which may facilitate greater talin recruitment. This may also operate as a positive feedback mechanism, as data presented in Chapter 3 demonstrates that knockdown of talin decreased the number of total and active integrin β1 containing adhesions. Lipid raft integrity is clearly important for talin recruitment to adhesions with PI(4,5)P2 being the most notable component; affecting local PI(4,5)P2 synthesis results in talin being less efficiently recruited to adhesions and glycosphingolipid cleavage treatment has shown to redistribute talin away from adhesions (Legate et al., 2011; Singh et al., 2010).

Other focal adhesion proteins have also been shown to be dependent on lipid raft composition for recruitment. FAK, paxillin, and PIPKIγ localization at adhesions depend upon lipid raft integrity, and FAK specifically has been shown to bind to PI(4,5)P2 and facilitate clustering which increase recruitment of other adhesion proteins (Singh et al., 2010; Goñi et al., 2014). PI(3,4)P2 can also bind to the adhesion-related protein lamellipodin (Bae et al., 2010), which indicates that PI(4,5)P2 is not the only phospholipid involved with adhesions. It is highly likely that the distribution of phospholipids is highly dynamic at adhesions and this plays a key role in the recruitment of adhesion proteins which then facilitates adhesion strengthening, maturation and ultimately migration of the cell.

A schema for how the interplay between all these dynamic components may operate can be described as follows and is illustrated in Figure 6.1. Integrins, localised to the plasma membrane, are situated within lipid rafts that undergo a spike in local PIP3 which triggers the recruitment of kindlin 1 or kindlin 2 to membranes at forming adhesions (Fig 6.1a). This recruitment, aided by the dynamics within the lipid raft, result in the binding of the membrane tethered kindlin to the membrane distal NPXY motif of the integrin β subunit tail. The localised PIP3 meanwhile would then be rapidly hydrolysed into PI(3,4)P2 or is recruited to the lipid raft in a β1 integrin dependent manner. This change in phospholipid composition, combined with kindlin binding to the integrin tail, would allow for talin to

localise to the lipid raft, and bind to the integrin β subunit (Fig 6.1b). This would then enable talin to recruit PIPKIγ to adhesions which would increase local levels of PI(4,5)P2. The increase in local PI(4,5)P2 would then lead to further recruitment of kindlins, as kindlins have a high affinity for PI(4,5)P2 (Perera et al., 2011) (Fig 6.1c). The end result of this would be the clustering of integrins and recruitment of further downstream proteins to the forming adhesion (Fig 6.1d). These include FAK, Src and ILK. Kindlin 1 and kindlin 2 then remain at adhesions, perhaps in complex with ILK or migfilin which would provide a link with kindlins to the actin cytoskeleton (Tu et al., 2003; Brahme et al., 2013). The binding to integrin tail may switch to be dependent upon ILK or another protein rather than remaining directly bound post-initiation. However formation of a link between integrins and the actin cytoskeleton would also explain the large defects in migration following kindlin 2 knockdown, which were much greater than the defects seen in cells knocked down in talin. This would also suggest that kindlin 2 is more than just an adapter for talin recruitment.

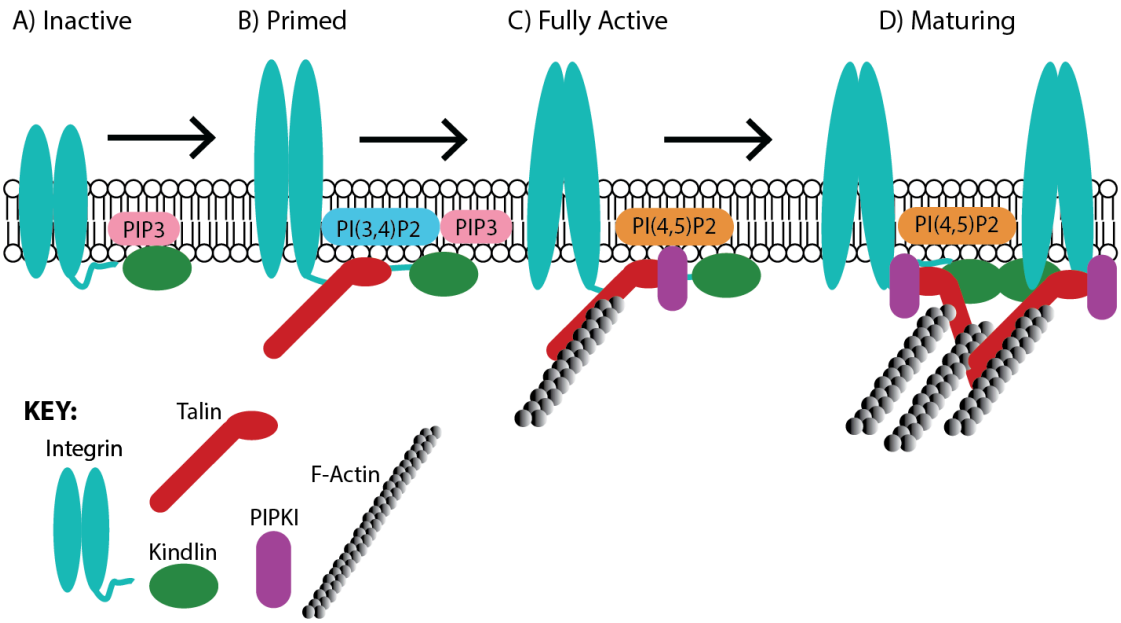

Figure 6.1 Proposed model of the interplay between phospholipids and integrin activators at forming adhesions.

A model showing the proposed hypothesis for the interplay between phospholipids and integrin activators at forming adhesions. A) Integrins are in an inactive conformation, a small localised increase in PIP3 levels results in kindlin being targeted to the plasma membrane. B) Kindlin binds to the cytoplasmic tail of β integrins at the membrane distal NPxY motif followed by an increase in PI(3,4)P2 which is β1 integrin dependent. The binding of kindlin to the β integrin cytoplasmic tail and the change in the phospholipid composition together contributes to recruit talin to the membrane proximal NPxY motif on the β integrin tail. This binding results in the integrin adopting an extended or primed conformation. C) Talin then recruits PIPKIγ which results in the localised production of PI(4,5)P2 which further facilitates the recruitment of other adhesion proteins in addition to talin and kindlin proteins. Talin attaches to the actin cytoskeleton exerting tension and further facilitating protein recruitment. The integrin is now fully active and would be ligand bound. D) Finally, tension, lipid raft dynamics and integrin clustering through recruited proteins such as talin and kindlin result in adhesion maturation and further connections to the actin cytoskeleton.

6.4 Extracellular forces and adhesion maturation

Talin and kindlin mediated integrin activation were studied in this thesis on both a traditional 2D surface, as well as a more physiologically relevant 3D CDM model. CDM, like ECM *in vivo* has different mechanical properties to the traditional 2D substrates beyond just dimensionality, but also differences in pore size, and stiffness (Jayo and M. Parsons, 2012). Matrix stiffness plays a key role in focal adhesion biology as a number of key adhesion proteins, including talin, are mechanosensitive (Yao et al., 2014; Schiller and Fässler, 2013). Indeed, a key step in the regulation of talin at adhesions appears to be in the force applied across it. At less than 5 pN it has been hypothesised that talin is recruited to adhesions and auto-inhibition is relieved by interaction with phospholipids. Upon binding to the integrin β tail and to actin, force can be exerted across talin revealing cryptic vinculin binding sites (Yao et al., 2014). This has been shown to occur around 5 pN of applied force. As more force is applied across talin, more vinculin can bind and cross-link talin to support it and strengthen the adhesion, however beyond 25 pN vinculin can be displaced. It was thought that force could function as a checkpoint, ensuring that talin is successfully bound to both integrin and actin before further recruitment of focal adhesions may happen (Yao et al., 2014).

This study was examining the force across a single molecule, whereas in an actual adhesion there will be multiple talin molecules present which

could then be crosslinked to actin and each other via vinculin. If the main role of kindlins in integrin activation and adhesion maturation is the clustering of integrins and recruitment of additional adhesion proteins, as has been suggested by others (Calderwood et al., 2013), then kindlins may serve to expand the amount of adhesion proteins recruited so that the tension across the adhesion is spread, in order to prevent crossing this 25 pN threshold. Furthermore, this potential role in clustering and recruitment of adhesion proteins may be different for each of the kindlin isoforms as they have been shown to have different binding partners, as discussed in the introduction. As kindlin expression alone is not sufficient for integrin activation, then perhaps the phenotypic changes and the large effect on migration observed in kindlin 2 knockdown fibroblasts in this thesis is due to kindlins role in supporting adhesion formation to ensure that tension does not cross the 25 pN threshold.

6.5 Integrin activation in pathological settings

Kindlins have been shown to be involved in several adhesion-linked diseases including, leukocyte adhesion deficiency syndrome (LAD) and Kindler syndrome. Kindler syndrome is caused by mutations in kindin-1 that result in loss of function, and the link between the actin cytoskeleton and the ECM in keratinocytes (Siegel et al., 2003). Kindler syndrome patients suffer from skin blistering, increased photosensitivity and gum

diseases (Kindler, 1954; Ashton, 2004). In cells it was found that Kindler syndrome patient keratinocytes showed reduced wound closure compared with control cells and cells had multiple narrow leading edges in addition to reduced proliferation and reduced adhesion (Herz et al., 2006; Has et al., 2008). LAD-III patients have a mutation in kindlin-3 and this results in a failure to activate β1, β2 and β3 integrins in hematopoietic cells (Moser, Bauer, et al., 2009). This lack of integrin activations results in impaired platelet activation due to there being a defect in leukocytes being able to adhere to epithelial cells. To date, no human mutations have been identified in humans that results in loss of kindlin-2 function. This suggests that loss of kindlin-2 may be lethal, which has been seen in the mouse knockout model (Dowling et al., 2008). In support of data in this thesis, this further suggests that kindlin-2 either plays a more significant role in adhesion regulation than kindlin-1, or potentially that kindlin-2 has as yet unexplored roles outside of integrin activation that are essential for cell survival.

Kindlin 1 was recently found to function in regulating the mitotic spindle in cancer cells, and upon shRNA knockdown of kindlin 1 resulted in abnormal spindle formation and reduced cell survival (Patel et al., 2013). This role was found to be both dependent upon kindlins interaction with both integrins and polo-like kinase 1 (PLK-1). Interestingly, kindlin 2 was still expressed in these cells, again demonstrating that kindlin 2 cannot compensate for loss of kindlin 1 and vice versa. Data presented in this

thesis demonstrated that shRNA knockdown of kindlin 1 resulted in an increase in cells becoming bi-nucleated (not shown) which agrees with the reported role of kindlin 1 in spindle orientation. Moreover, this suggests that kindlin-1, but not kindlin-2 may act as a link between the adhesion and cell cycle machinery to control proliferation in a range of disease contexts.

A key step in metastatic cancer progression is the inability of cells to undergo apoptosis in response to loss of cell-matrix adhesion, a process known as anoikis (Taddei et al., 2012). Talin, through its activation of integrins and recruitment of other proteins, has been shown to promote cell survival and proliferation, in particular through the Akt pathway (Sakamoto et al., 2010). Talin and its activation of β1 integrin in particular have been shown to play key roles in cancer metastasis. It was shown that inside-out activation of β1 integrins through talin is required for liver colonisation by MDA-MB 435 cancer cells that were injected into the veins of chick embryos (Kato et al., 2012). It was also shown that metastatic melanoma cells had increased β1 activation (Kato et al., 2012). Data in Chapter 3 of this thesis showed that knockdown of talin or kindlin 2 in NIH3T3 cells resulted in a significant reduction in the number of active β1 integrin containing focal adhesions in cells within a more physiologically relevant CDM model. It was also shown in Chapter 3 that knockdown of kindlin 2 has a far larger affect on migration of NIH3T3 fibroblasts within CDM than knockdown of either kindlin 1 or talin. Taken together with other published studies, these data suggest that there may be a role for kindlins

in cancer cell metastasis and that talin and kindlin interaction with β1 integrin in particular could offer new ways to target metastatic disease.

In conclusion, this thesis has shown that kindlins play a critical role in integrin activation and migration in fibroblasts in both 2D and 3D substrates, particularly kindlin 2. It has shown clear evidence for the first time that kindlin arrives to sites of forming adhesions before talin at the same adhesion within the same cell. It has also raised questions about the role of specific kindlins in activating specific integrins. Furthermore, the relationship between integrin activators, integrins and phospholipids within lipid rafts has been shown to be a deeply complex system. This work has also put forward a model of how this dynamic process may function at the early stages of adhesion formation, which has implications on our understanding of adhesion protein recruitment during cellular migration. This thesis has shown the limits of what is known about the interplay between talin, kindlins, integrins and phospholipids and it is clear that this is a very fertile field for future investigation.

Bibliography

Abercrombie, M. & Dunn, G. A. (1975) Adhesions of fibroblasts to substratum during contact inhibition observed by interference reflection microscopy. *Experimental Cell Research*. 92 (1), 57–62.

Abercrombie, M. et al. (1971) The locomotion of fibroblasts in culture. IV. Electron microscopy of the leading lamella. *Experimental Cell Research*. 67 (2), 359–367.

Abercrombie, M., Heaysman, J. E. & Pegrum, S. M. (1970a) The locomotion of fibroblasts in culture. I. Movements of the leading edge. *Experimental Cell Research*. 59 (3), 393–398.

Abercrombie, M., Heaysman, J. E. & Pegrum, S. M. (1970b) The locomotion of fibroblasts in culture. II. "Ruffling". *Experimental Cell Research*. 60 (3), 437–444.

Abercrombie, M., Heaysman, J. E. & Pegrum, S. M. (1970c) The locomotion of fibroblasts in culture. III. Movements of particles on the dorsal surface of the leading lamella. *Experimental Cell Research*. 62 (2), 389–398.

Adair, B. D. et al. (2005) Three-dimensional EM structure of the ectodomain of integrin {alpha}V{beta}3 in a complex with fibronectin. *The Journal of Cell Biology*. [Online] 168 (7), 1109–1118.

Anthis, N. J. & Campbell, I. D. (2011) The tail of integrin activation. *Trends in biochemical sciences*. [Online] 36 (4), 191–198.

Anthis, N. J., Haling, J. R., et al. (2009) Beta integrin tyrosine phosphorylation is a conserved mechanism for regulating talin-induced integrin activation. *Journal of Biological Chemistry*. [Online] 284 (52), 36700–36710.

Anthis, N. J., Wegener, K. L., et al. (2009) The structure of an integrin/talin complex reveals the basis of inside-out signal transduction. *The EMBO Journal*. [Online] 28 (22), 3623–3632.

Ashton, G. H. S. (2004) Kindler syndrome. *Clinical and experimental dermatology*. 29 (2), 116–121.

Askari, J. A. et al. (2010) Focal adhesions are sites of integrin extension. *The Journal of Cell Biology*. [Online] 188 (6), 891–903.

Bachir, A. I. et al. (2014) Integrin-Associated Complexes Form

Hierarchically with Variable Stoichiometry in Nascent Adhesions. *CURBIO*. [Online] 24 (16), 1845–1853.

Bae, Y. H. et al. (2010) Profilin1 regulates PI (3, 4) P2 and lamellipodin accumulation at the leading edge thus influencing motility of MDA-MB-231 cells. *Proceedings of the National Academy of Sciences*. [Online] 107 (50), 21547–21552.

Bialkowska, K. et al. (2010) The integrin co-activator Kindlin-3 is expressed and functional in a non-hematopoietic cell, the endothelial cell. *Journal of Biological Chemistry*. [Online] 285 (24), 18640–18649.

Bledzka, K. et al. (2012) Spatial Coordination of Kindlin-2 with Talin Head Domain in Interaction with Integrin Cytoplasmic Tails. *Journal of Biological Chemistry*. [Online] 287 (29), 24585–24594.

Bledzka, K. et al. (2010) Tyrosine phosphorylation of integrin beta3 regulates kindlin-2 binding and integrin activation. *Journal of Biological Chemistry*. [Online] 285 (40), 30370–30374.

Bouaouina, M. et al. (2012) A Conserved Lipid-binding Loop in the Kindlin FERM F1 Domain Is Required for Kindlin-mediated IIb 3 Integrin Coactivation. *Journal of Biological Chemistry*. [Online] 287 (10), 6979–6990.

Brahme, N. N. et al. (2013) Kindlin Binds Migfilin Tandem LIM Domains and Regulates Migfilin Focal Adhesion Localization and Recruitment Dynamics. *Journal of Biological Chemistry*. [Online] 288 (49), 35604–35616.

Cai, X. et al. (2008) Spatial and temporal regulation of focal adhesion kinase activity in living cells. *Molecular and Cellular Biology*. [Online] 28 (1), 201–214.

Calderwood, D. A. et al. (2013) Talins and kindlins: partners in integrin-mediated adhesion. *Nature Reviews Molecular Cell Biology*. [Online] 14 (8), 503–517.

Calderwood, D. A. et al. (2002) The phosphotyrosine binding-like domain of talin activates integrins. *Journal of Biological Chemistry*. [Online] 277 (24), 21749–21758.

Calderwood, D. A. et al. (1999) The Talin head domain binds to integrin beta subunit cytoplasmic tails and regulates integrin activation. *Journal of Biological Chemistry*. [Online] 274 (40), 28071–28074.

Campbell, I. D. & Humphries, M. J. (2011) Integrin structure, activation, and interactions. *Cold Spring Harbor Perspectives in Biology*. [Online] 3 (3), a004994–a004994.

Cantor, J. M. et al. (2008) Integrin-associated proteins as potential therapeutic targets. *Immunological reviews*. [Online] 223 (1), 236–251.

Carisey, A. et al. (2013) Vinculin Regulates the Recruitment and Release of Core Focal Adhesion Proteins in a Force-Dependent Manner. *Current Biology*. [Online] 23 (4), 271–281.

Caswell, P. T. et al. (2008) Rab-coupling protein coordinates recycling of alpha5beta1 integrin and EGFR1 to promote cell migration in 3D microenvironments. *The Journal of Cell Biology*. [Online] 183 (1), 143–155.

Chen, J. et al. (2003) Bistable regulation of integrin adhesiveness by a bipolar metal ion cluster. *Nature Structural Biology*. [Online] 10 (12), 995–1001.

Chigaev, A. et al. (2003) FRET Detection of Cellular a4-Integrin Conformational Activation. *Biophysj*. [Online] 85 (6), 3951–3962.

Choi, C. K. et al. (2011) Cross-Correlated Fluctuation Analysis Reveals Phosphorylation-Regulated Paxillin-FAK Complexes in Nascent Adhesions. *Biophysj*. [Online] 100 (3), 583–592.

Critchley, D. R. (2009) Biochemical and Structural Properties of the Integrin-Associated Cytoskeletal Protein Talin. *Annual review of biophysics*. [Online] 38 (1), 235–254.

Cukierman, E. (2001) Taking Cell-Matrix Adhesions to the Third Dimension. *Science*. [Online] 294 (5547), 1708–1712.

Cukierman, E. et al. (2002) Cell interactions with three-dimensional matrices. *Current Opinion in Cell Biology*. 14 (5), 633–639.

Cukierman, E. et al. (2001) Taking cell-matrix adhesions to the third dimension. *Science*. [Online] 294 (5547), 1708–1712.

de Pereda, J. M. et al. (2005) Structural basis for phosphatidylinositol phosphate kinase type Igamma binding to talin at focal adhesions. *Journal of Biological Chemistry*. [Online] 280 (9), 8381–8386.

Deakin, N. O. & Turner, C. E. (2011) Distinct roles for paxillin and Hic-5 in regulating breast cancer cell morphology, invasion, and metastasis. *Molecular biology of the cell*. [Online] 22 (3), 327–341.

Deakin, N. O. & Turner, C. E. (2008) Paxillin comes of age. *Journal of Cell Science*. [Online] 121 (Pt 15), 2435–2444.

del Rio, A. et al. (2009) Stretching single talin rod molecules activates vinculin binding. *Science*. [Online]

Doherty, G. J. & McMahon, H. T. (2008) Mediation, modulation, and consequences of membrane-cytoskeleton interactions. *Annual review of biophysics*. [Online] 3765–95.

Dowling, J. J. et al. (2008) Kindlin-2 is an essential component of intercalated discs and is required for vertebrate cardiac structure and function. *Circulation Research*. [Online] 102 (4), 423–431.

Dyson, J. M. et al. (2001) The SH2-containing inositol polyphosphate 5-phosphatase, SHIP-2, binds filamin and regulates submembraneous actin. *The Journal of Cell Biology*. [Online] 155 (6), 1065–1079.

Efimov, A. et al. (2008) Paxillin-dependent stimulation of microtubule catastrophes at focal adhesion sites. *Journal of Cell Science*. [Online] 121 (3), 405–405.

Elliott, P. R. et al. (2010) The Structure of the talin head reveals a novel extended conformation of the FERM domain. *Structure*. [Online] 18 (10), 1289–1299.

Emsley, J. et al. (2000) Structural basis of collagen recognition by integrin alpha2beta1. *Cell*. [Online] 101 (1), 47–56.

Erneux, C. et al. (2011) SHIP2 multiple functions: A balance between a negative control of PtdIns(3,4,5)P 3level, a positive control of PtdIns(3,4)P 2production, and intrinsic docking properties. *Journal of Cellular Biochemistry*. [Online] 112 (9), 2203–2209.

Fra, A. M. et al. (1994) Detergent-insoluble glycolipid microdomains in lymphocytes in the absence of caveolae. *Journal of Biological Chemistry*. 269 (49), 30745–30748.

Fraley, S. I. et al. (2010) A distinctive role for focal adhesion proteins in three-dimensional cell motility. *Nature Cell Biology*. [Online] 12 (6), 598–604.

Franco, S. J. et al. (2004) Calpain-mediated proteolysis of talin regulates adhesion dynamics. *Nature Cell Biology*. [Online] 6 (10), 977–983.

Franke, T. F. et al. (1997) Direct regulation of the Akt proto-oncogene product by phosphatidylinositol-3,4-bisphosphate. *Science*. 275 (5300), 665–668.

Friedl, P. & Wolf, K. (2010) Plasticity of cell migration: a multiscale tuning model. *The Journal of Cell Biology*. [Online] 188 (1), 11–19.

Friedl, P. et al. (2001) Amoeboid leukocyte crawling through extracellular matrix: lessons from the Dictyostelium paradigm of cell movement. *Journal of leukocyte biology*. 70 (4), 491–509.

Gahmberg, C. G. et al. (2009) Regulation of integrin activity and signalling. *Biochimica et Biophysica Acta (BBA) - General Subjects*. [Online] 1790 (6), 431–444.

Galbraith, C. G. et al. (2007) Polymerizing actin fibers position integrins primed to probe for adhesion sites. *Science*. [Online] 315 (5814), 992–995.

Gardel, M. L. et al. (2010) Mechanical integration of actin and adhesion dynamics in cell migration. *Annual review of cell and developmental biology*. [Online] 26315–333.

Gaus, K. et al. (2006) Integrin-mediated adhesion regulates membrane order. *The Journal of Cell Biology*. [Online] 174 (5), 725–734.

Geiger, B. et al. (2001) Transmembrane crosstalk between the extracellular matrix--cytoskeleton crosstalk. *Nature Reviews Molecular Cell Biology*. [Online] 2 (11), 793–805.

Ginsberg, M. et al. (1985) Inhibition of fibronectin binding to platelets by proteolytic fragments and synthetic peptides which support fibroblast adhesion. *Journal of Biological Chemistry*. 260 (7), 3931–3936.

Gomez, T. M. & Letourneau, P. C. (2014) Actin dynamics in growth cone motility and navigation. *Journal of neurochemistry*. [Online] 129 (2), 221–234.

Goñi, G. M. et al. (2014) Phosphatidylinositol 4,5-bisphosphate triggers activation of focal adhesion kinase by inducing clustering and conformational changes. *Proceedings of the National Academy of Sciences of the United States of America*. [Online] 111 (31), E3177–E3186.

Gorter, E. & Grendel, F. (1925) ON BIMOLECULAR LAYERS OF LIPOIDS ON THE CHROMOCYTES OF THE BLOOD. *The Journal of experimental medicine*. [Online] 41 (4), 439–443.

Goswami, D. et al. (2008) Nanoclusters of GPI-Anchored Proteins Are Formed by Cortical Actin-Driven Activity. *Cell*. [Online] 135 (6), 1085–1097.

Goult, B. T. et al. (2013) Structural studies on full-length talin1 reveal a compact auto-inhibited dimer: Implications for talin activation. *JOURNAL OF STRUCTURAL BIOLOGY*. [Online] 184 (1), 21–32.

Goult, B. T. et al. (2010) Structure of a double ubiquitin-like domain in the talin head: a role in integrin activation. *The EMBO Journal*. [Online] 29 (6), 1069–1080.

Gowrishankar, K. et al. (2012) Active Remodeling of Cortical Actin

Regulates Spatiotemporal Organization of Cell Surface Molecules. *Cell*. [Online] 149 (6), 1353–1367.

Hagelberg, C. & Allan, D. (1990) Restricted diffusion of integral membrane proteins and polyphosphoinositides leads to their depletion in microvesicles released from human erythrocytes. *Biochem J*.

Hakkinen, K. M. et al. (2011) Direct Comparisons of the Morphology, Migration, Cell Adhesions, and Actin Cytoskeleton of Fibroblasts in Four Different Three-Dimensional Extracellular Matrices. *Tissue Engineering Part A*. [Online] 17 (5-6), 713–724.

Harburger, D. S. & Calderwood, D. A. (2009) Integrin signalling at a glance. *Journal of Cell Science*. [Online] 122 (9), 1472–1472.

Harburger, D. S. et al. (2009) Kindlin-1 and -2 directly bind the C-terminal region of beta integrin cytoplasmic tails and exert integrin-specific activation effects. *Journal of Biological Chemistry*. [Online] 284 (17), 11485–11497.

Harunaga, J. S. & Yamada, K. M. (2011) Cell-matrix adhesions in 3D. *Matrix Biology*. [Online] 30 (7-8), 363–368.

Has, C. et al. (2008) C-terminally truncated kindlin-1 leads to abnormal adhesion and migration of keratinocytes. *The British journal of dermatology*. [Online] 159 (5), 1192–1196.

Hato, T. et al. (2006) Identification of critical residues for regulation of integrin activation in the beta6-alpha7 loop of the integrin beta3 I-like domain. *Journal of thrombosis and haemostasis : JTH*. [Online] 4 (10), 2278–2280.

Heath, J. P. & Dunn, G. A. (1978) Cell to substratum contacts of chick fibroblasts and their relation to the microfilament system. A correlated interference-reflexion and high-voltage electron-microscope study. *Journal of Cell Science*. 29197–212.

Herz, C. et al. (2006) Kindlin-1 is a phosphoprotein involved in regulation of polarity, proliferation, and motility of epidermal keratinocytes. *Journal of Biological Chemistry*. [Online] 281 (47), 36082–36090.

Hirata, H. et al. (2014) Force-dependent vinculin binding to talin in live cells: a crucial step in anchoring the actin cytoskeleton to focal adhesions. *AJP: Cell Physiology*. [Online] 306 (6), C607–C620.

Humphries, J. D. et al. (2006) Integrin ligands at a glance. *Journal of Cell Science*. [Online] 119 (Pt 19), 3901–3903.

Hynes, R. O. (2002a) Integrins: bidirectional, allosteric signaling machines. *Cell*. 110 (6), 673–687.

Hynes, R. O. (2002b) Integrins: bidirectional, allosteric signaling machines. *Cell*. 110 (6), 673–687.

Ithychanda, S. S. et al. (2009) Migfilin, a molecular switch in regulation of integrin activation. *Journal of Biological Chemistry*. [Online] 284 (7), 4713–4722.

Izzard, C. S. (1988) A precursor of the focal contact in cultured fibroblasts. *Cell motility and the cytoskeleton*. [Online] 10 (1-2), 137–142.

J E Ferrell, J. & Huestis, W. H. (1984) Phosphoinositide metabolism and the morphology of human erythrocytes. *The Journal of Cell Biology*. [Online] 98 (6), 1992–1998.

Jayo, A. & Parsons, M. (2012) Imaging of cell adhesion events in 3D matrix environments. *European Journal of Cell Biology*. [Online] 91 (11-12), 824–833.

Kahner, B. N. et al. (2012) Kindlins, Integrin Activation and the Regulation of Talin Recruitment to αIIbβ3 Maddy Parsons (ed.). *PLoS ONE*. [Online] 7 (3), e34056.

Kanchanawong, P. et al. (2010) Nanoscale architecture of integrin-based cell adhesions. *Nature*. [Online] 468 (7323), 580–584.

Karaköse, E. et al. (2010) The kindlins at a glance. *Journal of Cell Science*. [Online] 123 (Pt 14), 2353–2356.

Kato, H. et al. (2012) The primacy of β1 integrin activation in the metastatic cascade. *PLoS ONE*. [Online] 7 (10), e46576.

Kemp-O'Brien, K. & Parsons, M. (2013) Using FRET to analyse signals controlling cell adhesion and migration. *Journal of microscopy*. [Online] 251 (3), 270–278.

Khaitlina, S. Y. (2001) Functional specificity of actin isoforms. *International review of cytology*. 20235–98.

Kharaishvili, G. et al. (2014) *The role of cancer-associated fibroblasts, solid stress and other microenvironmental factors in tumor progression and therapy resistance*. [Online] 14 (1), 1–8.

Kiema, T. et al. (2006) The molecular basis of filamin binding to integrins and competition with talin. *Molecular cell*. [Online] 21 (3), 337–347.

Kim, C. et al. (2011) Basic amino-acid side chains regulate transmembrane integrin signalling. *Nature*. [Online] 1–7.

Kindler, T. (1954) Congenital poikiloderma with traumatic bulla formation and progressive cutaneous atrophy. *The British journal of dermatology*.

66 (3), 104–111.

Klämbt, C. (2009) Modes and regulation of glial migration in vertebrates and invertebrates. *Nature Reviews Neuroscience*. [Online] 10 (11), 769–779.

Klockenbusch, C. & Kast, J. (2010) Optimization of formaldehyde cross-linking for protein interaction analysis of non-tagged integrin beta1. *Journal of Biomedicine and Biotechnology*. [Online] 2010 (5), 927585–13.

Klooster, ten, J. P. et al. (2006) Targeting and activation of Rac1 are mediated by the exchange factor beta-Pix. *The Journal of Cell Biology*. [Online] 172 (5), 759–769.

Kobayashi, T. et al. (2014) Matrix metalloproteinase-9 activates TGF- and stimulates fibroblast contraction of collagen gels. *AJP: Lung Cellular and Molecular Physiology*. [Online] 306 (11), L1006–L1015.

Krauss, K. & Altevogt, P. (1999) Integrin leukocyte function-associated antigen-1-mediated cell binding can be activated by clustering of membrane rafts. *Journal of Biological Chemistry*. [Online] 274 (52), 36921–36927.

Kubow, K. E. & Horwitz, A. R. (2012) Reducing background fluorescence reveals adhesions in 3D matrices. *Nature Cell Biology*. [Online] 14 (12), 1344–1344.

Kwiatek, J. M. et al. (2013) Characterization of a New Series of Fluorescent Probes for Imaging Membrane Order Ludger Johannes (ed.). *PLoS ONE*. [Online] 8 (2), e52960.

Ladoux, B. & Nicolas, A. (2012) Physically based principles of cell adhesion mechanosensitivity in tissues. *Reports on Progress in Physics*. [Online] 75 (11), 116601.

Lai-Cheong, J. E. et al. (2008) Colocalization of Kindlin-1, Kindlin-2, and Migfilin at Keratinocyte Focal Adhesion and Relevance to the Pathophysiology of Kindler Syndrome. *Journal of Investigative Dermatology*. [Online] 128 (9), 2156–2165.

Lai-Cheong, J. E. et al. (2010) The role of kindlins in cell biology and relevance to human disease. *International Journal of Biochemistry and Cell Biology*. [Online] 42 (5), 595–603.

Lawson, C. & Schlaepfer, D. D. (2012) Integrin adhesions: who‘s on first? What’s on second? Connections between FAK and talin. *Cell Adhesion & Migration*. [Online] 6 (4), 302–306.

Lawson, C. et al. (2012) FAK promotes recruitment of talin to nascent

adhesions to control cell motility. *The Journal of Cell Biology*. [Online] 196 (2), 223–232.

Lämmermann, T. & Sixt, M. (2009) Mechanical modes of 'amoeboid' cell migration. *Current Opinion in Cell Biology*. [Online] 21 (5), 636–644.

Le Clainche, C. & Carlier, M. F. (2008) Regulation of Actin Assembly Associated With Protrusion and Adhesion in Cell Migration. *Physiological Reviews*. [Online] 88 (2), 489–513.

Legate, K. R. et al. (2011) Integrin adhesion and force coupling are independently regulated by localized PtdIns(4,5)2 synthesis. *The EMBO Journal*. [Online] 30 (22), 4539–4553.

Leitinger, B. & Hogg, N. (2002) The involvement of lipid rafts in the regulation of integrin function. *Journal of Cell Science*. 115 (Pt 5), 963–972.

Leslie, N. R. et al. (2008) Understanding PTEN regulation: PIP2, polarity and protein stability. *Oncogene*. [Online] 27 (41), 5464–5476.

Ling, K. et al. (2002) Type I gamma phosphatidylinositol phosphate kinase targets and regulates focal adhesions. *Nature*. [Online] 420 (6911), 89–93.

Liu, J. et al. (2011) Structural basis of phosphoinositide binding to kindlin-2 protein pleckstrin homology domain in regulating integrin activation. *Journal of Biological Chemistry*. [Online] 286 (50), 43334–43342.

Liu, W. et al. (2013) Mechanism for KRIT1 Release of ICAP1-Mediated Suppression of Integrin Activation. *Molecular cell*. [Online] 49 (4), 719–729.

Liu, Y. et al. (2012) Crystal structure of kindlin-2 PH domain reveals a conformational transition for its membrane anchoring and regulation of integrin activation. *Protein & Cell*. [Online] 3 (6), 434–440.

Locascio, A. & Nieto, M. A. (2001) Cell movements during vertebrate development: integrated tissue behaviour versus individual cell migration. *Current opinion in genetics & development*. 11 (4), 464–469.

Lundbæk, J. A. et al. (2003) Cholesterol-Induced Protein Sorting: An Analysis of Energetic Feasibility. *Biophysj*. [Online] 84 (3), 2080–2089.

Ma, Y.-Q. et al. (2008) Kindlin-2 (Mig-2): a co-activator of beta3 integrins. *The Journal of Cell Biology*. [Online] 181 (3), 439–446.

Mackinnon, A. C. et al. (2002) C. elegans PAT-4/ILK Functions as an Adaptor Protein within Integrin Adhesion Complexes. *Current Biology*. 12 (10), 787–797.

Malinin, N. L. et al. (2009) A point mutation in KINDLIN3 ablates activation of three integrin subfamilies in humans. *Nature Medicine*. [Online] 15 (3), 313–318.

McLaughlin, S. et al. (2002) PIP(2) and proteins: interactions, organization, and information flow. *Annual review of biophysics and biomolecular structure*. [Online] 31151–175.

Meves, A. et al. (2009) The Kindlin protein family: new members to the club of focal adhesion proteins. *Trends in Cell Biology*. [Online] 19 (10), 504–513.

Moissoglu, K. & Schwartz, M. A. (2012) Integrin signalling in directed cell migration. *Biology of the Cell*. [Online] 98 (9), 547–555.

Molony, L. et al. (1987) Properties of talin from chicken gizzard smooth muscle. *Journal of Biological Chemistry*. 262 (16), 7790–7795.

Mondal, S. et al. (2012) Phosphoinositide lipid phosphatase SHIP1 and PTEN coordinate to regulate cell migration and adhesion. *Molecular biology of the cell*. [Online] 23 (7), 1219–1230.

Monkley, S. J. et al. (2000) Disruption of the talin gene arrests mouse development at the gastrulation stage. *Developmental dynamics : an official publication of the American Association of Anatomists*. [Online] 219 (4), 560–574.

Montanez, E. et al. (2008) Kindlin-2 controls bidirectional signaling of integrins. *Genes & Development*. [Online] 22 (10), 1325–1330.

Moore, D. T. et al. (2012) Affinity of talin-1 for the β3-integrin cytosolic domain is modulated by its phospholipid bilayer environment. *Proceedings of the National Academy of Sciences of the United States of America*. [Online] 109 (3), 793–798.

Mory, A. et al. (2008) Kindlin-3: a new gene involved in the pathogenesis of LAD-III. *Blood*. [Online] 112 (6), 2591–2591.

Moser, M. et al. (2008) Kindlin-3 is essential for integrin activation and platelet aggregation. *Nature Medicine*. [Online] 14 (3), 325–330.

Moser, M., Bauer, M., et al. (2009) Kindlin-3 is required for β2 integrin–mediated leukocyte adhesion to endothelial cells. *Nature Medicine*. [Online] 15 (3), 300–305.

Moser, M., Legate, K. R., et al. (2009) The Tail of Integrins, Talin, and Kindlins. *Science*. [Online] 324 (5929), 895–899.

Mould, A. P. & Humphries, M. J. (2004) Regulation of integrin function through conformational complexity: not simply a knee-jerk reaction?

Current Opinion in Cell Biology. [Online] 16 (5), 544–551.

Mould, A. P. et al. (2003) Conformational changes in the integrin beta A domain provide a mechanism for signal transduction via hybrid domain movement. *Journal of Biological Chemistry*. [Online] 278 (19), 17028–17035.

Mould, A. P. et al. (2002) Integrin activation involves a conformational change in the alpha 1 helix of the beta subunit A-domain. *Journal of Biological Chemistry*. [Online] 277 (22), 19800–19805.

Murata, Y. & Okamura, Y. (2007) Depolarization activates the phosphoinositide phosphatase Ci-VSP, as detected in Xenopus oocytes coexpressing sensors of PIP2. *The Journal of Physiology*. [Online] 583 (Pt 3), 875–889.

Nishida, N. et al. (2006) Activation of leukocyte beta2 integrins by conversion from bent to extended conformations. *Immunity*. [Online] 25 (4), 583–594.

Oxley, C. L. et al. (2008) An integrin phosphorylation switch: the effect of beta3 integrin tail phosphorylation on Dok1 and talin binding. *Journal of Biological Chemistry*. [Online] 283 (9), 5420–5426.

Pankov, R. et al. (2000) Integrin dynamics and matrix assembly: tensin-dependent translocation of alpha(5)beta(1) integrins promotes early fibronectin fibrillogenesis. *The Journal of Cell Biology*. 148 (5), 1075–1090.

Parsons, M. et al. (2008) Quantification of integrin receptor agonism by fluorescence lifetime imaging. *Journal of Cell Science*. [Online] 121 (Pt 3), 265–271.

Pasapera, A. M. et al. (2010) Myosin II activity regulates vinculin recruitment to focal adhesions through FAK-mediated paxillin phosphorylation. *The Journal of cell …*. [Online]

Pasquali, C. et al. (2007) A chemical proteomics approach to phosphatidylinositol 3-kinase signaling in macrophages. *Molecular & cellular proteomics : MCP*. [Online] 6 (11), 1829–1841.

Patel, H. et al. (2013) Kindlin-1 regulates mitotic spindle formation by interacting with integrins and Plk-1. *Nature Communications*. [Online] 42056.

Perera, H. D. et al. (2011) Membrane binding of the N-terminal ubiquitin-like domain of kindlin-2 is crucial for its regulation of integrin activation. *Structure*. [Online] 19 (11), 1664–1671.

Petrich, B. G. (2009) Talin-dependent itegrin signalling in vivo. *Thrombosis*

and Haemostasis. [Online]

Porter, J. C. & Hogg, N. (1998) Integrins take partners: cross-talk between integrins and other membrane receptors. *Trends in Cell Biology*. 8 (10), 390–396.

Prasad, N. et al. (2001) SH2-containing inositol 5'-phosphatase SHIP2 associates with the p130(Cas) adapter protein and regulates cellular adhesion and spreading. *Molecular and Cellular Biology*. [Online] 21 (4), 1416–1428.

Quizi, J. L. et al. (2012) *SLK-mediated phosphorylation of paxillin is required for focal adhesion turnover and cell migration*. [Online] 1–8.

Rantala, J. K. et al. (2011) SHARPIN is an endogenous inhibitor of beta 1-integrin activation. *Nature Cell Biology*. [Online] 13 (11), 1315–1324.

Rentero, C. et al. (2011) Quantitative imaging of membrane lipid order in cells and organisms. *Nature Protocols*. [Online] 7 (1), 24–35.

Ridley, A. J. et al. (2003) Cell migration: integrating signals from front to back. *Science*. [Online] 302 (5651), 1704–1709.

Riveline, D. et al. (2001) Focal contacts as mechanosensors: externally applied local mechanical force induces growth of focal contacts by an mDia1-dependent and ROCK-independent mechanism. *The Journal of Cell Biology*. 153 (6), 1175–1186.

Rodius, S. et al. (2008) The talin rod IBS2 alpha-helix interacts with the beta3 integrin cytoplasmic tail membrane-proximal helix by establishing charge complementary salt bridges. *Journal of Biological Chemistry*. [Online] 283 (35), 24212–24223.

Roduit, C. et al. (2008) Elastic membrane heterogeneity of living cells revealed by stiff nanoscale membrane domains. *Biophysical Journal*. [Online] 94 (4), 1521–1532.

Rogalski, T. M. et al. (2000) The UNC-112 gene in Caenorhabditis elegans encodes a novel component of cell-matrix adhesion structures required for integrin localization in the muscle cell membrane. *The Journal of Cell Biology*. 150 (1), 253–264.

Rognoni, E. et al. (2014) Kindlin-1 controls Wnt and TGF-β availability to regulate cutaneous stem cell proliferation. *Nature Medicine*. [Online] 20 (4), 350–359.

Rossier, O. et al. (2012) Integrins β1 and β3 exhibit distinct dynamic nanoscale organizations inside focal adhesions. *Nature Cell Biology*. [Online] 14 (10), 1057–1067.

Saarikangas, J. et al. (2010) Regulation of the Actin Cytoskeleton-Plasma Membrane Interplay by Phosphoinositides. *Physiological Reviews*. [Online] 90 (1), 259–289.

Sakamoto, S. et al. (2010) Talin1 promotes tumor invasion and metastasis via focal adhesion signaling and anoikis resistance. *Cancer research*. [Online] 70 (5), 1885–1895.

Sanz-Moreno, V. & Marshall, C. J. (2009) Rho-GTPase signaling drives melanoma cell plasticity. *Cell cycle (Georgetown, Tex.)*. 8 (10), 1484–1487.

Scales, T. M. & Parsons, M. (2011) Spatial and temporal regulation of integrin signalling during cell migration. *Current Opinion in Cell Biology*. [Online] 23 (5), 562–568.

Schaller, M. D. & Parsons, J. T. (1995) pp125FAK-dependent tyrosine phosphorylation of paxillin creates a high-affinity binding site for Crk. *Molecular and Cellular Biology*. 15 (5), 2635–2645.

Schiller, H. B. & Fässler, R. (2013) Mechanosensitivity and compositional dynamics of cell–matrix adhesions. *Nature Publishing Group*. [Online] 14 (6), 509–519.

Senetar, M. A. et al. (2007) Talin2 is induced during striated muscle differentiation and is targeted to stable adhesion complexes in mature muscle. *Cell motility and the cytoskeleton*. [Online] 64 (3), 157–173.

Sero, J. E. et al. (2012) Paxillin controls directional cell motility in response to physical cues. *Cell Adhesion & Migration*. [Online] 6 (6), 502–508.

Serrels, B. et al. (2007) Focal adhesion kinase controls actin assembly via a FERM-mediated interaction with the Arp2/3 complex. *Nature Cell Biology*. [Online] 9 (9), 1046–1056.

Shevchenko, A. & Simons, K. (2010) *Lipidomics: coming to grips with lipid diversity*. [Online] 1–6.

Shi, X. et al. (2007) The MIG-2/Integrin Interaction Strengthens Cell-Matrix Adhesion and Modulates Cell Motility. *Journal of Biological Chemistry*. [Online] 282 (28), 20455–20466.

Siegel, D. H. et al. (2003) Loss of kindlin-1, a human homolog of the Caenorhabditis elegans actin-extracellular-matrix linker protein UNC-112, causes Kindler syndrome. *American journal of human genetics*. [Online] 73 (1), 174–187.

Simons, K. & Gerl, M. J. (2010) Revitalizing membrane rafts: new tools and insights. *Nature Reviews Molecular Cell Biology*. [Online] 11 (10), 688–699.

Simons, K. & Ikonen, E. (1997) Functional rafts in cell membranes. *Nature*. [Online] 387 (6633), 569–572.

Simons, K. & Sampaio, J. L. (2011) Membrane organization and lipid rafts. *Cold Spring Harbor Perspectives in Biology*. [Online] 3 (10), a004697–a004697.

Simons, K. & van Meer, G. (1988) Lipid sorting in epithelial cells. *Biochemistry*. 27 (17), 6197–6202.

Singer, S. J. & Nicolson, G. L. (1972) The fluid mosaic model of the structure of cell membranes. *Science*. 175 (4023), 720–731.

Singh, R. D. et al. (2010) Gangliosides and β1-Integrin Are Required for Caveolae and Membrane Domains. *Traffic*. [Online] 11 (3), 348–360.

Singhal, R. L. et al. (1995) Quercetin down-regulates signal transduction in human breast carcinoma cells. *Biochemical and Biophysical Research Communications*. 208 (1), 425–431.

Svensson, L. et al. (2009) Leukocyte adhesion deficiency-III is caused by mutations in KINDLIN3 affecting integrin activation. *Nature Medicine*. [Online] 15 (3), 306–312.

Taddei, M. L. et al. (2012) Anoikis: an emerging hallmark in health and diseases. *The Journal of pathology*. [Online] 226 (2), 380–393.

Tadokoro, S. et al. (2003) Talin binding to integrin beta tails: a final common step in integrin activation. *Science*. [Online] 302 (5642), 103–106.

Takagi, J. et al. (2002) Global conformational rearrangements in integrin extracellular domains in outside-in and inside-out signaling. *Cell*. 110 (5), 599–511.

Tamariz, E. & Grinnell, F. (2002) Modulation of fibroblast morphology and adhesion during collagen matrix remodeling. *Molecular biology of the cell*. [Online] 13 (11), 3915–3929.

Tamura, M. et al. (1998) Inhibition of cell migration, spreading, and focal adhesions by tumor suppressor PTEN. *Science*. [Online] 280 (5369), 1614–1617.

Tamura, M. et al. (1999) PTEN gene and integrin signaling in cancer. *Journal of the National Cancer Institute*. 91 (21), 1820–1828.

Tu, Y. et al. (2003) Migfilin and Mig-2 link focal adhesions to filamin and the actin cytoskeleton and function in cell shape modulation. *Cell*. 113 (1), 37–47.

Ussar, S. et al. (2008) Loss of Kindlin-1 Causes Skin Atrophy and Lethal Neonatal Intestinal Epithelial Dysfunction Veronica van Heyningen (ed.). *PLoS Genetics*. [Online] 4 (12), e1000289.

Ussar, S. et al. (2006) The Kindlins: Subcellular localization and expression during murine development. *Experimental Cell Research*. [Online] 312 (16), 3142–3151.

van Zijl, F. et al. (2011) Initial steps of metastasis: cell invasion and endothelial transmigration. *Mutation research*. [Online] 728 (1-2), 23–34.

Várnai, P. et al. (2005) Selective cellular effects of overexpressed pleckstrin-homology domains that recognize PtdIns(3,4,5)P3 suggest their interaction with protein binding partners. *Journal of Cell Science*. [Online] 118 (Pt 20), 4879–4888.

Vicente-Manzanares, M. et al. (2005) Cell migration at a glance. *Journal of Cell Science*. [Online] 118 (Pt 21), 4917–4919.

Walker, E. H. et al. (2000) Structural determinants of phosphoinositide 3-kinase inhibition by wortmannin, LY294002, quercetin, myricetin, and staurosporine. *Molecular cell*. 6 (4), 909–919.

Wang, S. et al. (2012) Tiam1 interaction with the PAR complex promotes talin-mediated Rac1 activation during polarized cell migration. *The Journal of Cell Biology*. [Online] 199 (2), 331–345.

Wang, Y. L. (1985) Exchange of actin subunits at the leading edge of living fibroblasts: possible role of treadmilling. *The Journal of Cell Biology*. 101 (2), 597–602.

Wei, Y. et al. (1999) A role for caveolin and the urokinase receptor in integrin-mediated adhesion and signaling. *The Journal of Cell Biology*. 144 (6), 1285–1294.

Wen, T. et al. (2010) Integrin α3 subunit regulates events linked to epithelial repair, including keratinocyte migration and protein expression. *Wound repair and regeneration : official publication of the Wound Healing Society [and] the European Tissue Repair Society*. [Online] 18 (3), 325–334.

Wong, K.-K. et al. (2010) Targeting the PI3K signaling pathway in cancer. *Current opinion in genetics & development*. [Online] 20 (1), 87–90.

Worth, D. C. & Parsons, M. (2010) Advances in imaging cell-matrix adhesions. *Journal of Cell Science*. [Online] 123 (21), 3629–3638.

Worth, D. C. et al. (2010) Alpha v beta3 integrin spatially regulates VASP and RIAM to control adhesion dynamics and migration. *The Journal of*

Cell Biology. [Online] 189 (2), 369–383.

Xiao, T. et al. (2004) Structural basis for allostery in integrins and binding to fibrinogen-mimetic therapeutics. *Nature*. [Online] 432 (7013), 59–67.

Xiong, J. P. et al. (2001) Crystal structure of the extracellular segment of integrin alpha Vbeta3. *Science*. [Online] 294 (5541), 339–345.

Yamada, K. M. et al. (2003) Dimensions and dynamics in integrin function. *Brazilian journal of medical and biological research = Revista brasileira de pesquisas médicas e biológicas / Sociedade Brasileira de Biofísica ... [et al.]*. 36 (8), 959–966.

Yan, B. et al. (2001) Calpain cleavage promotes talin binding to the beta 3 integrin cytoplasmic domain. *Journal of Biological Chemistry*. [Online] 276 (30), 28164–28170.

Yao, M. et al. (2014) Mechanical activation of vinculin binding to talin locks talin in an unfolded conformation. *Scientific Reports*. [Online] 4.

Yates, L. A. et al. (2012) Structural and Functional Characterization of the Kindlin-1 Pleckstrin Homology Domain. *Journal of Biological Chemistry*. [Online] 287 (52), 43246–43261.

Ye, F. et al. (2011) Molecular mechanism of inside-out integrin regulation. *Journal of thrombosis and haemostasis : JTH*. [Online] 9 Suppl 120–25.

Ye, F. et al. (2010) Recreation of the terminal events in physiological integrin activation. *The Journal of Cell Biology*. [Online] 188 (1), 157–173.

Ye, F. et al. (2013) The Mechanism of Kindlin-Mediated Activation of Integrin aIIbb3. *CURBIO*. [Online] 1–8.

Yoshinaga, S. et al. (2012) A phosphatidylinositol lipids system, lamellipodin, and Ena/VASP regulate dynamic morphology of multipolar migrating cells in the developing cerebral cortex. *The Journal of neuroscience : the official journal of the Society for Neuroscience*. [Online] 32 (34), 11643–11656.

Zamir, E. et al. (2000) Dynamics and segregation of cell-matrix adhesions in cultured fibroblasts. *Nature Cell Biology*. [Online] 2 (4), 191–196.

Zhang, L. et al. (2004) Mechanosensitivity of GIRK channels is mediated by protein kinase C-dependent channel-phosphatidylinositol 4,5-bisphosphate interaction. *Journal of Biological Chemistry*. [Online] 279 (8), 7037–7047.

Zhao, Y. et al. (2012) Regulation of cell adhesion and migration by Kindlin-

3 cleavage by calpain. *Journal of Biological Chemistry*. [Online] 287 (47), 40012–40020.

Zhu, Jianghai et al. (2008) Structure of a Complete Integrin Ectodomain in a Physiologic Resting State and Activation and Deactivation by Applied Forces. *Molecular cell*. [Online] 32 (6), 849–861.

Zhu, Jieqing et al. (2013) Complete integrin headpiece opening in eight steps. *The Journal of Cell Biology*. [Online] 201 (7), 1053–1068.